Title
Genetic analysis of neuronal morphogenesis in vivo

Author
Sweeney, Neal T

Publication Date
2006

Peer reviewed|Thesis/dissertation

Genetic Analysis of Neuronal Morphogenesis *in Vivo*

by

Neal T. Sweeney

DISSERTATION

Submitted in partial satisfaction of the requirements for the degree of

DOCTOR OF PHILOSOPHY

in

Neuroscience

in the

GRADUATE DIVISION
of the

UNIVERSITY OF CALIFORNIA, SAN FRANCISCO

Acknowledgements

I would like to thank Fen-Biao Gao for support, guidance, enthusiasm and for keeping an open door for any questions I had or anything I wanted to discuss. I have learned a great deal from him. After working closely together in the early days as the lab was just starting up, we gained a friendship that enabled us to work together as colleagues. I would also like to thank my thesis committee: Cori Bargmann, Grae Davis, Lou Reichardt, Mark Von Zastrow and Liqun Luo. They were very supportive and provided good ideas all along the way.

I'm also grateful to the members of the Gao Lab for discussions on topics scientific and otherwise, Wenjun Li for collaborating on the *flamingo* project, and Siddartha Mitra for listening to my many off-the-wall ideas and giving good advice on experimental directions.

I would like to thank Robin Osterhout for being such a great friend for so many years. Tahnee Stair deserves more appreciation than I can express – she has been an inspiration, a source of encouragement and I can't imagine life without her. I'm finally grateful to my parents who maintained interest in my project and support for me in good times and bad and were always there to help keep my chin up.

Preface

The material presented in Chapter Two, 'Genetic Manipulation of Single Neurons *in Vivo* Reveals Specific Roles of Flamingo in Neuronal Morphogenesis' has been published in *Developmental Biology* (2002) 247, 76-88. The authors were Neal T. Sweeney, Wenjun Li and Fen-Biao Gao. Chapter Three, 'The Coiled-Coil Protein Shrub Controls Neuronal Morphogenesis in *Drosophila*' has been accepted for publication by *Current Biology* and will be published in Vol. 16 (8) on May 23, 2006. The authors were Neal T. Sweeney, Jay E. Brenman, Yuh Nung Jan, and Fen-Biao Gao. Permission has been given by Elsevier to reprint copyrighted material from these two articles in this thesis.

Involvement of Co-Authors

The experiments presented in Chapter Two were done by Neal Sweeney in collaboration with Wenjun Li and Fen-Biao Gao. Neal Sweeney performed all the experiments presented in Chapters Three and Four with the exceptions of the isolation and mapping of the *shrub*^{4} mutation and the generation of the Shrub antibody and UAS-*shrub* transgenic lines, which were carried out by Jay E. Brenman and Fen-Biao Gao in Yuh Nung Jan's laboratory.

Fen-Biao Gao

Fen-Biao Gao, Ph.D.

Research Advisor

Genetic Analysis of Neuronal Morphogenesis *in Vivo*

by

Neal T. Sweeney

Abstract

Proper dendritic branching is required for neuronal function. Although a number of genes that regulate dendritic branching have recently been identified, the mechanisms by which these genes control morphogenesis remain unknown. As many genes are expressed in multiple tissues and at multiple developmental time points, it is important to determine the specific cell-autonomous roles for a particular gene in dendritic branching, independent of pleiotropic effects.

In addressing cell-autonomous mechanisms, mosaic analysis with a repressible cell marker (MARCM) was used to make single-cell mutant clones of several genes previously implicated in dendritic branching. These genes are expressed in both neurons and in adjacent cells, raising the question of whether dendritic phenotypes are attributable to extrinsic or intrinsic roles of the genes. Mutations in the *flamingo* gene cause dendritic overextension and experiments presented here illustrate that Flamingo can act cell-autonomously to limit dendritic extension of dorsally extended dendrites. Intrinsic roles

for Flamingo were also found in controlling axon extension and branching.

A second set of experiments focused on the role of *shrub*, another gene involved in dendritic branching. Shrub is homologous to yeast late endosomal protein Snf7, and is expressed in many, if not all, tissues of the *Drosophila* embryo. Several methods were used to test cell-autonomous roles of Shrub, all of which caused increased dendritic branching. Aberrant axonal branching was also seen in single-cell *shrub* mutant clones, suggesting a similar role in axonal morphogenesis. A series of further experiments showed that misregulation of the Delta/Notch signaling pathway, likely due to impaired endosomal-to-lysosomal transport, contributes to the dendritic phenotypes in *shrub* mutant cells. A final set of experiments explored the cell-autonomous roles of Delta, Notch, and Neuralized, a key regulator of Delta localization. Each of these genes was found to regulate dendritic branching in a cell-autonomous manner, suggesting that Delta regulates Notch activity in cis and/or has Notch-independent functions.

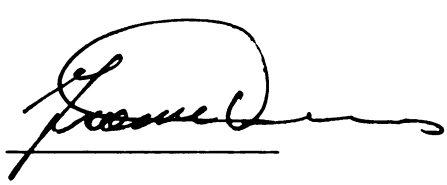

Graeme Davis, Ph.D.

Thesis Committee Chair

Table of Contents

Table of Figures

Chapter One:

General Introduction

Among the most distinguishing neuronal characteristics is a complex branched morphology. Morphological complexity derives largely from dendrites, which receive much of a neuron's sensory or synaptic input and are intimately related to a neuron's function. To attain these specific morphologies, developmental programs must exist to ensure that a neuron has a specific arbor attuned to its function.

Although there is great diversity in dendritic arbors across neuronal types and across species, dendritic development usually includes a number of specific growth stages (Craig and Banker, 1994; Scott and Luo, 2001). First, the neuron must attain cell polarity and extend one or more dendrites with molecular and morphological characteristics distinct from those of axons. The neuron must then regulate the guidance, branching, and extension of its dendritic tree. Dendritic specializations such as dendritic spines may be formed in certain neurons. Finally, dendritic structure is continually subject to modulations by various inputs including synaptic activity.

During these stages, neurons face a number of challenges in the development of a specific dendritic arbor. 1) Although axons and dendrites are both elongated, branched extensions from the cell body and are regulated by a number of common genes, they have significant differences in morphology. Are common or distinct mechanisms used to control axonal and dendritic branching? How does a single gene cause distinct axonal and dendritic phenotypes? 2) Guidance of dendrites to a specific region and regulation of dendritic branching and extension determine a neuron's receptive field and are essential for the correct wiring of neuronal circuits. What mechanisms are responsible for the specification of dendritic field? 3) The nervous system shows a striking diversity of dendritic branching patterns, even among adjacent neurons. How does a neuron select a

specific branching pattern? How do two neurons form distinct branching patterns in a common environment?

At each step of dendrite development, a neuron likely integrates a number of intrinsic and extrinsic cues in the attainment of a dendritic branching pattern. The importance of both intrinsic and extrinsic factors has been borne out by a number of studies using cell ablation and primary neuronal cultures. When adjacent neurons are ablated either using X-irradiation (Altman and Anderson, 1972), genetic mutations (Rakic and Sidman, 1973) or a laser beam (Gao et al 2000), the remaining neurons often retain their wild-type dendritic phenotypes and certain neurons in *Drosophila* show no changes in morphology (Gao et al., 2000). At the same time, some remaining neurons show dendritic overgrowth (Gao et al., 2000), branch orientation defects and loss of higher order branching (Altman and Anderson, 1972; Rakic and Sidman, 1973), supporting extrinsic influences. In primary cultures, isolated neurons are able to grow recognizable dendrites with spines and synapses, but fail to attain mature dendritic morphologies identical to those *in vivo*, again suggesting that extrinsic factors from other cell types are not required for dendritic growth per se but are important for certain aspects of dendritic elaboration (Baptista et al., 1994).

To understand the array of intrinsic and extrinsic factors that regulate dendritic morphogenesis, a number of recent studies have used genetic screens (e.g., Gao et al., 1999; Parrish et al., 2006; Medina et al., 2006; Reuter et al., 2003) and candidate-based approaches (e.g., Andersen et al., 2005; Lee et al., 2003; Lee et al., 2000; McAllister et al., 1995; Zou and Cline, 1999). Following the identification of a gene as affecting dendritic development, it is important to consider whether it may act as an intrinsic or

extrinsic regulator, or a combination of both. This question of cell-autonomy is important as it defines the locus for action of a particular gene, which is especially important for genes expressed both in the cell of interest and in adjacent cells, and facilitates explanatory models for different aspects of branching.

Common and Distinct Mechanisms in Axonal and Dendritic Morphogenesis

As polarized cells, neurons exhibit morphological and molecular differences between axons and dendrites. Dendrites differ from axons in their cytoskeletal composition and organization, branched morphology and localization of various proteins (Craig and Banker, 1994). Several *in vivo* studies in vertebrates (Myers et al., 1986; Westerfield et al., 1986) and invertebrates (Gao et al., 1999) have observed that axonal outgrowth from the cell body occurs first, followed by dendrite initiation at a later point, suggesting that the neuron may have distinct stages where axonal and dendritic growth predominate. Although a number of proteins have been found to affect both axons and dendrites, it is not known whether common mechanisms are used for axonal and dendritic morphogenesis and to what degree these are coordinately related. Interestingly, a number of genes similarly affect axons and dendrites, while others have selective or even opposite phenotypes (reviewed in Scott and Luo, 2001).

Among proteins that affect cytoskeletal polymerization and organization, axonal and dendrites phenotypes are often similar. These include small GTPases such as RhoA, Rac1 and Cdc42. RhoA, for example, limits both axonal and dendritic growth (Lee et al., 2000; Luo, 2000) while Rac1 promotes growth and branch formation in each (Li et al., 2000; Luo, 2000; Luo et al, 1996). Other cytoskeletal-associated proteins such as

Kakapo/Short Stop also similarly affect axons and dendrites (Gao et al., 1999; Kolodziej et al., 1995; Prokop et al., 1998). Kakapo contains actin binding and microtubule binding domains and likely acts as a cross-linker between two cytoskeletal components. Signaling proteins that regulate cytoskeletal dynamics, such as Enabled, also have similar axonal and dendritic phenotypes. Loss of Enabled leads to axonal and dendritic guidance defects, likely due to its ability to bind actin-associated proteins and actin filaments (Gao et al., 1999; Wills et al., 1999; Li et al., 2005). As common cytoskeletal mechanisms are used to produce axonal and dendritic growth and extension, cytoskeletal-interacting proteins produce similar phenotypes.

Regulatory mechanisms common to axonal and dendritic morphogenesis also include changes in glutamate receptor function during neuronal development. At early stages, AMPA receptors in hippocampal neurons lack the GluR2 subunit and can flux calcium, while adult receptors contain GluR2 and are impermeable to calcium (Shi et al., 2001; Zhu et al., 2000). Similarly, NMDA receptors in immature but not adult neurons lack the NR2A subunit, which reduces the duration of activation and consequently reduces calcium influx as neurons mature (Quinlan et al., 1999). Decreased calcium influx in turn alters the activity of calcium-dependent protein kinases such as CAMKII. Decreased CAMKII activity causes a slowing of both dendritic branching dynamics and axonal elaboration (Wu and Cline, 1998; Zou and Cline, 1999). Through this activity-dependent mechanism, axons and dendrites are coordinately stabilized as neurons mature.

A number of other genes have been shown to exert opposite effects on axons and dendrites, in some cases through polarized trafficking of downstream signaling molecules. In a study using mammalian cortical pyramidal neurons cultured on cortical

slices, axons extended toward the ventricle due to a chemorepulsive factor from cells near the marginal zone (Polleux et al, 1998). A soluble factor from the marginal zone again affected the cell one to two days later, but in this case as an attractant for dendrites (Polleux et al., 2000). Semaphorin 3A (Sema3A) was identified as a factor released from the marginal zone able to exert opposite effects on axons and dendrites (Polleux et al., 1998). Consistent with other work showing that cGMP levels can switch Sema3A between attractive and repellant influences on axons (Song et al., 1998), differences in cGMP levels between axons and dendrites levels were likely responsible for the opposite Sema3A phenotypes. Soluble guanylate kinase (sGC) regulates cGMP production was found to be localized specifically to cortical dendrites in these experiments (Polleux et al., 2000).

Another mechanism by which axonal and dendritic developmental may be differentially regulated through developmental switches. In a study of cultured retinal ganglion cells (RGCs), two phases of neuronal growth were observed, one primary axonal and one primarily dendritic (Goldberg et al., 2002). At embryonic day 20 (E20), the RGCs extended axons at a rate ten times that of axons from postnatal day 8 (P8) neurons. As for dendritic growth, E20 neurons grew few dendrites while P8 neurons grew primarily dendrites. An extracellular cue, likely from amacrine cells, was found to mediate this conversion between axonal and dendritic growth. Other experiments found that the switch was irreversible and not due to an intrinsic aging mechanism.

Regulation of Dendritic Field by Extrinsic and Intrinsic Mechanisms

Following dendritic outgrowth in a particular direction, the neuron faces the task of forming a dendritic arbor, sometimes branching hundreds of times and extending over a large area. Targeting of a dendritic arbor to a specific region is essential in the forming of synapses with specific synaptic partners or, in the case of sensory neurons, to innervate a certain region of the receptive field. Although dendrites usually elaborate near the cell body, guidance mechanisms are still essential and required for neuronal function. In some cases, extrinsic cues from other cells help to orient dendritic dendritic fields, while in other contexts without external landmarks, the neurons rely on intrinsic mechanisms.

Among the extrinsic mechanisms for regulating dendritic field is non-redundant coverage of a receptive field, also known as tiling. Dendrites of sensory neurons in the visual (Hitchcock, 1989; Wassle et al., 1981) and somatosensory systems (Gao et al., 2000; Grueber et al., 2002; Sagasti et al., 2005) form non-overlapping fields with neighboring neurons. This tiling mechanism has been extensively studied in *Drosophila* larval peripheral nervous system (PNS) neurons that innervate the epidermis (Emoto et al., 2004; Grueber et al, 2003). Terminal dendrites of adjacent cells repel each other so that the neurons cover the entire epidermis without overlap; two proteins, Tricornered kinase and Furry, are among the mediators of this process (Emoto et al., 2004). N-cadherin is another protein involved in contact-dependent interactions. In cultured hippocampal neurons (Zanata et al., 2002) and among projection neurons in the *Drosophila* olfactory bulb (Zhu and Luo, 2004), blocking N-cadherin leads to increased dendritic spine length and dendritic overgrowth. N-cadherin activates α- and β-catenins, which eventually activate Rac1, leading to dendritic branching and spine growth.

Another set of external cues are derived from early developmental landmarks, as found in studies of *Drosophila* motor neurons (Landgraf et al., 2003). These neurons also organize their dendrites into non-overlapping fields, but dendrite-dendrite interactions, muscle innervation, axonal targeting and glia cells play little or no role in this process. Instead, the early parasegmental organization of the embryo directs these myotopic maps and provides another extrinsic method by which dendritic field may be specified.

In other contexts, extrinsic cues do not exist or intrinsic cues play predominant roles in organizing dendritic fields, as is the case in the *Drosophila* olfactory system. In this system, each projection neuron (PN) targets dendrites to a single glomerulus and this targeting occurs before the PNs have been innervated, suggesting an intrinsic mechanism (Jefferis et al., 2001; Jefferis et al., 2004). PNs derived from different neuroblast lineages innervate non-overlapping sets of glomeruli, pointing to cell lineage as a factor. Moreover, the birth order of neurons within a particular neuroblast lineage is correlated with dendritic glomerular targeting (Jefferis et al., 2001). In addition, two transcription factors, Acj6 and Drifter, were found to be expressed selectively in different neuroblast lineages and could change dendritic targeting when misexpressed (Komiyama et al., 2003). Another interesting result using this system was obtained in studies of N-cadherin. N-cadherin was found to act non-autonomously to limit dendritic overgrowth, suggesting that this protein functions to bind together dendrites targeted to a common glomerulus (Zhu and Luo, 2004). Dendritic field specification also involves intrinsic cytoskeletal regulators including RhoA. In a number of model systems, constitutive activation of RhoA leads to reduced dendritic length, while blocking RhoA function with

dominant-negative constructs leads to increased length (Lee et al., 2000; Li et al., 2000; Wong et al., 2000).

Creating Neuronal Diversity: Regulation of Dendritic Branching Type

As dendrites grow out from the cell body, they often grow in close proximity to dendrites from other neurons. Despite this similar environment, there exists a great diversity of dendritic arbors in the nervous system, with hundreds or thousands of different classes of mammalian neurons based on morphology (Stevens, 1998). Among a single class of neurons, retinal alpha ganglion cells, dendritic branching patterns form the basis for up to 15 subclasses (Masland, 2001). In some cases, such as in the mammalian cortex, different classes of neurons have similar morphologies at early stages before undergoing dramatic changes to become morphologically distinct, suggesting an early intrinsic growth program followed by later refinement into different classes (Koester and O'Leary, 1992; Vercelli et al., 1992). How does a neuron develop a specific morphology despite sharing many environmental cues with neighboring neurons?

One mechanism for creating dendritic branching pattern diversity is the asymmetric inheritance of signaling molecules during cell division. This process has been extensively studied in the formation of cellular diversity among sensory organ precursor cells in *Drosophila,* but other studies suggest it could also be used to create diversity in dendritic branching. In the embryonic mouse cortex, distribution of Numb, one of the molecules known to be inherited asymmetrically, correlated with similarity of morphology between the daughter cells (Shen et al., 2002). Neurons with increased Numb inheritance showed shorter dendrites, consistent with previous studies showing

that Numb can suppress Notch activity and decreased Notch activity suppresses dendritic growth (Redmond et al., 2000; Sestan et al., 1999).

A number of transcription factors have also been identified as regulators of dendritic branching type. One of these is Hamlet, a Zn-finger transcription factor that is expressed in *Drosophila* external sensory (ES) neurons during dendritic branch extension but not in adjacent multiple dendritic (MD) neurons. ES cells normally have a single unbranched dendrite, but *hamlet* mutant neurons show complex branching patterns characteristic of MD neurons (Moore et al., 2002). Postmitotic expression of *hamlet* in MD neurons is sufficient to shift the dendrites to a simpler branching pattern, supporting a role in regulation between ES and MD branching types. Also able to create dendrite diversity are Cut and Abrupt, two transcription factors expressed in a complementary pattern in *Drosophila* PNS sensory neurons. Cut is highly expressed in highly branched type III and IV neurons but not in morphologically simpler type I neurons (Grueber et al., 2003), while Abrupt is expressed selectively in type I neurons (Li et al., 2004; Sugimura et al., 2004). Loss of Cut in type III and IV neurons leads to a dramatic reduction in branching while postmitotic expression of Cut in type I and II neurons leads to increased arborization. Complementary results were obtained for Abrupt, with higher levels of Abrupt expression leading to simpler branching patterns. The ability to regulate dendritic branching by expression of these genes postmitotically suggests either that Hamlet, Cut, and Abrupt are able to regulate dendritic morphology independent of cell fate, or that cell fate is not a one-time decision, with different aspects of cell identity able to be determined after a cell's final division (Jan and Jan, 2003).

Another mechanism for creating dendritic diversity was found in a study of cortical pyramidal cells. Neurotrophins including NT-3. NT-4, BDNF and NGF were applied exogenously and endogenously to slices from the ferret visual cortex (Baker et al., 1998; McAllister et al., 1995; Niblock et al., 2000). While each neurotrophin caused pyramidal cells to increase in length and complexity, the neurons showed layer-specific differences in response (McAllister et al., 1995; McAllister et al., 1997). Intrinsic differences in response likely created divergent responses to common cues. Neurotrophins activate MAP kinase and PI-3 kinase signaling pathways downstream of the Trk receptors, ultimately influencing Rho family kinases, which mediate actin cytoskeleton dynamics (Posern et al., 2000; Wu et al 2001). Neurotrophins may also lead to changes in local protein synthesis of cytoskeletal proteins (Aakalu et al., 2001; Kuhl and Skehel, 1998).

Cell class-specific responses to extracellular cues were also found in the *Drosophila* CNS, where dendrites of certain motor neurons cross to the contralateral side of the CNS midline, while dendrites of other neurons remain on the ipsilateral side. Contralateral dendrites are attracted by the midline attractant Netrin, while ipsilateral dendrites are repelled from the midline by Slit (Furrer et al., 2003). Since the contralateral and ipsilateral dendrites grow in close proximity, mechanisms must exist so that crossing dendrites are responsive to Netrin and insensitive to Slit and vice versa for ipsilateral dendrites. Interestingly, Slit does not appear to affect dendritic growth of all *Drosophila* neurons, as DA neurons are unresponsive (Gao et al., 1999), suggesting that different mechanisms may act in different systems and cell types to regulate dendritic branching type.

In Vivo Analysis of Intrinsic Mechanisms Controlling Dendritic Morphogenesis Using the *Drosophila* PNS

The studies described above have led to insights into different aspects of dendritic morphogenesis including differences between axonal and dendritic growth, and mechanisms to specify dendritic field and branching pattern. To move further, unbiased genetic analysis combined with *in vivo* visualization of dendritic morphology offers a powerful approach, evidenced by studies of axonal morphogenesis (reviewed in Tear et al., 1999). While *in vitro* approaches to dendritic branching have produced key findings, *in vivo* systems eliminate any potential confounds due to cellular context. In addition, genes that affect dendritic morphogenesis may affect multiple tissues at multiple stages of development, a pleitropy that raises potential confounds when trying to directly link a gene to a dendritic phenotype. To avoid these potential problems, an ideal genetic system would also enable individual genes to be manipulated in a single postmitotic neuron without affecting the surrounding environment.

A powerful genetic system that enables both dendritic morphology to be examined *in vivo* and cell-autonomous manipulation of individual genes is the *Drosophila* embryonic and larval PNS. In this system, each abdominal hemisegment contains 44 PNS sensory neurons, which include external sensory (ES), chordotonal (CH), and multidendritic (MD) neurons and are grouped into dorsal, lateral, and ventral clusters (Bodmer and Jan, 1987). Of the MD neurons, most are classified as dendritic arborization (DA) neurons, which elaborate extensive dendritic trees in a two-dimensional manner just under the epidermis (Bodmer and Jan, 1987). Expression of

green fluorescent protein (GFP) using neuronal subtype-specific Gal4 lines allows easy visualization of dendritic morphology in living embryos or larvae (Gao et al., 1999; 2000). In recent years, this system has been used to dissect the molecular pathways that control different aspects of dendritic morphogenesis. Enhancer trap lines have also been used to identify genes with DA neuron-specific expression patterns (e.g., Emoto et al., 2004; Sugimura et al., 2004). In addition, forward genetic screens in this and other assay systems in *Drosophila* have identified a number of molecular players in dendritic morphogenesis (e.g., Gao et al., 1999, Li and Gao, 2003; Medina et al., 2006; Parrish et al., 2006; Reuter et al., 2003; Zhu et al., 2005).

In experiments presented in this thesis, I used the *Drosophila* PNS system to explore the function of newly identified genes that affect dendritic morphogenesis. Following gene identification, a number of questions remain to be answered, including a gene's specific roles in axonal and dendritic growth. In addition, as a gene may act at different developmental stages and in different cell types, it is important to assess cell-autonomous roles and determine neuronal subtype-specific phenotypes. Furthermore, identifying interacting genes or signaling pathways leads to mechanistic insight.

In Chapter Two, I will first describe the generation of single-cell clones allowing wild-type DA neuron dendritic morphologies to be described in detail. This system was first used to address the cell-autonomous functions of Flamingo, which was previously found to affect dendritic extension (Gao et al., 1999; Gao et al., 2000), but cell-cell interaction motifs and Flamingo expression in both DA neurons and adjacent cells suggested that it could have intrinsic and/or extrinsic roles. In collaboration with colleagues, I show that Flamingo has a cell-autonomous role in DA neurons in limiting

dendritic extension and in regulating axonal extension and guidance.

MARCM clones were also used to examine the role of Shrub in dendritic branching, as described in Chapter Three. Shrub is expressed ubiquitously, again raising the possibility of cell-autonomous and non-autonomous effects. Single-cell *shrub* mutant clones showed ectopic dendritic and axonal branching. Further experiments supported a role for Shrub in the endosomal pathway, consistent with previous studies of its yeast ortholog, Snf7. Mouse orthologs of Shrub were also found to be functionally conserved, as they could rescue *shrub* mutant phenotypes in *Drosophila.*

A final set of experiments described in Chapter Four addresses the cell-autonomous roles of the Notch/Delta signaling pathway in dendritic morphogenesis. Notch upregulation was found to contribute to dendritic phenotypes in *shrub* mutants and cell-autonomous functions for Notch and Delta in promoting dendritic branching are described.

Chapter Two:

Genetic Manipulation of Single Neurons *in Vivo* Reveals Specific Roles of Flamingo in Neuronal Morphogenesis

Summary

To study the roles of intracellular factors in neuronal morphogenesis, we used the mosaic analysis with a repressible cell marker (MARCM) technique to visualize identifiable single multiple dendritic (MD) neurons in living *Drosophila* larvae. We found that individual neurons in the peripheral nervous system (PNS) developed clear morphological polarity and diverse dendritic branching patterns in larval stages. Each MD neuron in the same dorsal cluster developed a unique dendritic field, suggesting that they have specific physiological functions. Single-neuron analysis revealed that Flamingo did not affect the general dendritic branching patterns in postmitotic neurons. Instead, Flamingo limited the extension of one or more dorsal dendrites without grossly affecting lateral branches. In addition, Flamingo is required cell autonomously to promote axonal growth and to prevent premature axonal branching of PNS neurons. These results demonstrate that Flamingo plays a role in early neuronal differentiation and exerts specific effects on dendrites and axons.

Introduction

Neuronal morphogenesis is a critical step in neural development. Many neurons elaborate highly branched dendritic trees that can make thousands of synaptic connections with other neurons (Ramón y Cajal, 1911). The proper formation of dendritic fields and axonal arborizations is crucially important for the assembly of a functional nervous system (Masland, 2001). However, it remains unclear how the morphologies of different neurons are specified during development and to what extent this process is controlled by intrinsic factors or environmental cues.

The formation of dendritic fields is mainly affected by the extent and the direction of dendritic outgrowth and branching. The mechanisms controlling dendrite development have been studied with neuronal cell cultures (reviewed in Craig and Banker, 1994; Higgins et al., 1997; Bradke and Dotti, 2000). In recent years, various *in vivo* approaches have been taken to study neuronal morphology. For instance, different versions of green fluorescent protein (GFP) were used to label a small number of neurons in worms and flies (Roayaie et al., 1998; Lee and Luo, 1999; Gao et al., 1999). Local dye superfusion or virus-mediated GFP expression allowed the visualization of neurons in cultured hippocampal slices (Engert and Bonhoeffer, 1999; Maletic-Savatic et al., 1999). In another approach, transgenic mice were created in which red, green, yellow, or cyan fluorescent proteins were selectively expressed in a small subset of central nervous system (CNS) neurons (Feng et al., 2000). More recently, single-cell electroporation enabled ectopic gene expression in the brain of *Xenopus* tadpoles or rat hippocampal slices (Haas et al., 2001). These advances have greatly enhanced our ability to study

neuronal morphogenesis *in vivo* at the molecular level.

Both *in vitro* and *in vivo* approaches have revealed a number of key molecules that regulate dendritic and axonal outgrowth and branching (reviewed in Brose and Tessier-Lavigne, 2000; Jontes and Smith, 2000; Matus, 2000; Wong and Wong, 2000; McAllister, 2000; Whitford et al., 2002; Scott and Luo, 2001; Jan and Jan, 2001). For instance, neurotrophins and their receptors are important in controlling axonal growth (reviewed in Reichardt and Farinas, 1997) and in regulating dendritic morphology (McAllister et al., 1995; Lom and Cohen-Cory, 1999; Xu et al., 2000). Semaphorin 3A and Slit1, both of which are involved in axon guidance, also regulate the development of cortical dendrites (Polleux et al., 2000; Whitford et al., 2002). In *Xenopus*, the glycosylphosphatidyl-inositol (GPI)-linked molecule CPG15 promotes both dendritic growth and axonal arborization *in vivo* (Nedivi et al., 1998; Cantallops et al., 2000). Despite the recent progress, the molecular understanding of the intracellular machinery that controls the formation of specific neuronal morphology remains far from complete. For instance, it is not known how dendritic extension and branching are coordinated, nor is the differential regulation of dendritic and axonal development understood.

To study these issues, we used the peripheral nervous system (PNS) of *Drosophila* embryos as a model system in which GFP was expressed in multiple dendritic (MD) neurons to visualize dendritic outgrowth and branching (Gao et al., 1999). The easy visualization of these dendrites *in vivo* and their relatively discrete developmental phases made it feasible to carry out genetic screens to identify molecules that control distinct aspects of dendritic morphogenesis. This approach led to the identification of the *flamingo* mutations that result in the overextension of MD neuron dorsal dendrites (Gao

et al., 1999, 2000). The *flamingo* gene, which encodes a G protein-coupled receptor-like protein, also controls planar cell polarity in conjunction with *frizzled* (Usui et al., 1999; Chae et al., 1999; Lu et al., 1999). In mutant embryos, the activity of *flamingo* is altered not only in MD neurons but also in adjacent epithelial cells (Usui et al., 1999; Gao et al., 2000). In addition, Flamingo affects spindle orientation in adult sensory organ precursor cells (Lu et al., 1999). Therefore, it is not clear how Flamingo controls the formation of dendritic fields directly in postmitotic neurons and to what extent Flamingo functions cell-autonomously in this process.

To further understand the roles of Flamingo and other intrinsic factors in neuronal morphogenesis, we labeled single wild-type or mutant MD neurons with GFP in living *Drosophila* larvae using the mosaic analysis with a repressible cell marker (MARCM) technique (Lee and Luo, 1999). Here, we describe an assay system that allows the dendritic morphology of single identifiable MD neurons in the dorsal cluster to be studied *in vivo*. We show that individual PNS sensory neurons, unlike CNS neurons, develop clear morphological polarity and highly diverse dendritic branching patterns. Although located in the same dorsal cluster, individual MD neurons develop highly unique dendritic fields. This finding suggests that intrinsic properties of each MD neuron are important in controlling the development of its unique dendritic field and that each MD neuron fulfills a specific physiological function. Furthermore, our genetic analysis with single-neuron resolution reveals that Flamingo directly controls dendritic fields of different dorsal cluster MD neurons in a cell-autonomous fashion. Surprisingly, Flamingo does not affect the dendritic branching patterns in a global way; instead, it only limits the extension of one or more processes toward the dorsal midline without grossly

affecting the extension of lateral branches. Flamingo also has a cell-autonomous function in promoting axonal elongation and preventing premature axonal branching of PNS sensory neurons. Altogether, these studies demonstrate that Flamingo controls several aspects of neuronal morphogenesis and exerts differential effects on initial dendritic and axonal growth.

Results

GFP Labeling of Single PNS Sensory Neurons in Living *Drosophila* Larvae

Each abdominal hemisegment of *Drosophila* embryos and larvae contains 44 peripheral neurons that can be grouped into dorsal, lateral, and ventral clusters (Campos-Ortega and Hartenstein, 1985; Ghysen et al., 1986; reviewed in Jan and Jan, 1993) (Figure 2-1A). Our studies primarily focus on the dorsal cluster, which contains four external sensory (ES) neurons and eight MD neurons that can be further classified into three groups: one bipolar dendrite (BD) neuron, six dendritic arborization (DA) neurons, and one internal sensory neuron whose dendrites include a spring-like structure that contacts motorneuron axon terminals (Figure 2-1B). Gal4 line *109(2) 80* labels all the eight MD neurons but not the four ES neurons in the dorsal cluster (Gao et al., 1999).

To label single MD neurons in *Drosophila* larval PNS with GFP, we used the MARCM technique (Lee and Luo, 1999). This technique allows the labeling of a clone of cells by GFP due to the loss of the Gal80 repressor via FLP recombinase-mediated mitotic recombination in precursor cells. With the UAS-Gal4-targeted expression system (Brand and Perrimon, 1993), all of the larval PNS sensory neurons could be labeled by mCD8–GFP under the control of $Gal4^{C155}$, which allows marker expression in all postmitotic neurons (Lin and Goodman, 1994) (Figure 2-1C). mCD8–GFP was targeted to the cell membrane; therefore, the cell body of each sensory neuron in each dorsal cluster could be easily identified in larval stages. In contrast, CNS neurons were tightly packed together and could not be distinguished individually (Figure 2-1C). When Gal80 was ubiquitously expressed under the control of the *Drosophila* tubulin promoter,

mCD8–GFP expression was suppressed in all PNS sensory neurons (Figure 2-1D). Since MD neuron precursor cells divide 5–7 hr after egg laying (AEL), we heat-shocked embryos 4–6 hr AEL to induce FLP recombinase expression and then examined larvae for the presence of single-neuron clones. We found that about 10% of the larvae contained a single PNS sensory neuron labeled by mCD8–GFP in one of the dorsal clusters (Figure 2-1E). At a much lower frequency, we could find larvae in which two neurons were labeled by mCD8–GFP in the same dorsal cluster.

Morphological Diversity of PNS Sensory Neurons

With the MARCM-based single-neuron assay system, recombination events occur in a random fashion at low frequency. As there are only 12 PNS sensory neurons in each dorsal cluster, it is possible to find larvae in which only one of the 12 neurons is labeled by mCD8–GFP. Indeed, we obtained images of the dendritic branching patterns of each subtype of PNS neurons in the dorsal cluster, as well as images of other PNS sensory neurons in the lateral and ventral clusters. Since our genetic studies mainly focus on the dorsal cluster, only the development of dendritic fields of dorsal cluster MD neurons is described here in detail.

We found that, even in the relatively simple *Drosophila* nervous system, different neurons developed strikingly diverse dendritic morphologies. *Drosophila* CNS neurons are unipolar cells similar to those in other insects (Shankland and Goodman, 1982). The CNS neuron in Figure 2-2A sends its axon across the ventral midline and elaborates neuronal processes in a three-dimensional manner that makes it difficult to reconstruct the neuron's morphology. This complex morphology also prevents clear differentiation

of its dendritic and axonal processes. In contrast, the morphological polarity of PNS sensory neurons is much easier to define. For example, each ES neuron extends a single dendrite without further branching in the direction opposite to that of its axon (Figure 2-2B). Dorsal cluster BD (dbd) neurons extend two unbranched dendrites along the anterior–posterior axis and an axon ventrally toward the CNS (Figure 2-2C). Most MD neurons develop highly diverse dendritic branching patterns (Figure 2-2D) and share morphological similarity with dendrites of mammalian CNS neurons, such as the tapering of dendrites with further branching and extension (Craig and Banker, 1994). The dendritic complexity of some MD neurons is also comparable to that of many mammalian CNS neurons (Ramón y Cajal, 1995).

Some MD neurons (Figure 2-2D) have processes similar to the "headless" spines on many developing mammalian neurons (Peters and Kaiserman-Abramof, 1970). These processes are typically 5–10 μm long in third instar larvae, extend to both sides of the dendritic branches, and are more numerous on dendrites distal to the cell body. Though the physiological function of these processes in *Drosophila* is unclear, further studies with single-neuron resolution might enhance our understanding of the formation and the maintenance of these fine structures *in vivo*.

Development and Organization of MD Neuron Dendritic Fields in the Dorsal Cluster

Most MD neurons in the dorsal cluster, including the BD neuron and the six DA neurons, elaborate their dendrites underneath the epidermis. These neurons probably function as touch receptors or proprioceptors (Bodmer and Jan, 1987). Labeling single PNS neurons

in living larvae allowed us to study how the dendritic fields of different MD neurons are formed and organized in the same dorsal cluster, although their cell bodies are close to each other.

Our single-neuron analysis also reveals that each MD neuron has a defined dendritic field. Among larvae at the same stage, the general branching pattern for a particular MD neuron remains the same. For instance, the ddaC neuron sends its primary dendrite dorsally; this dendrite soon branches into secondary and tertiary branches that cover the whole hemisegment from the anterior segment boundary to the posterior segment boundary (Figure 2-3A) and from the dorsal midline to the lateral cluster of PNS neurons (data not shown). The ddaC neuron also extends many smaller dendritic processes more or less parallel to the dorsal midline. Interestingly, these dendritic processes from the same ddaC neuron never overlap (Figure 2-3A), suggesting a "self-avoidance" mechanism, as previously described for axonal branches of a single mechanosensory neuron in leeches (Kramer et al., 1985; Kramer and Stent, 1985; Wang and Macagno, 1998). Similar to the ddaC neuron, the ddaD neuron in the dorsal cluster sends dendrites covering the area between segment boundaries (Figure 2-3B). However, it only sends out four or five major branches to cover the area between the dorsal midline and its cell body, with fewer smaller branches. Some terminal branches of the ddaD neuron appear to cross the segment boundaries (Figure 2-3B). Unlike the ddaC and ddaD neurons, the four other DA neurons in the dorsal cluster have more restricted dendritic fields. The ddaF and ddaE neurons send out only a few branches toward either the anterior or the posterior segment boundaries with their most dorsal dendritic branches falling short of the dorsal midline. Strikingly, unlike other MD neurons, none of the

dendritic branches of the ddaF and ddaE neurons have any spine-like processes (Figures 2-3C and 2-3D). The ddaB neuron has one or two dendritic branches that reach the dorsal midline, and a few branches that extend toward the anterior segment boundary (Figure 2-3E). The ddaA neuron is the most lateral MD neuron in the dorsal cluster and extends its dendrites mainly along the anteroposterior axis (Figure 2-3F). The dendritic fields of the ddaC and ddaD neurons overlap with each other and with the dendritic fields of four other MD neurons. However, the dendritic fields of ddaE and ddaF neurons have minimal overlap. The presence of different dendritic fields in the same dorsal cluster raises the possibility that each MD neuron has a defined physiological function and that the dendritic morphology of each MD neuron is largely determined by its intrinsic properties.

Flamingo Has a Cell-Autonomous Function in Postmitotic Neurons to Control the Extension of Dorsal Dendrites of MD Neurons

Previous studies have identified Flamingo as a regulator of dendritic growth (Gao et al., 1999, 2000) and of the spindle orientation in sensory organ precursor (SOP) cells (Lu et al., 1999). To address whether Flamingo has a direct role in controlling neuronal morphogenesis in postmitotic neurons and to assess the cell-autonomous function of Flamingo, we generated single neuron mutant clones homozygous for the *flamingo*^{E59} (Usui et al., 1999) and *flamingo*^{72} (Gao et al., 1999) alleles in wild-type larvae.

When dorsal cluster MD neurons were devoid of *flamingo* gene activity, one or more dendritic processes overextended toward the dorsal midline in about 15% of more than 100 *flamingo*^{E59} mutant neurons (Figures 2-4A–C) and in about 9% of 80 *flamingo*^{72}

mutant neurons (Fig. 4D). Surprisingly, the basic architecture of the dendritic branching patterns was not obviously altered. For instance, ddaC neuron still extended a primary dendrite dorsally, which branched into several secondary and tertiary dendrites (Figure 2-4A). In addition, the ddaF or ddaE neuron still sent out lateral branches normally toward either the anterior or posterior segment boundaries (Figures 2-4B–D). The total length of the lateral branches of ddaF or ddaE neurons and the dendritic fields covered by these branches also appeared to be normal. For instance, the average total length of the lateral branches of wild-type ddaE neurons is 1.2 ± 0.2 μm (n = 10), which is the same as that of *flamingo*^{EC59} mutant ddaE neurons (1.3 ± 0.2 μm, n = 4). In some cases, two *flamingo*^{EC59} mutant MD neurons in opposite dorsal clusters were simultaneously labeled by mCD8–GFP, and their overextended dorsal dendrites crossed the dorsal midline and invaded the dendritic field of another MD neuron in the opposite hemisegment (data not shown). These data demonstrate that Flamingo does not control the general dendritic branching patterns of MD neurons. Instead, Flamingo has a cell-autonomous function in limiting the extension of dorsal dendrites with little or no effect on lateral branches. These studies also demonstrate that Flamingo plays a direct role in dendritic morphogenesis in postmitotic neurons, which is independent of its function in precursor cells.

Cell-Autonomous Function of Flamingo in Axonal Growth and Guidance

Flamingo is expressed on both dendrites and axons of MD neurons (Gao et al., 2000), suggesting that Flamingo may also regulate axonal morphogenesis. To investigate whether the *flamingo* mutations that affect dendritic initiation and extension also affect

axon development, we examined the axons of single MD neurons containing *flamingo*^{E59} mutations in wild-type larvae. In 10% of more than 100 *flamingo*^{E59} mutant neurons, their axons did not fully extend to the CNS (Figure 2-5A). This finding was consistent with the axonal phenotype in living *flamingo*^{E59} mutant embryos, in which axonal break points could be found in the axon bundles of dorsal cluster MD neurons (Figures 2-5B and 2-5C). In addition, the axons of PNS neurons failed to fasciculate as tightly as those of wild-type embryos (Figure 2-5B). Axonal breaks were previously found in the CNS of *flamingo*^{E59} mutant embryos (Usui et al., 1999). Interestingly, 70% of the mutant axons that failed to fully extend also branched at their termini (e.g., the ddaF neuron in Figure 2-5D), while wild-type PNS axons never branched before reaching the CNS. In some cases, a thin process derived from the axon extended dorsally (Figure 2-5A). Similar axonal phenotypes were found in *flamingo*^{72} mutant single-neuron clones (Figure 2-4D). These studies demonstrate that Flamingo has a cell-autonomous function in promoting axonal elongation and in preventing premature branching of axons before reaching their synaptic targets.

Next, we asked whether Flamingo also affects axon guidance. We found that the axons of some *flamingo* mutant ES neurons veered dramatically from the normal path before halting in ectopic locations (Figure 2-5E). Similar pathfinding defects were also found for axons of MD neurons. These findings suggest that Flamingo has a cell-autonomous function in controlling axon guidance either directly or indirectly.

Discussion

To study how neuronal morphogenesis is controlled by intracellular factors during development, we used the MARCM technique (Lee and Luo, 1999) to visualize single wild-type or mutant PNS neurons in living *Drosophila* larvae. We found that dendritic fields of MD neurons in the dorsal cluster are highly organized. Individual MD neurons have their own specific, well-defined dendritic fields. Genetic manipulation in single neurons revealed that Flamingo controls the formation of MD neuron dendritic fields by limiting the extension of one or more dorsally oriented branches with minimal effects on lateral branches. In addition, Flamingo is required cell autonomously for promoting axonal growth and for preventing premature axonal branching *in vivo*.

An Assay System to Study Intrinsic Mechanisms Controlling Neuronal Morphogenesis in Living *Drosophila* Larvae

Many genes function in several biological processes at multiple developmental stages. Consequently, mutations in these genes often cause pleiotropic developmental defects. An ideal approach for studying the roles of intrinsic factors in neuronal morphogenesis would be to manipulate gene activity in a single postmitotic neuron *in vivo* without disturbing the surrounding environment. Therefore, pleiotropic effects of the gene could be eliminated. Taking advantage of the MARCM technique (Lee and Luo, 1999), we were able to study the dendritic and axonal growth of single identifiable MD neurons in living *Drosophila* larvae (Figure 2-1).

MD neurons are an excellent model system because the mechanisms that control their generation have been well studied (Bodmer et al., 1989; Brewster and Bodmer,

1995; Vervoort et al., 1997; Orgogozo et al., 2001; reviewed in Jan and Jan, 2000). Some MD neurons share a common precursor cell and therefore belong to "solo" MD lineages that do not produce other cell types (Bodmer et al., 1989; Brewster and Bodmer, 1995). Other dorsal cluster MD neurons are generated from MD–ES lineages that also give rise to ES neurons and support cells in ES organs (Brewster and Bodmer, 1995); however, the exact order of cell division in MD–ES lineages remains controversial (Vervoort et al., 1997; Orgogozo et al., 2001). If the FLP recombinase-mediated recombination occurs before the formation of the MD neuron precursor cell, then two MD neurons or the MD neuron and the ES neuron in the same lineage will be labeled by GFP. Therefore, the presence of a single mCD8–GFP-labeled MD neuron itself indicates that the somatic recombination occurs during the last cell division that gives rise to the MD neuron. Since most MD neurons except BD neurons are not associated with support cells (Brewster and Bodmer, 1995; Vervoort et al., 1997; Orgogozo et al., 2001), the mCD8–GFP-labeled MD neuron will be the only mutant cell, whereas other cells in the lineage and other neurons in the same cluster remain wild type. If both an MD neuron and an ES neuron are labeled by GFP, it may indicate that the two neurons are derived from the same cell lineage. For instance, our study indicates that ddaF neuron is generated from the MD–ES lineage (Figure 2-4).

Using this assay system to study neuronal morphogenesis with single-neuron resolution offers several advantages. First, each dorsal cluster contains only a few neurons, which elaborate their dendrites in a relatively two-dimensional plane. We can study dendritic and axonal growth of the same identifiable MD neuron *in vivo* and compare wild-type and mutant neurons with ease and precision. Second, we can

continuously image the dendrites or the spine-like processes of a single wild-type or mutant MD neuron in a living animal over a period of several days. Third, since the FRT-mediated somatic recombination can occur during the last cell division that gives rise to the MD neuron, the cell-autonomous function of a gene in dendritic morphogenesis and axonal growth can be demonstrated independently of effects the gene may have on the proliferation or cell fate of neuronal precursor cells (Lee and Luo, 1999). Such a single-neuron assay system could be used to identify and characterize intracellular factors that affect neuronal morphogenesis. One potential drawback is the perdurance of wild-type protein and mRNA in the GFP-labeled mutant single neurons, which may mask the mutant phenotype during early stages of neuronal differentiation for some genes. This is probably why a low percentage of *flamingo* mutant single neurons show either dendritic or axonal defects.

How Are the Dendritic Fields of Different MD Neurons Specified during Development?

Individual MD neurons in the dorsal cluster have specific and distinct dendritic fields. The dendrites of the ddaC neuron cover the whole area of the hemisegment, whereas other MD neurons have their own unique territories. This finding suggests that each MD neuron has a specific physiological function in the *Drosophila* PNS, as in the vertebrate retina where different cell types with unique shapes represent distinct physiological entities (Masland, 2001). Indeed, Pickpocket, a *Drosophila* protein homologous to vertebrate epithelial Na^+ channel molecules, is only expressed in one MD neuron in the dorsal cluster (Adams et al., 1998). It is reasonable to speculate that other unidentified

channel molecules may be specifically expressed in different MD neurons to carry out certain sensory functions. In addition, the axons of different MD neurons project into different regions of the CNS, indicating different functions of MD neurons in neuronal circuitry (Schrader and Merritt, 2000).

How are the dendritic fields of MD neurons in *Drosophila* PNS specified during development? A laser ablation study in *Drosophila* suggested that one subtype of MD neurons had no effect on the formation of dendritic field of other MD neurons in the same dorsal cluster (Gao et al., 2000). In addition, competition between dendrites of homologous neurons near the dorsal midline plays a role in defining their dendritic fields (Gao et al., 2000). However, the competition mechanism probably functions as a means to fine tune the mature dendritic territory as occurs in the retina, where adjacent ganglion cell dendrites compete to define their territories (Perry and Linden, 1982). The close clustering of the MD neuron cell bodies in the same area suggests that intrinsic properties of each MD neuron may play major roles in determining the size and location of its dendritic field.

Specific Function of Flamingo in Controlling Dendritic Fields

In studies of neuronal morphogenesis, it is important to differentiate the direct and indirect effects of the gene of interest. Similar to other important regulators, Flamingo functions in different cell types and at different developmental stages (Usui et al., 1999; Chae et al., 1999; Lu et al., 1999; Gao et al., 2000). Our studies here provide evidence that Flamingo has a direct role in controlling dorsal dendritic growth in postmitotic neurons.

Although individual MD neurons in the dorsal cluster differ greatly in their dendritic fields, the defects caused by *flamingo* mutations appear to be similar: mostly one process of the mutant neurons overextends toward the dorsal midline. Surprisingly, the general dendritic architecture of these MD neurons is not affected dramatically (Figure 2-4). In addition, our findings suggest that Flamingo is not a cell type-specific regulator of dendritic morphology, nor does it affect dendritic branching patterns in a global way. It seems that Flamingo functions cell autonomously in controlling dendritic fields of different MD neurons by limiting the overextension of their dorsal dendrites. On the contrary, other mutants identified from the genetic screen (Gao et al., 1999), such as *tumbleweed*, appear to affect both dorsal and lateral dendrites in a more general way. Our studies also demonstrate that Flamingo function in neuronal morphogenesis is independent of its function in precursor cells.

How does Flamingo mainly control dorsal dendrite extension in postmitotic neurons? In a previous study, we found that neuronal morphogenesis of dorsal cluster MD neurons can be separated into relatively discrete developmental phases. These neurons always extend their axons first toward the ventral nerve cord. The extension of dorsal dendrites toward the dorsal midline ceases at 16–17 h AEL, before lateral dendrites extend toward the adjacent segment boundaries (Gao et al., 1999). If different development phases are controlled by different mechanisms, Flamingo may function mainly during dorsal dendrite extension. Indeed, Flamingo prevents precocious initiation of dorsal dendrites that contributes to the longer dorsal dendrites before 16 h AEL in *flamingo* mutant embryos (experiment performed by Fen-Biao Gao, Sweeney et al., 2000). The failure to stop after 17 AEL also contributes to the longer dorsal dendrites in

flamingo mutant embryos (Gao et al., 2000). Accordingly, the level of *flamingo* mRNA expression decreases during late embryogenesis (Chae et al., 1999), and Flamingo expression also decreases in the first instar larvae (data not shown). Flamingo likely acts during early neuronal differentiation to control the initiation and extension of dorsal dendrites.

Experiments on mouse Flamingo ortholog Celsr2 suggest that in mammals Flamingo may at later developmental stages to maintain dendritic arbors (Shima et al., 2004). In these experiments gene knockdown was performed by biolistic transfection of siRNA plasmids. Transfection was performed after dendritic trees were already significantly developed, and decreased branching was attributed to dendritic retraction. Whether one of the several mouse Flamingo orthologs also plays early developmental roles or whether Flamingo may play additional roles in *Drosophila* remains to be seen.

Flamingo Also Functions Cell Autonomously in Controlling Axonal Development

GFP labeling of single mutant neurons provides an opportunity to study whether genes that control dendrite development also affect other aspects of neuronal morphogenesis, such as axon growth. We found that Flamingo is required cell autonomously for promoting axonal growth. Since axons extend several hours earlier than dendrites, it is possible that the perdurance of Flamingo prevents the appearance of axonal phenotypes in some mutant neurons. Indeed, more *flamingo* mutant neurons exhibited dendritic defects than axonal defects. Two studies of axonal targeting on Drosophila photoreceptors found that Flamingo is involved in competitive interactions between adjacent growth cones in forming correct targets, although mutant axons still reached the

target tissue and fasciculation was not affected (Lee et al., 2003; Senti et al., 2003). Since only the initial segment of the MD neuron axon could be imaged in our experiments, it is possible that target formation in the CNS was similarly affected.

Since Flamingo has been shown to be involved in planar cell polarity in Drosophila wing and eye (Usui et al., 1999), as well as in mammalian tissues (Curtin et al., 2003), it is interesting to consider whether Flamingo may affect the polarity of MD neurons. Although MD neuron polarity has not been investigated in detail, the neurons show morphological polarity with dendrites extending toward the dorsal midline and branching extensively and axons extending ventrally without branching before reaching the CNS. In addition, *Drosophila* microtubule motor proteins that are plus- and minus-end directed are selectively sorted into axons and dendrites, respectively, which is consistent with microtubule polarity in mammalian neurons (Clark et al., 1997). In single-neuron *flamingo* clones, we found several changes in morphology and growth that suggest changes in polarity including early dendrite initiation, extensively branched axons extending toward the dorsal midline, and long unbranched dendrites. Another study on Flamingo function in the Drosophila CNS found that some overextended dendrites fail to stain for dendrite marker Nod, suggesting a change in polarity (Reuter et al., 2003). On the other hand, other molecules that regulate planar cell polarity in the Drosophila eye, such as Frizzled and Dishevelled do not affect photoreceptor axon targeting as Flamingo does (Senti et al., 2003) and *frizzled* does not genetically interact with *flamingo* (Gao et al., 2000). Even so, the role of neuronal polarity in explaining Flamingo dendritic phenotypes deserves further consideration.

Different molecules downstream of Flamingo might mediate its differential

functions in dendrites and axons; alternatively, the same downstream molecules could transduce different signals in the two compartments (e.g., through the cyclic nucleotide pathway; Song et al., 1998; Polleux et al., 2000). Further dissection of the Flamingo pathway will help to elucidate how dendritic initiation and axonal growth are coordinated during development. Since Flamingo is highly conserved from flies to humans (Usui et al., 1999; Chae et al., 1999), it is likely that Flamingo also plays an essential role in controlling neuronal morphogenesis in mammals.

Figures

Figure 2-1. GFP labeling of single neurons in *Drosophila* larvae

(A) 22C10 antibody staining of PNS sensory neurons in a wild-type stage 16 embryo. D, dorsal cluster; L, lateral cluster; V, ventral cluster. (B) Schematic representation of all 12 neurons in each dorsal cluster of abdominal hemisegments. Ovals, dda neurons; black circles, des neurons; diamond, dbd neuron; square, the internal sensory neuron whose dendrites contact motorneuron axons. The six dda neurons are ddaA, ddaB, ddaC, ddaD, ddaE, and ddaF. (C) Labeling of all the PNS and CNS neurons with mCD8–GFP. Bracket indicates all the 12 PNS sensory neurons in the dorsal cluster. Arrow indicates the CNS. Only a few segments are shown here. (D) Suppression of mCD8–GFP expression by the *tubP-Gal80* transgene. (E) mCD8–GFP labeling of a single dorsal cluster neuron. Genotypes: (A) *GAL4*^{C155}, *UAS-mCD8-GFP, hs-FLP1/+*; *FRT*^{G13}*/Cyo*. (B, C) *GAL4*^{C155}, *UAS-mCD8-GFP, hs-FLP1/+*; *FRT*^{G13}*/ FRT*^{G13}, *tubP-GAL80*.

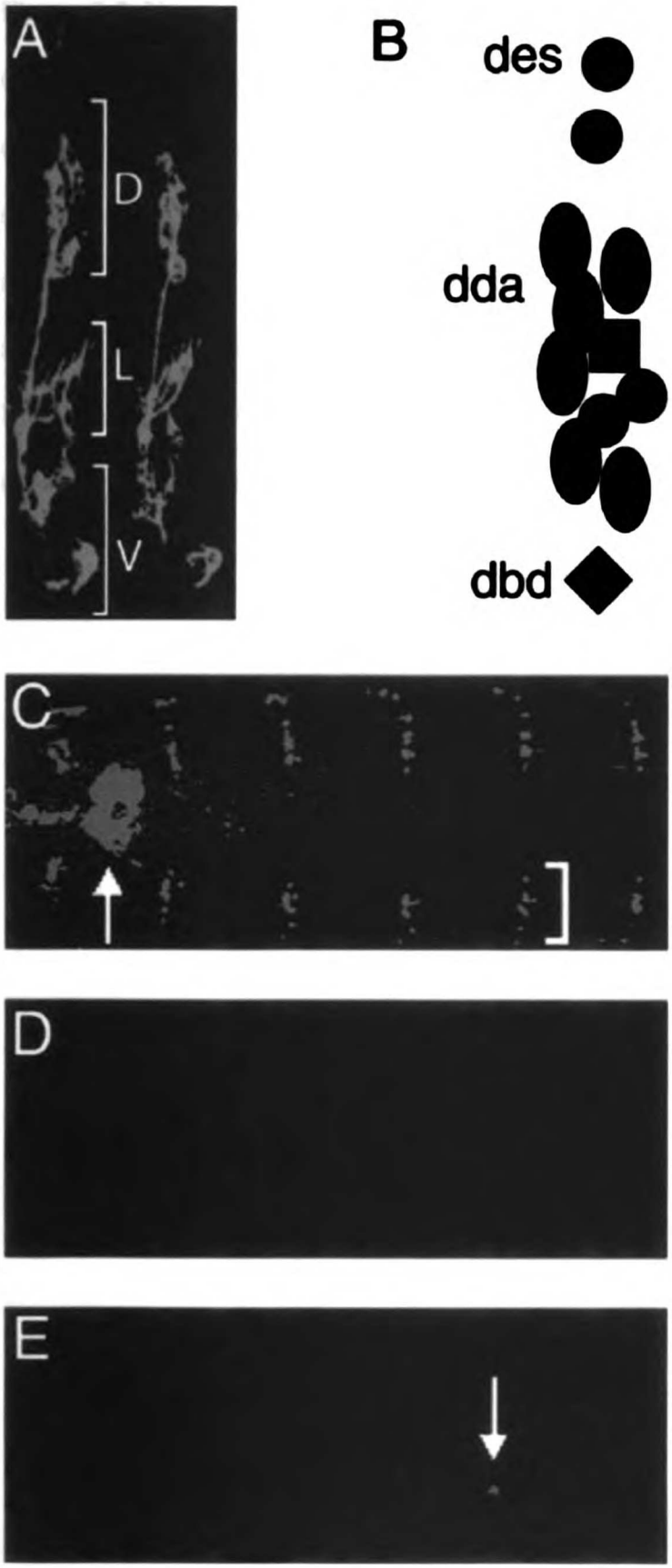

Figure 2-2. Neuronal polarity and diversity of neuronal morphology in *Drosophila*

(A) A CNS neuron sends its axon past the ventral midline (dotted line). Its neurites elaborate three-dimensionally in the CNS. (B) An ES neuron in a dorsal cluster has a single dendrite extending dorsally in the opposite direction of axon extension. (C) A BD neuron in a dorsal cluster with two unbranched dendrites running along the anterior–posterior axis. (D) An MD neuron with numerous spine-like protrusions in a lateral cluster. Arrows indicate the axons of mCD8–GFP-labeled neurons. The bar represents 10 μm for (A) and 40 μm for (B–D).

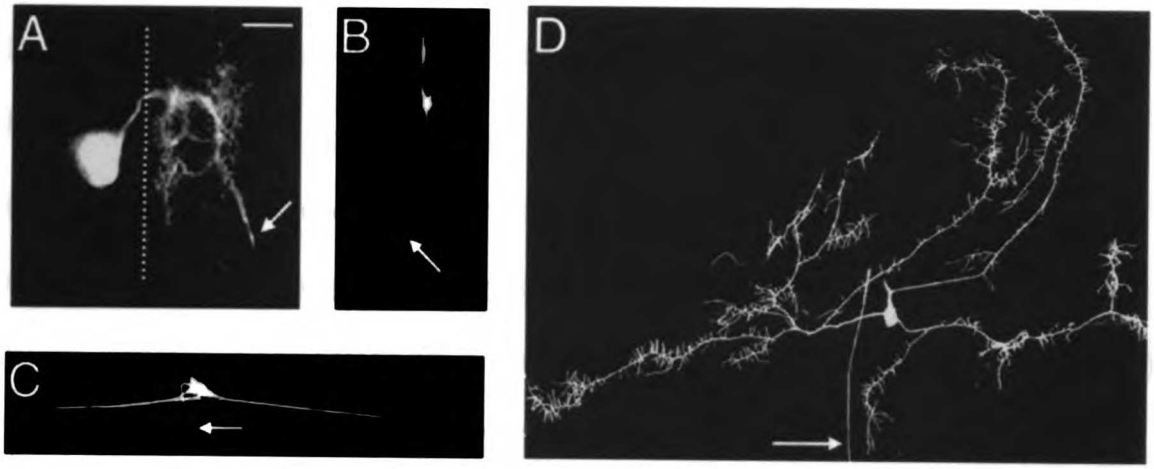

Figure 2-3. Dendritic fields of the six dda neurons in the dorsal cluster in wild-type larvae

(A) The ddaC neuron sends out dendrites that cover a large area from the anterior segment boundary to the posterior segment boundary and from the dorsal midline to the lateral cluster. (B) The ddaD neuron has fewer dendritic branches than ddaC neuron. (C) Dendrites of the ddaF neuron only cover the anterior half of the hemisegment. *Gal4*^{C155} also drives low-level expression of CD8–GFP in epithelial cells. Therefore, CD8–GFP-labeled single epithelial cells can be seen in some larvae (asterisk). The arrowhead indicates an ES neuron. (D) Dendrites of the ddaE neuron only cover the posterior half of the hemisegment. (E) The ddaB neuron extends dendrites to the anterior segment boundary and the dorsal midline. (F) The ddaA neuron extends dendrites along the anteroposterior axis and exhibits spine-like structures. Vertical black arrows show segment boundaries.

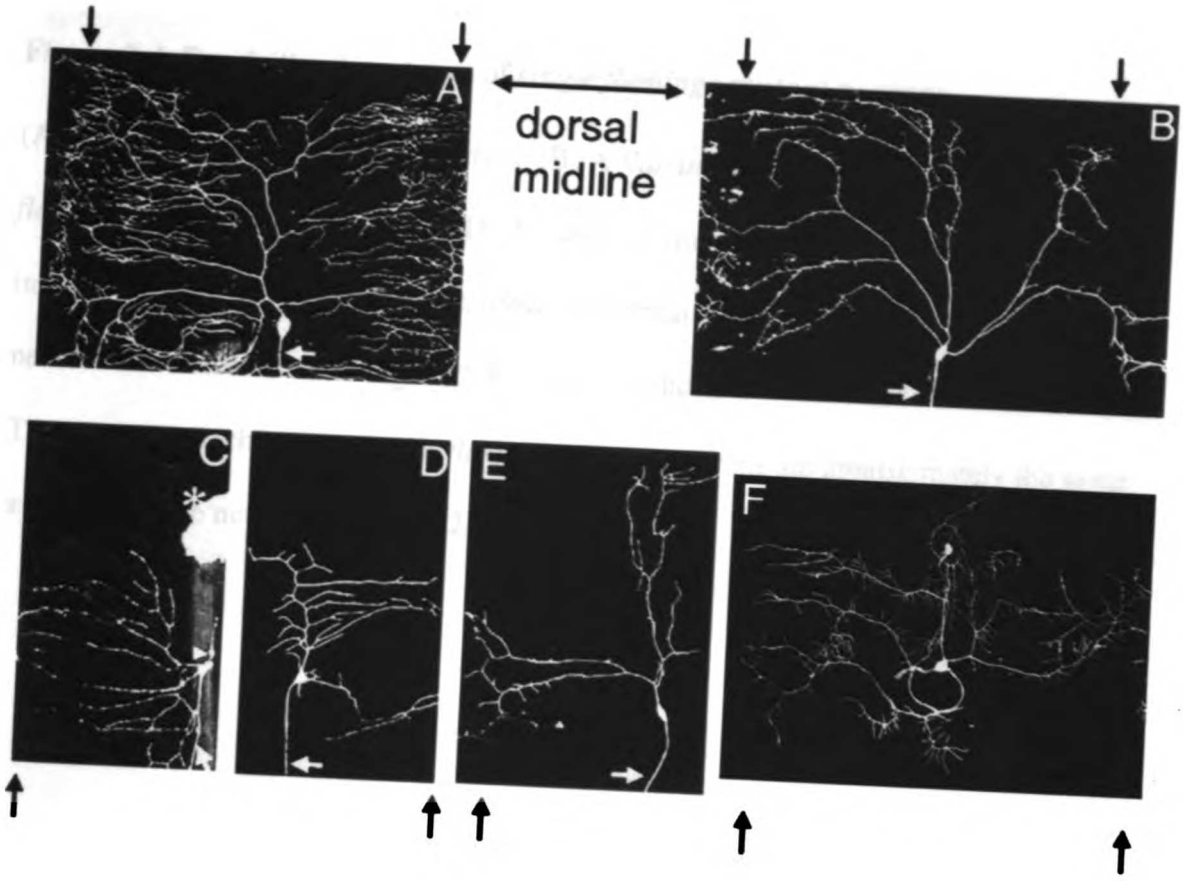

Figure 2-4. Dendritic phenotypes of single *flamingo* mutant neurons

(A) A *flamingo*^{E59} mutant ddaC neuron. (B) A *flamingo*^{E59} mutant ddaF neuron. (C) A *flamingo*^{E59} mutant ddaE neuron. (D) A *flamingo*^{72} mutant ddaE neuron. The arrowhead in (D) indicates the axon that fails to develop normally. The axonal phenotype of ddaE neuron is described later in Figure 2-5. Arrows indicate overextended dendritic branches. The general branching patterns of *flamingo* mutant neurons are approximately the same as the wild type neurons in Figure 2-3.

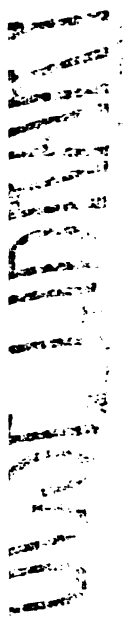

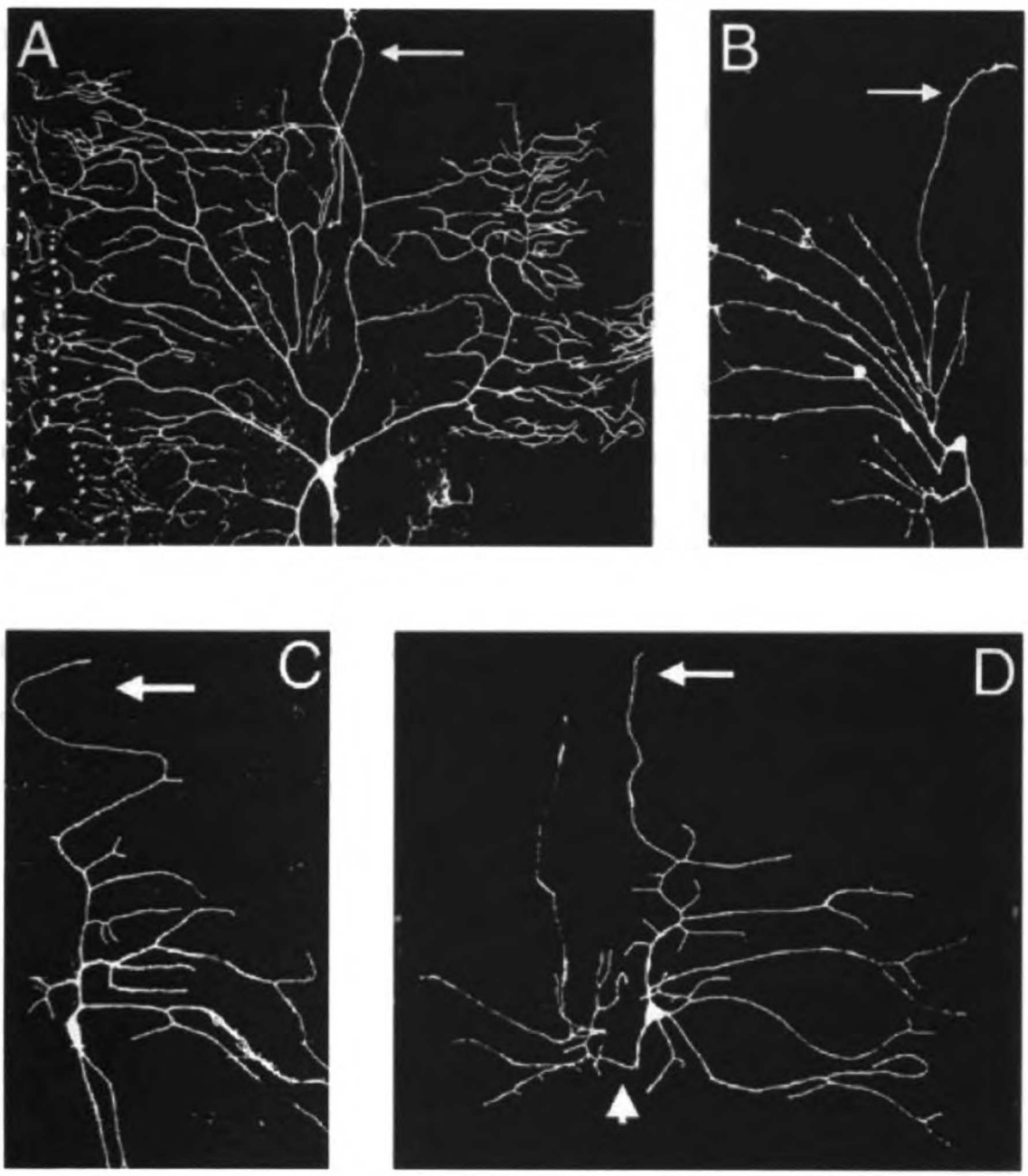

Figure 2-5. Axonal defects in *flamingo* mutant neurons

(A) A mCD8–GFP-labeled two-neuron *flamingo*^{E59} mutant clone in a dorsal cluster. Asterisk indicates the cell body of an ES neuron. The arrowhead indicates the cell body of the ddaF neuron. The arrow shows the axonal break point of the ddaF neuron. A thin process derived from the axon extends dorsally. (B) GFP-labeled dorsal cluster MD neurons in a living *flamingo* mutant embryo. Bracket indicates the cell bodies of MD neurons. Arrow indicates axonal break point of the axon from one dorsal cluster neuron. (C) An enlarged image of the area indicated by the arrow in (B). (D) A mCD8–GFP-labeled *flamingo*^{72} mutant ddaF neuron. Arrow indicates premature termination and branching of the axon. Arrowhead indicates the cell body. (E) A *flamingo*^{E59} mutant ES neuron in the dorsal cluster. Arrow indicates the axon that terminates at the wrong place. Asterisk indicates the cell body.

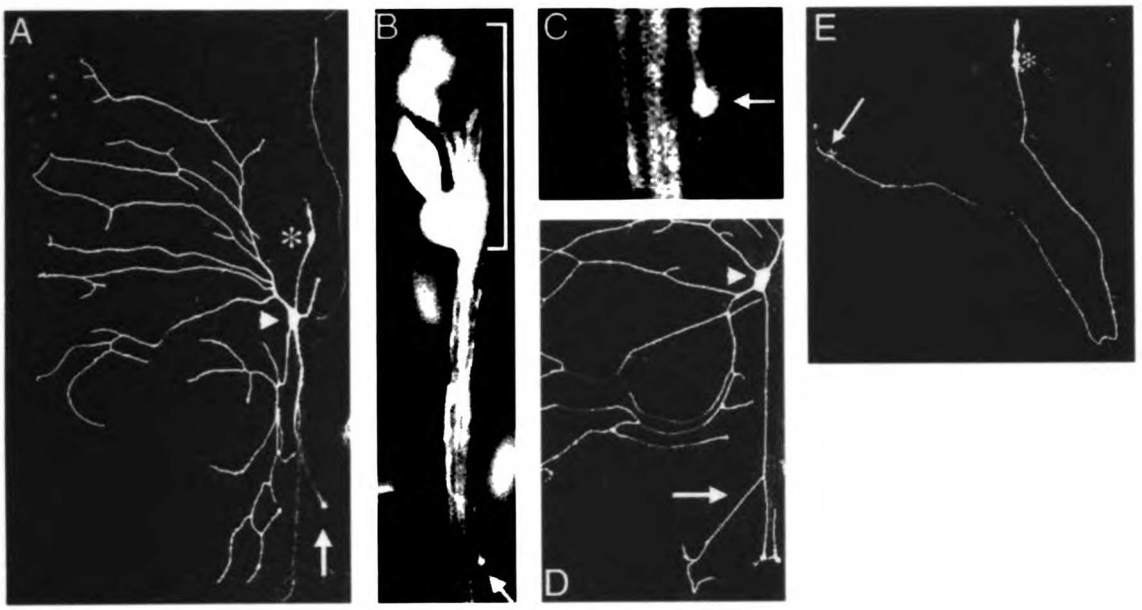
A
B
C
D
E

Chapter Three:

The Coiled-Coil Protein Shrub Controls Neuronal Morphogenesis in *Drosophila*

Summary

The diversity of neuronal cells, especially in the size and shape of their dendritic and axonal arborizations is a striking feature of the mature nervous system. Dendritic branching is a complex process, and the underlying signaling mechanisms remain to be further defined at the mechanistic level (Konur and Ghosh, 2005; Jan and Jan, 2003; Masland, 2004). Here we report the identification of mutations in the *shrub* gene that increased dendritic branching. Single-cell clones of *shrub* mutant dendritic arborization (DA) sensory neurons in *Drosophila* larvae showed ectopic dendritic and axonal branching in neurons, indicating a cell-autonomous function for *shrub* in neuronal morphogenesis. *shrub* encodes an evolutionarily conserved coiled-coil protein homologous to the yeast protein Snf7, a key component in the endosomal sorting complex required for transport (ESCRT-III) which is involved in the formation of endosomal compartments known as multivesicular bodies (MVBs) (Babst, 2005). We found that mouse orthologs could substitute for Shrub in mutant *Drosophila* embryos and loss of Shrub function caused abnormal distribution of several early or late endosomal markers in DA sensory neurons. Our findings demonstrate that the novel coiled-coil protein Shrub functions in the endosomal pathway and plays an essential role in neuronal morphogenesis.

Results and Discussion

shrub Mutant Embryos Exhibit Reduced Dendritic Fields and Altered Dendritic Branching Patterns

Each abdominal hemisegment of the *Drosophila* embryo and larvae contains 44 PNS sensory neurons, including multidendritic (MD) neurons. Of the MD neurons, most are classified as dendritic arborization (DA) neurons, which elaborate extensive dendritic trees in a two-dimensional manner just under the epidermis (Bodmer and Jan, 1987). Expression of green fluorescent protein (GFP) with neuronal subtype-specific GAL4 lines allows easy visualization of dendritic morphology in living embryos or larvae (Gao et al., 1999; Gao et al., 2000). Forward genetic screens in this and other assay systems in *Drosophila* have identified a number of potentially novel loci where mutations led to striking alterations in dendritic branching and arborization (e.g. Gao et al., 1999; Medina et al., 2006; Reuter et al., 2003).

A mutation at the *shrub* locus (*shrub*^{4}), mapped to 44F-45E, dramatically decreased the size of the dendritic fields of DA neurons (Gao et al., 1999). *shrub*^{4} mutant embryos die before reaching larval stage. To further characterize the dendritic phenotype, we collected wild-type and *shrub*^{4} mutant embryos at three different time points. At 15–16 hr after egg laying (AEL), wild-type dorsal cluster DA neurons extended two dorsally oriented dendrites with few lateral branches, whereas the dorsal dendrites in *shrub*^{4} mutants often branched several times to produce multiple dorsally oriented dendrites (Figure 3-1A). Time-lapse analysis demonstrates that the lateral branching process is highly dynamic, and some lateral branches are stabilized by 18–20

hr AEL (Figure 3-1A and Gao et al., 1999). At 17–18 and 19–20 hr AEL, DA neurons in *shrub*^{4} mutants exhibited greatly reduced dendritic fields, and lateral branches often failed to reach the adjacent segment boundaries. Under higher confocal magnification, however, we could see numerous fine dendritic processes that are difficult to discern in the image presented in Figure 3-1. To quantify the changes in dendritic arborization in *shrub*^{4} mutants, we calculated the aggregate dendritic field for the six dorsal cluster DA neurons as described (Li et al,. 2004). The average dendritic field of dorsal clusters was reduced in *shrub*^{4} mutant embryos (Figure 3-1B). Dendritic growth was similarly affected in embryos with the *shrub*^{4} mutation in trans to a deficiency covering 44F-45E (*Df(2R)Np5, In(2LR)w45-32n*) (data not shown), suggesting that the *shrub*^{4} dendritic phenotype was not due to mutations at other cytological locations.

Identification of the *shrub* Gene

To clone *shrub*, we found two P-element insertion lines between 44F and 45E that failed to complement the lethality of *shrub*^{4}. Both lines contained insertions in the 5′ region of a novel gene CG8055. *P{lacW}l(2)k11201*^{k11201} was inserted 128 nucleotides upstream of the ATG start codon, and precise excision of the P-element rescued the lethality. *P{EPgy2}CG8055*^{EY05194} was inserted 73 nucleotides upstream of the coding region in the first exon of *CG8055*, and exhibited a phenotype similar to *shrub*^{4} (Figure 3-1C). We found a 31-nucleotide deletion in the coding region of *CG8055*, suggesting that *CG8055* is *shrub* (Figure 3-1C). No mutations were found in other adjacent genes. Wild-type Shrub protein has 226 amino acids and contains two coiled-coil domains with many basic

residues clustered near the amino terminus and many acidic residues clustered near the carboxy terminus (Figure 3-1D).

We also generated a rabbit polyclonal antibody against a fusion protein of GST and full-length Shrub. Western blot analysis with this antibody showed a robust band in wild-type embryonic extracts but not in *shrub*^{4} mutant extracts near 36 kDa,which was larger than the predicted size of Shrub (25 kDa) (Figure 3-1E). This difference is likely due to the high percentage of charged amino acids, which can alter protein mobility in polyacrylamide gels. Related proteins in yeast show similar shifts in SDS-PAGE migration (Babst et al., 2002).

Shrub is an uncharacterized novel protein in *Drosophila* homologous to yeast Snf7 (Tu et al., 1993), a class E Vps protein (also known as Vps32) involved in the trafficking of transmembrane proteins to the lysosome via MVBs (Babst et al., 2002). In epithelial cells, Shrub seems to be diffusely localized in the cytoplasm as shown by immunostaining (data not shown), consistent with the localization of Snf7 in yeast (Babst et al., 2002). Shrub and its mammalian homologues are highly conserved at the amino acid level. Three Snf7 orthologs are present in the human genome, hSnf7-1, hSnf7-2, and hSnf7-3 (also known as CHMP4B, CHMP4A, and CHMP4C, respectively) (Katoh et al., 2003; Peck et al., 2004). In the mouse genome, there are two uncharacterized orthologs that we named mSnf7-1 and mSnf7-3, which correspond to hSnf7-1 and hSnf7-3, respectively.

Phenotypic Rescue and Functional Conservation of Shrub Homologues

To further confirm that the nonsense mutation in *shrub*^{4} is responsible for the dendritic phenotype, we performed two genetic rescue experiments. The *shrub*^{4} mutation is lethal in late embryogenesis, but concomitant ubiquitous expression of Shrub with *tubulin-Gal4* allowed survival of 99% of mutant embryos to the third instar larval stage, suggesting that *shrub* is indeed responsible for the lethality in *shrub*^{4} mutants (Figure 3-2A). Moreover, mSnf7-1 and mSnf7-3 could partially rscue the lethality of *shrub*^{4} mutants (Figure 2A). These data suggest both mammalian homologues can functionally replace Shrub in *shrub*^{4} mutants.

In the second rescue experiment, two copies of the UAS-*shrub* transgene were expressed in PNS neurons with *Gal4 109(2) 80*, and the average dendritic field size of dorsal cluster DA neurons was calculated (Figure 3-2B–E). Expression of UAS-*shrub* in *shrub*^{4} mutants increased the average dendritic field to wild-type levels. The rescued dorsal clusters contained a number of lateral branches, which were largely absent in *shrub*^{4} mutant clusters.

Cell-Autonomous Roles of Shrub

shrub mRNA is expressed during embryogenesis in many, if not all, cell types, including neurons and epithelial cells (data not shown). To further examine the cell-autonomous function of Shrub in dendritic branching, we used the MARCM technique (Lee and Luo, 1999) to reduce *shrub* activity in single DA neurons in third instar larvae. This technique allowed cell-autonomous dendritic phenotypes to be examined and quantified in each of the six dorsal cluster DA neurons (Grueber et al., 2002; Sweeney et al., 2002).

The dorsal cluster ddaE and ddaF neurons (Sweeney et al., 2002) have simple dendritic branching patterns extending over a limited area of the hemisegment with few higher-order branches. For example, wild-type ddaE neurons extend several branches posteriorly toward the adjacent segment boundary. These branches have the same apparent diameter proximal and distal to the cell body and no fine spine-like protrusions as occur in other DA neurons (Figure 3-3A). The shape of the dendritic trees of *shrub*^{4} mutant ddaE neurons was similar to wild-type, but the number of dendritic termini increased significantly due to an increase in fine, higher-order branches (Figure 3-3B, 3-3-3E). *shrub*^{4} mutant clones of ddaF and ddaB neurons showed similar results (Figure 3-4).

To further confirm these cell-autonomous phenotypes, we also used a UAS-*shrub-RNAi* transgenic line. This RNAi construct could effectively downregulate the expression of endogenous Shrub as shown by western blotting analysis (Figure3-3). When the RNAi transgenes were expressed in ddaE and ddaF neurons in the dorsal cluster driven by *Gal4*^{221}, the dendritic phenotype was similar to that of *shrub*^{4} MARCM clones: increased dendritic termini due to downregulation of *shrub* expression (Figure 3-3C–E). The RNAi phenotype was less severe than in *shrub*^{4} MARCM clones because RNAi likely led to a partial reduction of *shrub* expression.

ddaC neurons develop complex arbors that cover the entire area of the dorsal hemisegment (Figure 3-3F). *shrub*^{4} mutant ddaC neurons showed a nearly 100% increase in dendritic termini (Figure 3-3G, 3-3H). Moreover, *shrub*^{4} mutant ddaC neurons exhibited a high degree of branching complexity near the cell body, while much of the dendritic branching in wild-type ddaC neurons occured near the edges of the dendritic

field. Dendritic fields of *shrub*^{4} mutant ddaC neurons (Figure 3-3G) were also reduced in size, consistent with the dendritic phenotype seen in *shrub*^{4} mutant embryos (Figure 3-1A). *shrub*^{4} mutant phenotypes were seen in other dorsal cluster DA neurons. Of the six dorsal cluster DA neurons, ddaA and ddaD neurons are distinguished by the numerous actin-rich spine-like protrusions that extend from the dendritic shafts (Andersen et al., 2005; Li et al., 2005). As compared to wild-type, *shrub*^{4} mutant ddaA or ddaD neurons extended longer spine-like protrusions (Figure 3-5).

shrub Mutant Neurons Exhibit Ectopic Axonal Branching

We used several neuron-specific antibodies to immunostain *shrub*^{4} mutant embryos and found no gross morphological changes in axon fasciculation or guidance in the PNS or CNS (Figure 3-6A–B and data not shown). Changes in synaptic growth or arborization were not examined. We hypothesized that the absence of gross axonal phenotypes in *shrub*^{4} mutants could be due to a maternal contribution of the *shrub* gene. Maternal germline recombination (see Experimental Procedures) was used to create maternal knockout embryos derived from *shrub*^{4} mutant germline cells. These embryos showed severe defects in neuronal specification and differentiation (data not shown), supporting an essential role for maternally contributed Shrub at early embryonic stages.

PNS axons normally extend unbranched to the ventral nerve cord and form synapses on CNS neurons. Ectopic axonal branches were found in 21% of *shrub*^{4} mutant neurons generated by the MARCM technique (Figure 3-6D, 3-6E). Since a large portion of PNS axons inside the larval body cannot be visualized with this technique, we suspect

that the percentage of *shrub*^{4} mutant neurons exhibiting ectopic axonal branching is actually much higher.

shrub Mutation Causes Abnormal Distribution of Endosomal Markers

To confirm the subcellular localization of Shrub in *Drosophila* sensory neurons, we generated a UAS-*shrub-GFP* transgenic line. Expression of Shrub-GFP in ddaE neurons with *Gal4*^{221} caused an overbranching phenotype similar to that in *shrub*^{4} mutants (Figure 3-7B); branching in neurons overexpressing untagged Shrub did not vary from wild-type (Figure 3-7C). This finding suggests that Shrub-GFP acts as a dominant-negative form and further comfirms the cell-autonomous function of Shrub in controlling dendritic morphogenesis.

To assess endosome/lysosome function in a cell with reduced Shrub function, we used Spinster, a transmembrane protein and marker for late endosomes and lysosomes in *Drosophila* (Sweeney and Davis, 2002). Spinster-RFP was localized to puncta in the cell body and throughout the dendrites and axons of PNS neurons (Figure 3-7E). However, co-expression of Shrub-GFP led to accumulation of Spinster-RFP in large vesicles in the cell body and dendrites (Figure 3-7F). Spinster-GFP localization in DA neurons of *shrub*^{4} mutant embryos was abnormal (data not shown). We also examined different Rab proteins. The late endosomal marker Rab7-GFP and the early endosomal marker Rab5-GFP were redistributed when co-expressed with *shrub* RNAi (Figure 3-7G–J). Co-expression of *shrub* RNAi did not affect recycling endosomal markers Rab4-RFP (Figure 3-7K and 3-7L) and Rab11-GFP (data not shown). These results are consistent with a role for Shrub in protein transport through the endosomes to lysosomes.

Expression of Shrub-GFP in the eye using *long-GMR-Gal4* resulted in dramatic retinal degeneration (Figure 3-7M), consistent with the lethality in mutant eye clones of other endosomal gens such as *Vps25* (Thompson et al., 2005; Vaccari and Bilder, 2005).

The endosomal pathway modulates many cell-signaling pathways through internalization and subsequent sorting of receptor molecules (Le Borgne et al., 2005; Sorkin and Von Zastrow, 2002). The control of neuronal morphogenesis by Shrub could be mediated by one or more receptor signaling pathways. Indeed, Notch processing and activity were affected by *shrub* mutations, which contribute to the *shrub* dendritic phenotype. Our findings are consistent with the reports that *Drosophila* Vps25, a component in the ESCRT-II complex, controls epithelial cell proliferation through regulating Notch trafficking in endosomes (Thompson et al., 2005; Vaccari and Bilder, 2005). Moreover, mutations in *Drosophila Vps23/Tsg101*, a component in the ESCRT-I complex, also resulted in increased Notch signaling (Moberg et al., 2005).

Our studies here reveal the importance of the ESCRT complexes in the control of neuronal morphogenesis. The ESCRT complexes have been associated with several neurodegenerative diseases. The hereditary spastic paraplegia protein Spastin interacts with CHMP1B, an ESCRT-III complex-associated protein (Reid et al., 2005). More recently, a specific mutation within the *CHMP2B* gene, which encodes the ortholog of Vps2, another component of the ESCRT-III complex, was found in 11 affected members of a Danish frontotemporal dementia family but not in unaffected family members or in control populations (Skibinski et al., 2005). Further understanding of the molecular and physiological consequences of defects in ESCRT complex function may offer new insights into age-dependent neurodegenerative disorders.

Figures

Figure 3-1. Dendritic phenotypes in *shrub* mutant embryos and cloning of the *shrub* gene

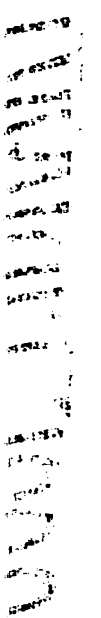

(A) Dendritic morphogenesis of dorsal cluster DA neurons in wild-type (WT) and *shrub*^{4} mutant embryos. Numerous fine processes in *shrub*^{4} mutant embryos could be seen under higher confocal magnification. Embryos were collected at 1-hr intervals and imaged at 15–16 hr, 17–18 hr, and 19–20 hr after egg laying (AEL). Scale bar: 20 μm. (B) Quantification of dendritic field area for dorsal cluster DA neurons in WT and *shrub*^{4} mutant embryos as described (Li et al., 2004). Segments A2–A6 were examined in embryos at 17–18 hr AEL, and 20 segments per genotype were quantified. ***: $p < 0.001$. All values are mean ± SEM. (C) Genomic organization of the *shrub* locus. The boxes represent exons, and the lines indicate introns. Black areas show the coding region of *shrub*. The 31-nucleotide deletion in the *shrub*^{4} allele is located in the second exon. One P element (*P{lacW}l(2)k11201*^{k11201}) is inserted in the regulatory region and one P element (*P{EPgy2}CG8055*^{EY05194}) is inserted in the first exon. (D) Domain organization of the Shrub protein. The black boxes indicate coiled-coil domains, and the positive and negative symbols represent regions with a high percentage of positively and negatively charged amino acids. The deletion in the *shrub*^{4} allele is located in the first coiled-coiled domain. (E) Western blot analysis with rabbit antibody raised against the Shrub-GST fusion protein indicates that Shrub is not expressed in *shrub*^{4} mutant embryos. Anti-β-tubulin was used as a loading control. Numbers indicate molecular mass in kDa. Since no smaller bands were detected, truncated Shrub is likely unstable or present only at very

low levels. A nonspecific band near 43 kDa is present in both wild-type and *shrub*^{4} extracts.

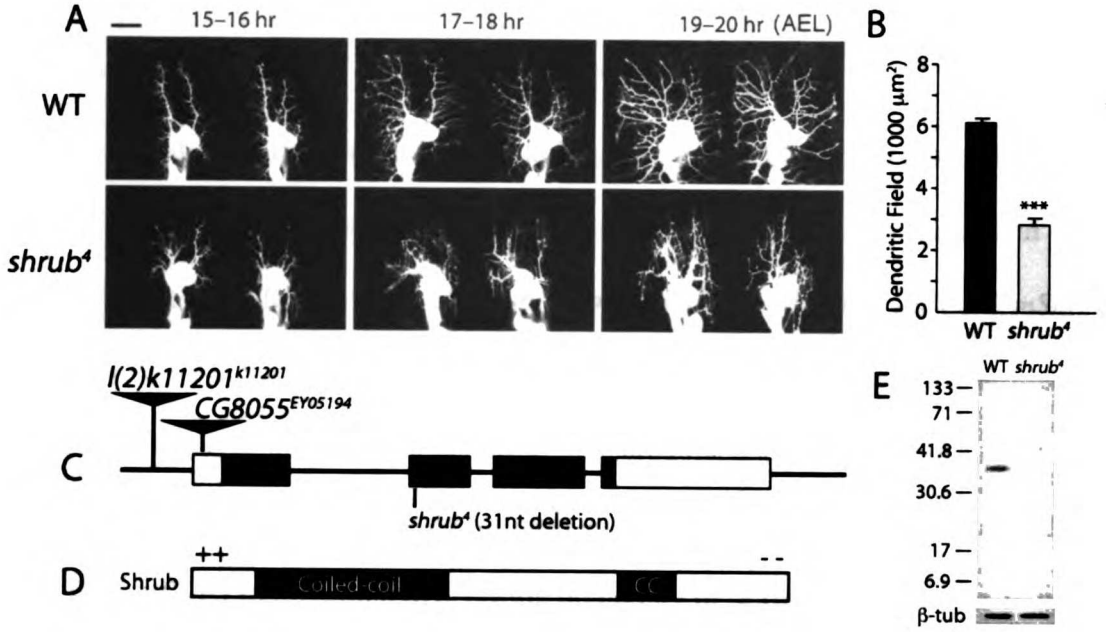
A
15–16 hr
17–18 hr
19–20 hr (AEL)
WT
shrub4
B
Dendritic Field (1000 µm²)
8
6
4
2
0
***
WT
shrub4
C
l(2)k11201k11201
CG8055EY05194
shrub4 (31nt deletion)
D
Shrub
++
- -
Coiled-coil
CC
E
WT
shrub4
133
71
41.8
30.6
17
6.9
β-tub

Figure 3-2. Rescue of the *shrub* mutant lethality and dendritic phenotypes and functional conservation of mammalian homologues

(A) Quantification of third instar larval viability in *shrub*^{4} mutants and rescued lines. Survival rate is expressed as the number of surviving larvae divided by maximum possible larvae with the genotype of *shrub*^{4}; *tubulin-Gal4*/UAS-*shrub* (or UAS-*mSnf7-1* or UAS-*mSnf7-3*). Survival beyond larval stages was not examined; see Experimental Procedures. (B) Quantification of dendritic field area for dorsal cluster DA neurons as described in Figure 1 legend. n = 20 for each genotype. All values are mean ± SEM. *: $p < 0.05$. (C–E) Representative dendritic branching of dorsal cluster DA neurons in wild-type (C), *shrub*^{4} mutant (D), and *shrub*^{4}; UAS-*shrub* (E) embryos at 17–18 hr AEL are shown. Scale bar: 20 μm. Expression of UAS-*GFP* driven by *Gal4 109(2)80* were used to visualize dendritic morphology.

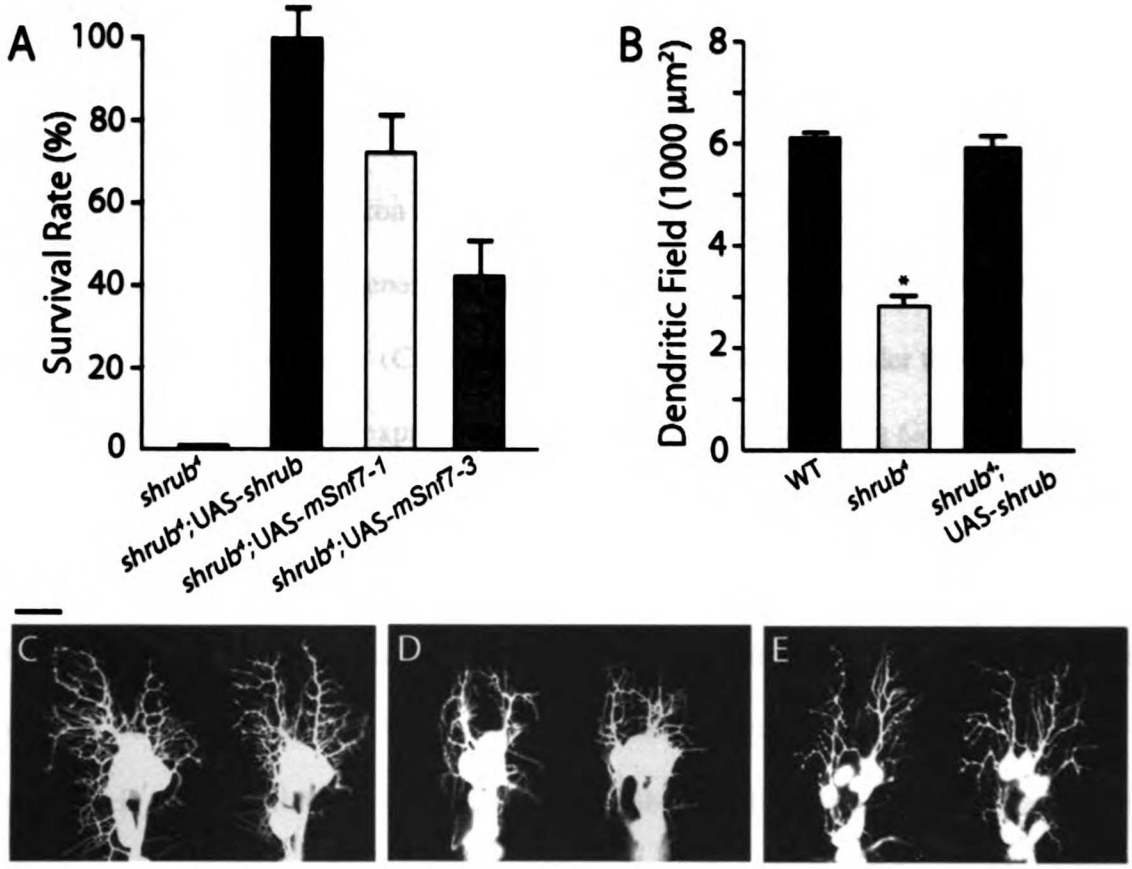
A
Survival Rate (%)
100
80
60
40
20
0
shrub4
shrub4;UAS-shrub
shrub4;UAS-mSnf7-1
shrub4;UAS-mSnf7-3
B
Dendritic Field (1000 µm2)
8
6
4
2
0
*
WT
shrub4
shrub4; UAS-shrub
C
D
E

Figure 3-3. The cell-autonomous function of *shrub* in dendritic branching as shown by single-cell MARCM analysis

(A) A wild-type ddaE neuron with smooth dendrites extending toward the posterior segment boundary. This neuron is labeled by GFP with the MARCM technique. (B) A *shrub*^{4} mutant ddaE neuron generated by MARCM shows increased dendritic branching especially near the cell body. (C) A ddaE neuron labeled by GFP under the control of *Gal4*^{221}. (D) A ddaE neuron expressing a *shrub* RNAi construct using *Gal4*^{221} that also exhibits increased dendritic branching. (E) Quantification of dendritic ends in wild-type or *shrub*^{4} mutant ddaE neurons. The first two columns are from MARCM analyses (n = 20 for *shrub*^{4} mutant neurons and n = 11 for wild-type neurons), and the last two columns are from wild-type ddaE neurons, and ddaE neurons expressing *shrub* RNAi, respectively. (F) A wild-type ddaC neuron that elaborates dendrites covering a large area between segment boundaries. (G) A *shrub*^{4} mutant ddaC neuron with increased dendritic termini and a reduced dendritic field, a phenotype consistent with the dendritic phenotype in *shrub*^{4} mutant embryos (Figure 3-1A). (H) Quantification of dendritic ends in wild-type or *shrub*^{4} mutant ddaC neurons. Values are mean ± SEM. ***: $p < 0.001$, **: $p < 0.01$. Scale bar: 50 μm. (I) Western blot analysis with anti-Shrub antibody. Lane 1 is lysate from wild-type embryos, lane 2 is lysate from embryos expressing UAS-*shrub-RNAi* by *tubulin-Gal4* and lane 3 is lysate from *shrub*^{4} mutant embryos. Numbers indicate molecular mass in kDa; the Shrub band is near 36 kDa, and the nonspecific band near 43 kDa serves as a loading control.

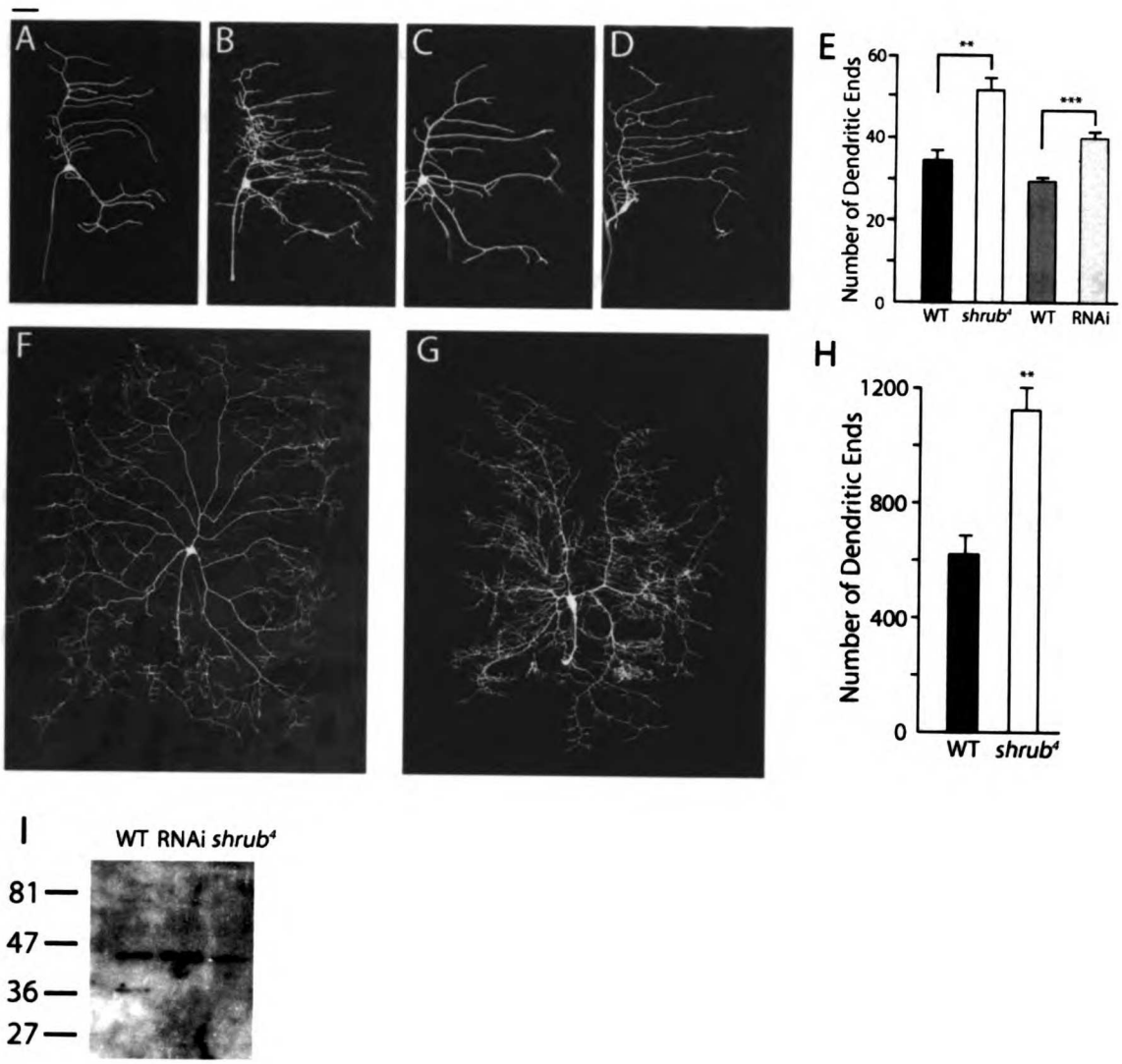
A
B
C
D
E
Number of Dendritic Ends
60
40
20
0
**
***
WT
shrub4
WT
RNAi
F
G
H
Number of Dendritic Ends
1200
800
400
0
**
WT
shrub4
I
WT RNAi shrub4
81
47
36
27

Figure 3-4. Dendritic phenotpes of *shrub* mutant ddaF and ddaB neurons generated by the MARCM technique

(A) A wild-type ddaF neuron labeled by GFP with the MARCM technique. Dendritic branches of ddaF neurons mostly extend towards the anterior segment boundary. Bar: 50 μm. (B) A *shrub*^{4} mutant ddaF neuron that exhibits increased dendritic branching. (C) Quantification of dendritic branches of wild-type or *shrub*^{4} mutant ddaF and ddaB neurons. *: $p < 0.05$. ***: $p < 0.001$. (D) A wild-type ddaB neuron labeled by GFP with the MARCM technique. (E) A *shrub*^{4} mutant ddaB neuron that exhibits increased dendritic branching.

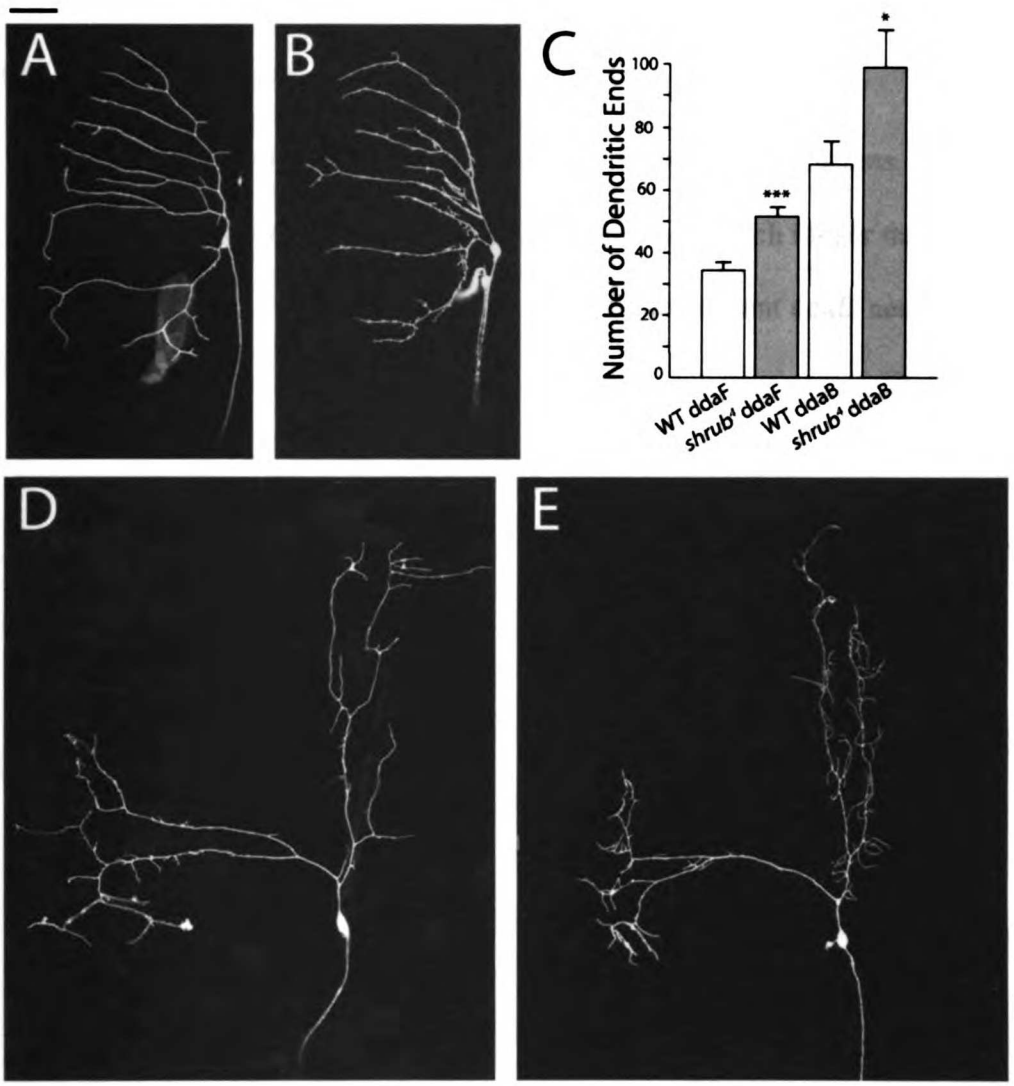
A
B
C
Number of Dendritic Ends
100
80
60
40
20
0
***
*
WT ddaF
shrub⁴ ddaF
WT ddaB
shrub⁴ ddaB
D
E

Figure 3-5. Dendritic Phenotype of *shrub* mutant ddaA and ddaD neurons generated by the MARCM technique

(A) A wild-type ddaA neuron that exhibits numerous spine-like protrusions. (B) A *shrub*^{4} mutant ddaA neuron whose spine-like protrusions are much longer than that on wild-type ddaA neurons. (C) and (D) wild-type and *shrub*^{4} mutant ddaD neurons, respectively. Bar: 50 μm.

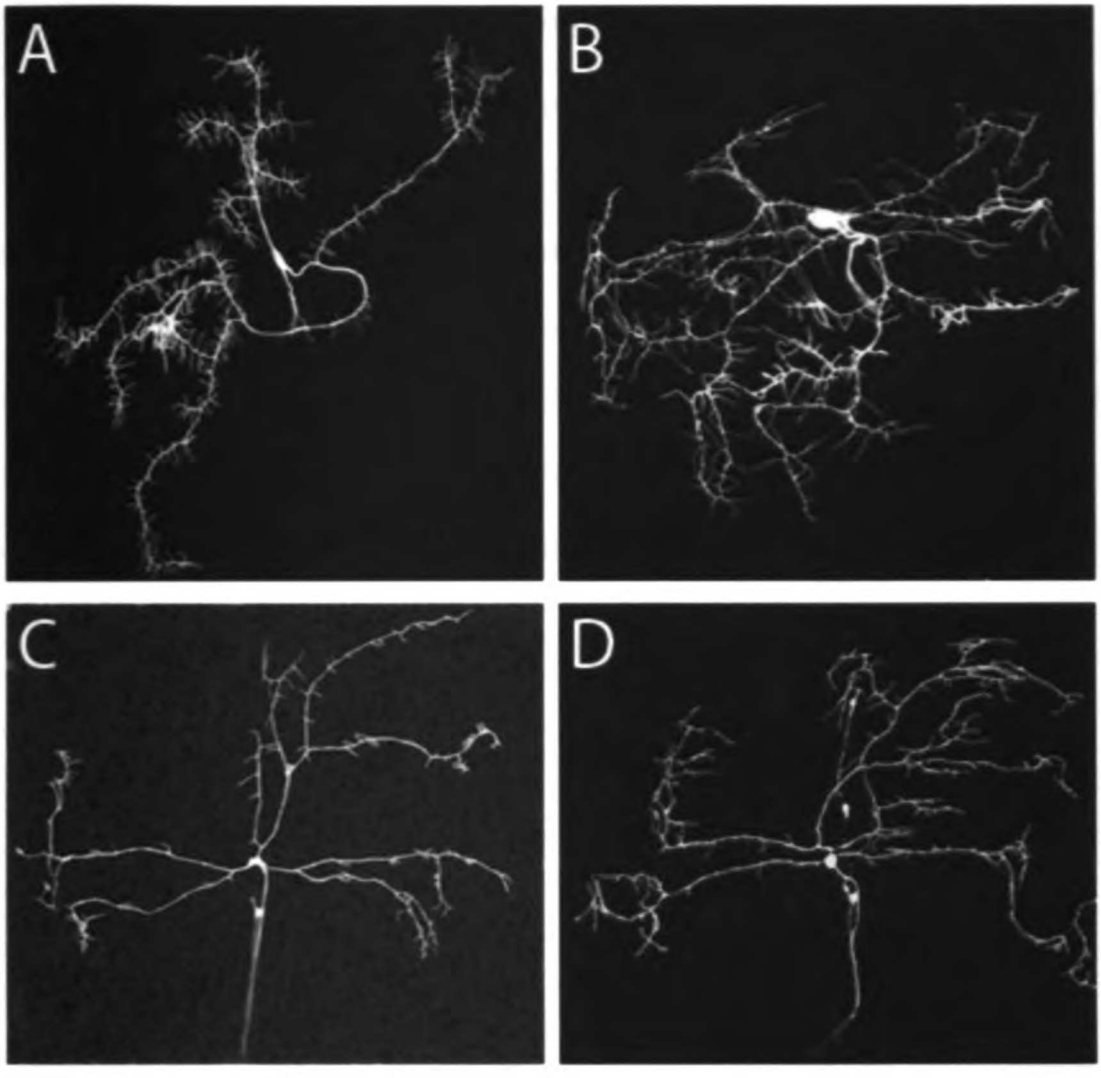
A
B
C
D

Figure 3-6. Ectopic axonal branching phenotypes of *shrub* mutant neurons

(A) Wild-type embryos at stage 16 were stained with 22C10 antibody to show the axonal tracks of PNS sensory neurons. (B) *shrub*^{4} zygotic mutant embryos did not exhibit detectable axonal guidance or fasciculation defects as realved by 22C10 antibody staining. D, dorsal cluster cell bodies; A, dorsal cluster axon bundle. (C) The axon of a wild-type GFP-labeled DA sensory neuron extends towards to ventral nerve cord without premature branching. (D) and (E) Ectopic axonal branching of *shrub*^{4} mutant DA neurons generated by MARCM. The arrows indicate abnormal axonal branching.

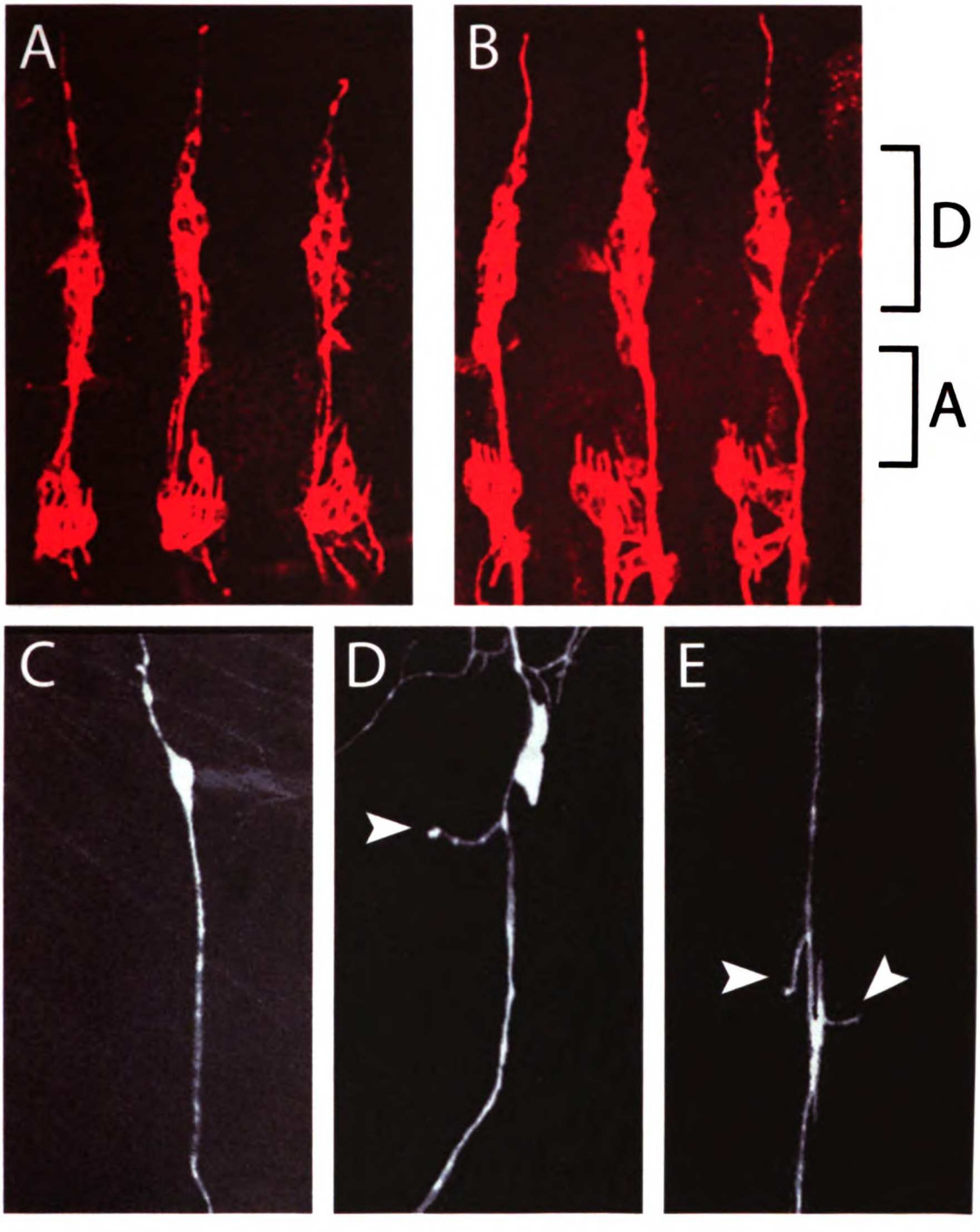
A
B
D
A
C
D
E

Figure 3-7. Shrub-GFP functions as a dominant negative form and reduced Shrub activity affects the distribution of endosomal markers

(A) A wild-type ddaE neuron labeled by *Gal4*^{221}. (B) A ddaE neuron in which *Gal4*^{221} drives expression of UAS-*shrub-GFP*. (C) A ddaE neuron in which *Gal4*^{221} drives expression of UAS-*shrub*. (D) Quantification of dendritic branching of ddaE neurons that are either wild-type (n = 27) or overexpressing UAS-*shrub-GFP* (n = 73) or UAS-*shrub* (n = 35). In this experiment, the number of dendritic ends was counted from early third instar larvae; therefore, the value for the wild-type control is slightly smaller than that in other experiments. Values are mean ± SEM. ***: $p < 0.001$. (E) Subcellular localization of Spinster-RFP in a wild-type ddaE neuron shows punctate localization in cell body and dendrites. *Gal4 109(2)80* drives target gene expression in panels E–K. (F) Subcellular localization of Spinster-RFP in a ddaE neuron co-expressing Shrub-GFP. Large accumulations of Spinster-RFP were found in cell body and dendrites. (G–L) A ddaE neuron expressing the following markers: late endosomal marker Rab7-GFP (G); late endosomal marker Rab7-GFP and *shrub* RNAi (H); early endosomal marker Rab5-GFP (I); early endosomal marker Rab5-GFP and *shrub* RNAi (J); recycling endosomal marker Rab4-RFP (K); recycling endosomal marker Rab4-RFP and *shrub* RNAi (L). (M) Expression of UAS-*shrub-GFP* by *long-GMR-Gal4* causes retinal degeneration. Black spots indicate dead pigment cells.

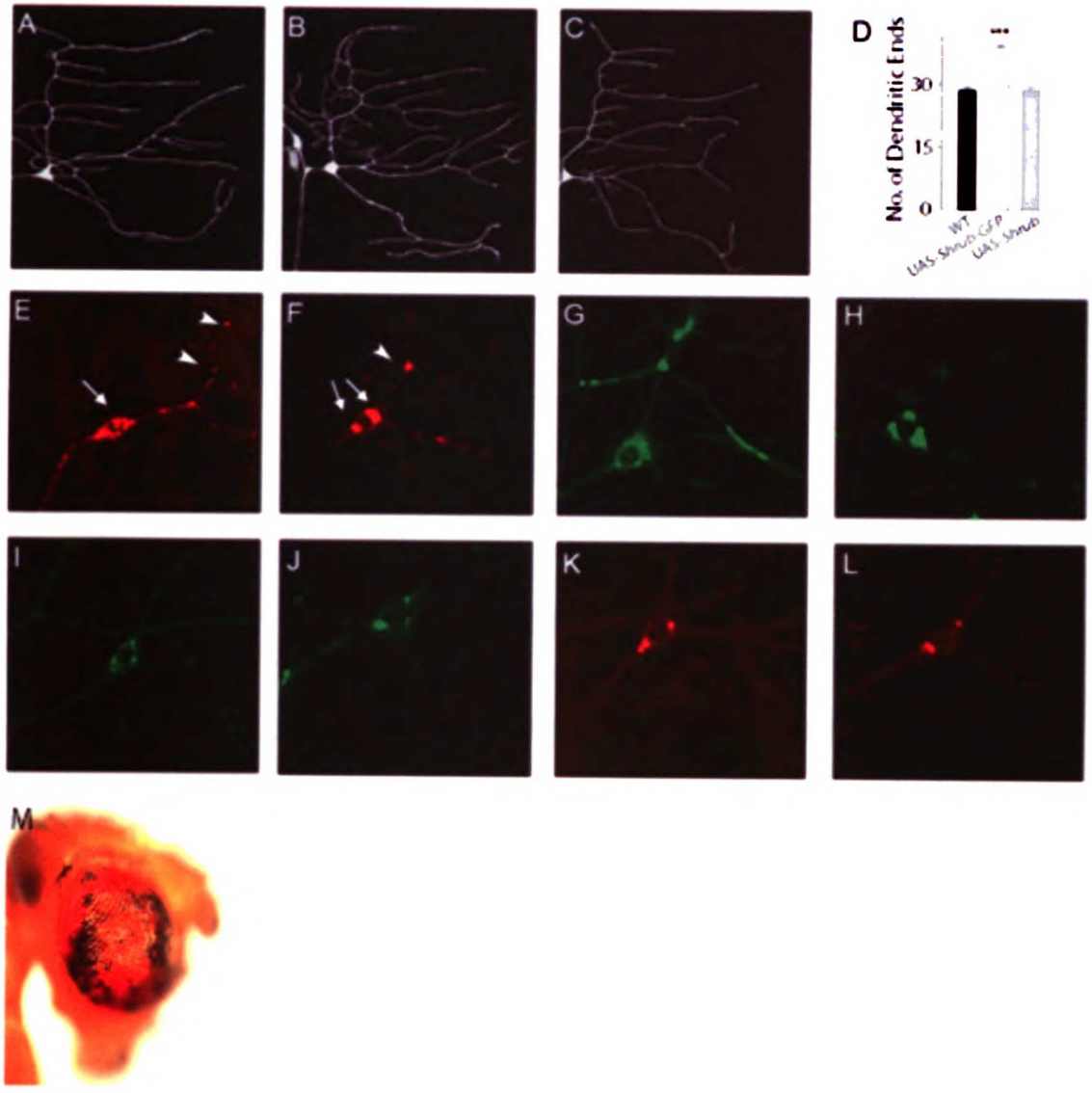
A
B
C
D
No. of Dendritic Ends
30
15
0
WT
UAS-Shrub-GFP
UAS-Shrub
E
F
G
H
I
J
K
L
M

Chapter Four:

Cell-Autonomous Regulation of Dendritic Morphogenesis by the Delta/Notch Signaling Pathway

Summary

Dendritic branching is a complex process controlled by many signaling pathways, including Notch. Here we report that mutations in the *shrub* gene enhanced signaling by the Notch pathway. *shrub* encodes an evolutionarily conserved coiled-coil protein homologous to the yeast protein Snf7, which is involved in the formation of a subset of late endosomal compartments known as multivesicular bodies. *shrub* mutant embryos had elevated expression levels of processed Notch C-terminal fragment and a fragment of the Notch ligand Delta, as well as Notch-dependent transcription. Further genetic studies revealed cell-autonomous functions for Notch and Delta in promoting dendritic branching. These data support a model in which control of dendritic morphogenesis by Shrub involves endosomal regulation of the Delta/Notch signaling pathway.

Introduction

In both flies and mammals, the Notch pathway is pivotal in multiple developmental processes in different tissues, such as neurogenesis, neuronal differentiation, and learning and memory (reviewed in Artavanis-Tsakonas et al., 1999; Yoon and Gaiano, 2005). Notch, a large type-I transmembrane glycoprotein, is processed into two fragments that form a membrane receptor complex. Upon binding to one of its ligands (Delta and Jagged family proteins), the Notch intracellular domain (NICD) is released from the plasma membrane and translocates into the nucleus to control gene expression (reviewed in Artavanis-Tsakonas et al., 1999; Yoon and Gaiano, 2005).

The diversity of neuronal cells, especially in the size and shape of their dendritic and axonal arborizations is a striking feature of the mature nervous system (Ramón y Cajal, 1995; Masland, 2004). A role for Notch in dendritic morphogenesis was first indicated by the presence of Notch and its ligands in mammalian cortical neurons, both *in vivo* and in primary cultures (Berezovska et al., 1998, 1999; Sestan et al., 1999; Redmond et al., 2000). Transfection of full-length Notch1 or its constitutively active form into cultured primary neurons (Berezovska et al., 1999; Sestan et al., 1999; Redmond et al., 2000) or N2a neuroblastoma cells (Franklin et al., 1999) induces C-promoter binding factor (CBF-1)–dependent transcription, inhibits dendritic growth (Berezovska et al., 1999; Redmond et al., 2000; Sestan et al., 1999), and promotes dendritic branching (Redmond et al., 2000). Essential roles for Notch signaling in axonal development have also been identified (Giniger et al., 1993; Crowner et al., 2003).

Regulation of Notch signaling involves a number of post-translational mechanisms, including endocytosis (Le Borgne et al., 2005), which modulates many cell-

signaling pathways through internalization and subsequent sorting of transmembrane proteins (Sorkin and Van Zastrow, 2002). After internalization to the early endosome, some cargoes are recycled back to the plasma membrane. Others move through the late endosome to the lysosome for degradation, with monoubiquitination often serving as a positive signal for lysosomal sorting (Babst, 2005). Evidence for endocytic targeting of Notch includes a conserved dileucine motif required for its internalization and downregulation (Shaye and Greenwald, 2002). In flies, Notch accumulates intracellularly and shows increased signaling in mutant clones in which transport to the late endosome is disrupted (Jekely and Rorth, 2003; Moberg et al., 2005; Thompson et al., 2005; Vaccari and Bilder, 2005). Moreover, two E3 ubiquitin ligases, Nedd4 and suppressor of Deltex, regulate the cell-surface expression and subcellular sorting of Notch for eventual signaling activation or degradation (Sakata et al, 2004; Wilkin et al., 2004). Delta has also been localized to late endosome compartments (Piddini and Vincent, 2003), and internalization of Delta in signal-sending cells by a dynamin-mediated mechanism affects Notch signaling (Parks et al., 2000). In addition, Delta is ubiquitinated by Neuralized, which promotes its internalization and subsequent degradation (Lai et al., 2001).

A key step in the endocytic regulation of transmembrane proteins such as Notch and Delta occurs in a subset of late endosomal compartments known as multivesicular bodies (MVBs) (Gruenberg and Stenmark, 2004). Cargoes destined for degradation in the lysosome are sorted into vesicles within the MVB lumen, and the proteins required for this process have been characterized in yeast (Babst, 2005). MVB sorting requires three heteromeric protein complexes, called ESCRT-I, ESCRT-II, and ESCRT-III

(endosomal sorting complex required for transport), which are thought to act sequentially (Babst et al., 2002a, 2002b; Katzmann et al., 2001). Shrub is an ortholog of yeast Snf7, a key protein in the ESCRT-III complex. We describe the dendritic and axonal phenotypes and the misregulation of the Delta/Notch signaling pathway in *shrub* mutants. We show data suggesting that Shrub regulates Notch signaling through an endocytic mechanism and that changes in Notch/Delta signaling contribute to *shrub* dendritic phenotypes. Further examination of Notch/Delta signaling revealed cell-autonomous regulation of dendritic morphogenesis by Notch, Delta, and Neuralized, indicating a novel cell-autonomous role for Delta in dendritic morphogenesis.

Results

Shrub Modulates the Notch Signaling Pathway

Proteins that affect endosomal transport often affect one or more signaling pathways (Sorkin and Von Zastrow, 2002). To investigate possible changes in intracellular signaling in *shrub*^{4} mutant cells, the *shrub* RNAi construct was expressed in the eye, and antenna anlagen in the embryo and larval eye imaginal disc, with *eyeless-Gal4*. Reduced *shrub* expression in these tissues affected eye proliferation and cell fate (Figure 4-1C–F). Eye specification and determination involve multiple signaling pathways, including the EGFR and Notch signaling pathways (Kumar and Moses, 2001). Because both of these pathways are regulated by endocytosis, we determined if EGF or Notch signaling contribute to the effects of *shrub* mutations on dendritic morphogenesis. To test the role of EGFR signaling in dendritic branching, we overexpressed two copies of a dominant-negative EGFR isoform (Reichmann-Fried et al., 1994) with *Gal4*^{221} and did not observe a significant difference (data not shown), raising the possibility that the EGF signaling pathway does not play a major role in dendritic branching of ddaE and ddaF neurons at late embryonic or larval stages.

To determine if changes in Notch signaling contribute to dendritic phenotypes in *shrub*^{4} mutants, we performed western blot analysis of lysates from wild-type and *shrub*^{4} mutant embryos. The Notch antibody C17.9C6 is directed against the intracellular domain of Notch and identifies two major species on a western blot, a full-length fragment (N-FL) of ~300 kDa and a processed transmembrane fragment (N-TM) of ~120 kDa, which consists of the transmembrane and intracellular domains (Fehon et al, 1990).

N-FL levels were unchanged in wild-type and mutants, but the N-TM fragment was increased approximately 3.5-fold in *shrub*^{4} mutants (based on two independent western blot experiments) (Figure 4-2A). This suggests that loss of Shrub function leads to decreased degradation or increased production of N-TM. Delta protein levels were also assessed with the C594.9B antibody, which is directed against an extracellular epitope and identifies a full-length fragment of ~98 kDa (L isoform) as well as several processed fragments of 86–92 kDa (I1 isoform) and ~83 kDa (I2 isoform) in late embryos (Klueg et al., 1998). In *shrub*^{4} mutant embryos, the level of the ~83 kDa isoform was upregulated approximately six fold (Figure 4-2B).

To demonstrate that the alterations in Delta/Notch protein levels actually led to changes in Notch signaling, we examined Notch-dependent transcription activity with a *E(spl)m8-lacZ* reporter line (Lecourtois and Schweisguth, 1995). This line expresses β-galactosidase under the control of an *Enhancer of split-m8* promoter. In *shrub*^{4} mutant embryos, the reporter activity increased significantly in DA and other sensory neurons and surrounding epidermal cells (Figure 4-2C–L), indicating that loss of Shrub function resulted in upregulated Notch signaling. Consistent with Shrub affecting the Notch pathway, expression of dominant-negative Shrub-GFP with *Gal4-1348* (Huppert et al., 1997) resulted in a wing vein phenotype identical to that caused by elevated Notch signaling (Figure 4-1A–B)

Cell-Autonomous Functions of Notch in Dendritic Branching

To investigate whether the misregulation of the Notch signaling pathway is partially responsible for the *shrub*^{4} dendritic phenoptype, we examined the cell-autonomous

functions of Notch and Delta in dendritic branching. First, we used the MARCM technique and the null Notch allele $N^{264\text{-}39}$ to make single-neuron *Notch* mutant clones (Mari-Beffa et al., 1991). In *Notch*$^-$ ddaC neurons, the main dendritic branches still extended from the cell body, but the branches often failed to reach the segment boundaries and showed decreased elaboration. Quantification of dendritic termini revealed 50% fewer dendritic ends in *Notch*$^-$ than wild-type ddaC neurons (316.1 ± 33.8, n = 11 vs. 609.2 ± 49.4, n = 6, $p < 0.001$) (Figure 4-3A–C). Expression of a Notch dominant–negative construct (N-DN) (Jonsson and Knust, 1996) in ddaC neurons with $Gal4^{477}$ also led to fewer dendritic branches than in wild-type (464.2 ± 34.4, n = 6 vs. 613.6 ± 19.6, n = 7, $p < 0.01$). These experiments support a cell-autonomous role for Notch in promoting dendritic branching.

To further test the possibility that increased Notch signaling contributes to *shrub*^{4} dendritic phenotypes, we expressed a constitutively active form of Notch ($Notch^{\Delta E}$) (Fuerstenberg and Giniger, 1998). Deletion of the Notch extracelluar domain in this construct creates a ligand-independent activated form consisting of the transmembrane and intracellular portions of the receptor. Since this fragment was upregulated and Notch activity was increased in *shrub*^{4} mutants (Figure 4-2), we were interested in whether overexpression would lead to a phenocopy of the *shrub*^{4} phenotype. Expression of $Notch^{\Delta E}$ cell-autonomously in ddaC neurons with $Gal4^{477}$ increased branching as compared to wild-type (717.8 ± 23.1, n = 7, vs. 613.6 ± 19.6, n = 9, $p < 0.01$) (Figure 4-3C, bars 3 and 4), consistent with increased Notch signaling contributing to *shrub*^{4} dendritic phenotypes

We found a similar Notch$^{\Delta E}$ overexpression phenotype in both ddaE neurons (38.0 ± 1.1, n = 49, vs. 29.7 ± 0.7, n = 56, $p < 0.001$) and in vpda neurons of the ventral cluster (67.8 ± 1.5, n = 66, vs. 38.5 ± 0.5, n = 71, $p < 0.001$) (Figure 4-3D–F). They all showed an increase in fine dendritic processes, a phenotype similar to that of *shrub*^{4} mutant neurons, neurons that express *shrub* RNAi, or neurons expressing a Shrub dominant-negative isoform (Chapter Three).

Shrub Affects Delta Subcellular Localization

Our finding that Shrub affects late endosomal markers and Delta protein levels prompted us to investigate the subcellular localization of Delta. To do so, we expressed a UAS-*Delta-GFP* construct with *Gal4 109(2)80*, which is expressed in all DA neurons and a small cluster of epithelial cells per segment. In epithelial cells, Delta-GFP (De Joussineau, et al., 2003) localized to cell membranes and small intracellular puncta (Figure 4-4A). Epithelial cells co-expressing Delta-GFP and *shrub* RNAi, however, showed large intracellular accumulations of Delta-GFP (Figure 4-4B). Antibody staining experiments showed that Delta was concentrated on membranes in wild-type epithelial cells but in intracellular vesicle-like structures in *shrub*^{4} mutant embryos (data not shown). Delta-GFP in DA neurons often localized to dendritic branch points and dendritic termini, suggesting a possible role in regulating dendritic branching (Figure 4-4C). This dramatic redistribution caused by *shrub* mutations may reflect impairment in Delta transport to the lysosome and raises the possibility that the abnormal processing of Delta may contribute to *shrub*^{4} dendritic phenotypes.

Cell-Autonomous Roles of Delta in Dendritic Branching

To further test the role of Delta in dendritic branching, we used the *Delta* mutant allele $Dl^{S148504}$ (Salzberg et al., 1997) to produce single-cell *Delta*$^-$ MARCM clones. *Delta*$^-$ clones showed significantly decreased dendritic branching: *Delta*$^-$ ddaC neurons had 54% fewer dendritic ends than wild-type neurons (298.8 ± 111.5, n = 4 vs. 651.3 ± 59.3, n = 7, $p < 0.05$) (Figure 4-4C–D). As in *Notch*$^-$ clones, *Delta*$^-$ ddaC neurons had primary branches that failed to reach the segment boundaries, and dendritic elaboration was significantly reduced. These findings indicate that Delta also has a cell-autonomous function in controlling dendritic branching.

These data showing reduction of dendritic branching in *Delta*$^-$ neurons were further supported by experiments with UAS-*Neuralized*, the E3 ubiquitin ligase for Delta, which reduces Delta levels when overexpressed (Lai et al., 2001). Like the *Delta*$^-$ MARCM clones, ddaC neurons expressing two copies of *Neuralized* with $Gal4^{477}$ had less branching than wild-type neurons (524.2 ± 34.0, n = 5 vs. 613.6 ± 19.6, n = 7, $p < 0.05$). When overexpressed with $Gal4^{221}$, Neuralized led to a similar decrease in branching: ddaE neurons had fewer termini (20.9 ± 0.6, n = 46) than wild-type neurons (30.8 ± 0.5, n = 90, $p < 0.001$) (Figure 4-4G), as did vpda neurons (33.0 ± 0.7, n = 54 vs. 43.6 ± 1.0, n = 51, $p < 0.001$).

To create DA neurons with excess Delta, we overexpressed a truncated Delta construct (UAS-*Dl-D*) that lacks much of the intracellular domain (Huppert et al., 1997) and is likely resistant to degradation via Neuralized. This construct may mimic the Delta isoform shown to be elevated in $shrub^4$ mutants by western blot (Figure 4-1). ddaC neurons overexpressing Dl-D with $Gal4^{477}$ had more dendritic termini (705.5 ± 20.7, n =

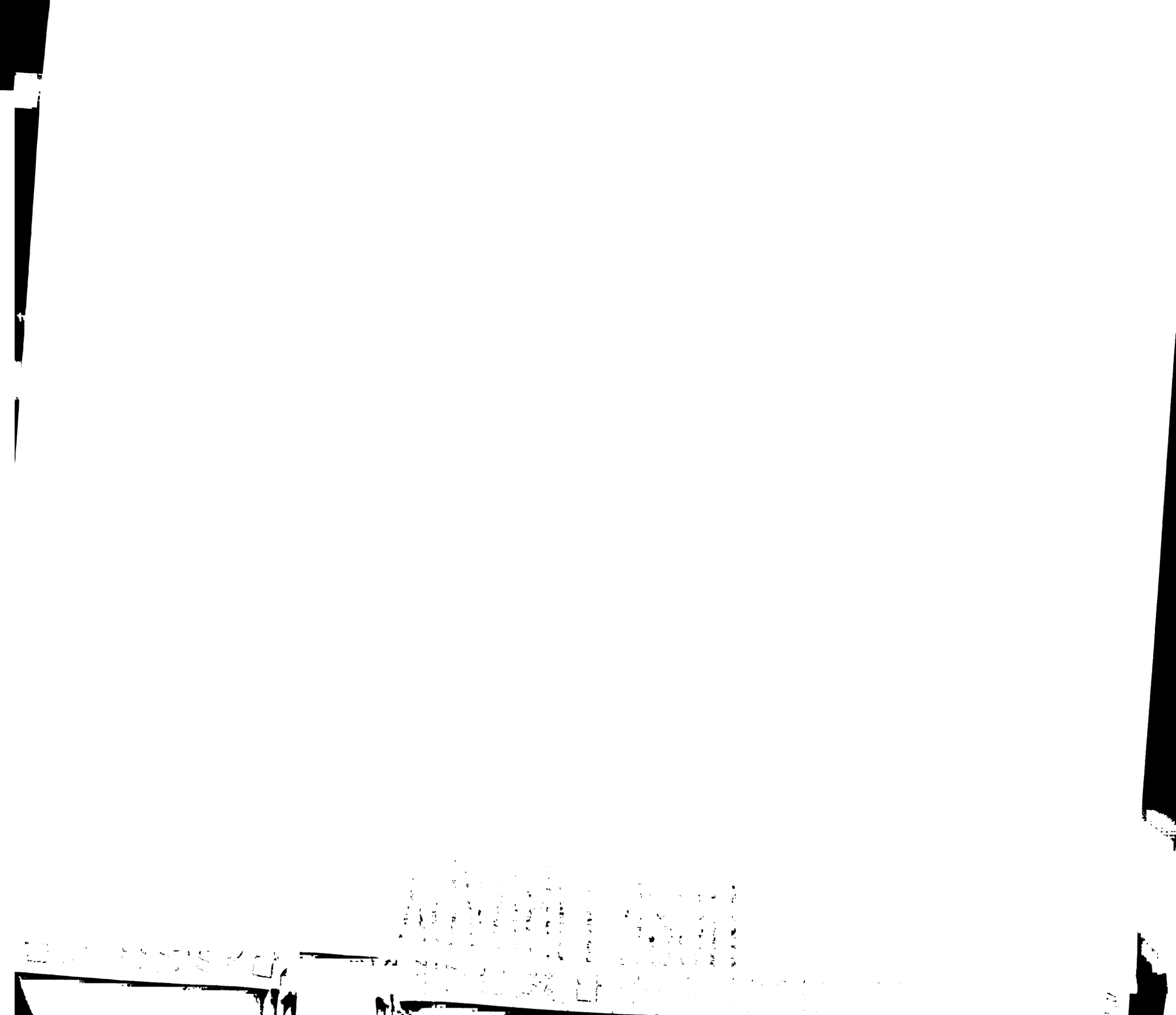

6) than wild-type neurons (613.6 ± 19.6, n = 7, $p < 0.01$), branching in ddaE neurons expressing Dl-D with *Gal4*^{221} was also greater than in wild-type neurons (36.4 ± 0.6, n = 96 vs. 30.8 ± 0.5, n = 90, $p < 0.001$). A similar dendritic phenotype was observed in vpda neurons expressing Dl-D (57.6 ± 1.2, n = 86, vs. 39.8 ± 0.5, n = 95, $p < 0.001$). These phenotypes were similar to that in *shrub*^{4} mutant neurons (Chapter Three) but opposite to that in *Delta*$^{-}$ neurons (Figure 4-4C–D).

Discussion

Shrub Modulates the Delta/Notch Signaling Pathway

Since endocytic pathways play a major role in regulating membrane receptor-mediated signaling (Sorkin and Von Zastrow, 2002), we wondered whether Shrub's effects on dendritic morphogenesis might involve changes in Notch signaling. Several lines of evidence indicate that Shrub plays a critical role in this pathway. First, N-TM was increased in *shrub*^{4} mutant embryos, while N-FL was unaffected. The N-TM band contains both the membrane-bound intracellular fragment and the γ-secretase-cleaved NICD fragment that acts as a transcriptional activator. Second, we found that the ~83 kDa Delta I2 isoform was selectively upregulated in *shrub*^{4} mutant embryos. This fragment results from C-terminal cleavage of Delta (Klueg et al., 1998), but little is known about the intracellular cleavage events. Our data suggest that this Delta fragment is selectively degraded by a Shrub-mediated pathway. Third, the loss of Shrub activity affected the subcellular distribution of Delta. Fourth, in *shrub*^{4} mutant embryos, Notch-dependent gene transcription was elevated in DA neurons and surrounding epithelial cells. Fifth, the *shrub* mutant phenotypes were partially rescued by reduced Notch activity. Sixth, dominant-negative Shrub expressed in the wing produced phenotypes consistent with increased Notch signaling. These findings provide additional evidence that endosomal regulation plays an important role in the Notch signaling pathway (Le Borgne et al., 2005)

It has been recently reported that *Drosophila* Vps25, a component in the ESCRT-II complex, controls epithelial cell proliferation through regulating Notch trafficking in

endosomes (Thompson et al., 2005; Vaccari and Bilder, 2005). Moreover, mutations in *Drosophila Vps23/Tsg101*, a component in the ESCRT-I complex, also resulted in the increased Notch signaling and accumulation of the Notch ~120 kDa fragments (Moberg et al., 2005). Taken together, these studies and our findings reported here strongly suggest that all three ESCRT complexes are required for the modulation of Notch signaling through the endosomal compartment. The detailed mechanisms of this regulatory process remain to be further investigated.

Delta Has a Cell-Autonomous Role in Controlling Dendritic Branching

An unexpected finding in this study was the cell-autonomous function of Delta in dendritic branching, which was prompted by our observations that the loss of Shrub function affects the processing and localization of Delta. Expression of a Delta-GFP construct indicated that Delta was present in vesicular structures in DA neuron dendrites, and cell-autonomous functions were assessed with MARCM. Interestingly, loss of Delta decreased dendritic branching (Figure 4-4). How might Delta function in a cell-autonomous manner to control dendritic branching? One possibility is that Delta expressed in DA neurons acts in cis to activate Notch on the same cell. This hypothesis is supported by the finding that Delta and Notch had similar cell-autonomous effects on the dendritic branching of DA neurons (Figures 4-3 and 4-4). Loss of Delta activity may lead to reduced cell-autonomous Notch activity, which in turn leads to decreased dendritic branching. Alternatively, Delta may have a Notch-independent function, as proposed for mammalian Delta1 (Ikeuchi and Sisodia, 2003; Six et al., 2003). Further genetic analysis is needed to distinguish between the two possibilities.

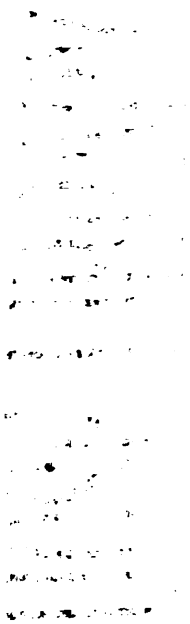

Implications for Neurodegenerative Diseases

The findings in this study indicate that alterations in the Delta/Notch signaling pathway contribute to dendritic phenotypes seen in *shrub*^{4} mutant neurons, revealing the importance of the endosomal-lysosomal pathway in the control of dendritic morphogenesis. Abnormalities in the endosomal-lysosomal pathway are among the neuropathologic hallmarks of Alzheimer's disease (Nixon, 2005), and both Notch and Delta are substrates for presenilin-dependent γ-secretase cleavage (De Strooper et al., 1999; Ikeuchi and Sisodia, 2003). Whether *shrub* mutations affect γ-secretase activity remains unknown. More recently, a specific mutation within the *CHMP2B* gene was found in 11 affected members of a Danish frontotemporal dementia family (FTD3) but not in unaffected family members or in control populations (Skibinski et al., 2005). The yeast ortholog of human CHMP2B, Vps2, interacts directly with Snf7 (Babst, 2005). Our results here raise the possibility that misregulation of the Notch signaling pathway may also contribute to the pathogenesis of FTD. Further understanding of the molecular and physiological consequences of defects in processing transmembrane proteins may offer new avenues for designing therapeutic intervention for age-dependent neurodegenerative disorders.

Figures

Figure 4-1. Expression of Shrub-GFP and *shrub* RNAi in the wing and eye cause phenotypes consistent with elevated Notch activity

(A)A wild-type wing expressing *Gal4-1348*. (B) A wing expressing Shrub-GFP by *Gal4-1348* shows vein breaks (arrowhead) identical to those produced by activated Notch expressed by *Gal4-1348* (Huppert et al., 1997). (C) A wild-type eye expressing *eyeless-Gal4*. (D–G) *shrub* RNAi expression with *eyeless-GAL4* leads to eye overgrowth (D), eye tissue in ectopic regions (E), complete eye loss (F), and ectopic tissues in eye regions (G).

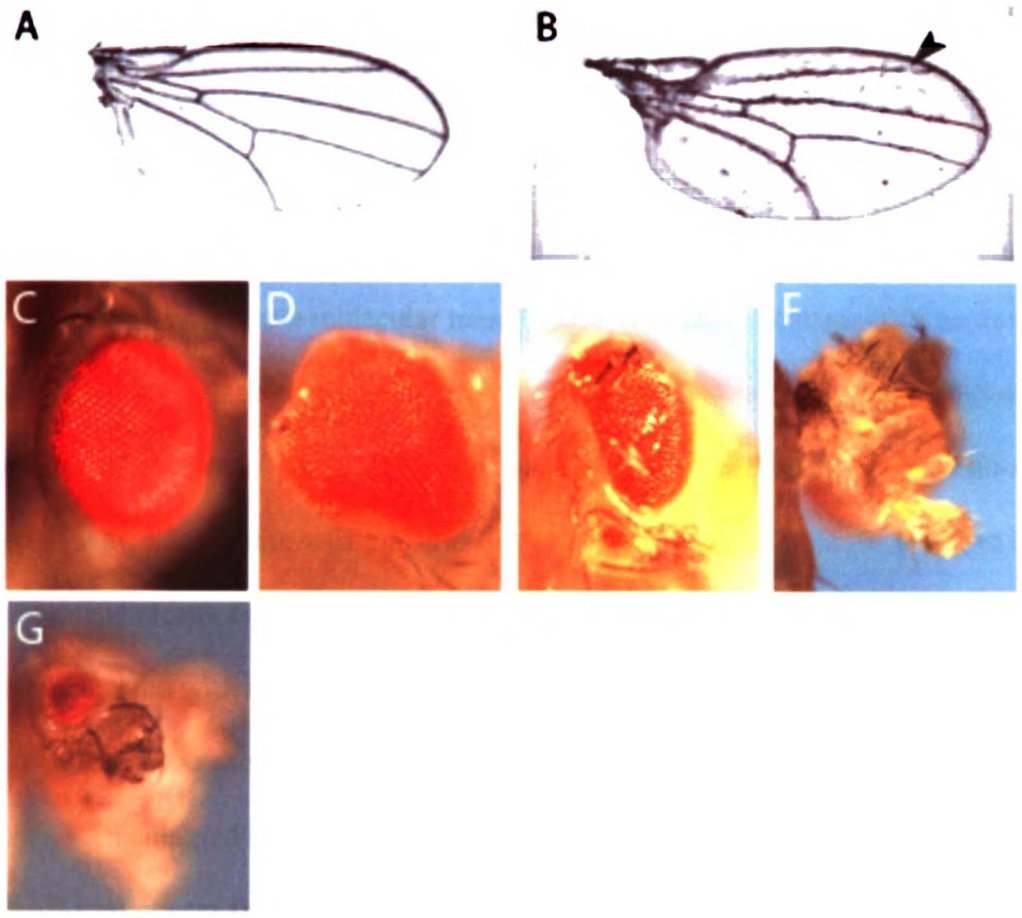
A
B
C
D
F
G

Figure 4-2. Shrub modulates the Delta/Notch signaling pathway

(A) Western blot analysis of Notch in wild-type and *shrub*^{4} mutant embryos. Notch full-length (N-FL) and transmembrane domain (N-TM) could be detected. (B) Delta isoforms in wild-type and *shrub*^{4} mutant embryos. Anti-β-tubulin (β-tub) was used as a loading control. Numbers indicate molecular mass in kDa. (C) Dorsal cluster PNS neurons in wild-type embryos labeled with anti-Futsch antibody. (D) Notch-dependent transcription in wild-type embryos as shown by LacZ staining. (E) Merged image from panels (C) and (D). (F) An enlarged image of one dorsal cluster from Panel C. (G) An enlarged image of one dorsal cluster from panel E. (H) Dorsal cluster PNS neurons in *shrub*^{4} mutant embryos labeled with anti-Futsch antibody. (I) Notch-dependent transcription in *shrub*^{4} mutant embryos as shown by LacZ staining. (J) An merged image from panels (F) and (G). (K) An enlarged image of one dorsal cluster from Panel H. (L) An enlarged image of one dorsal cluster from Panel J. The arrow indicates the ddaE neuron that shows increased Notch-dependent transcription.

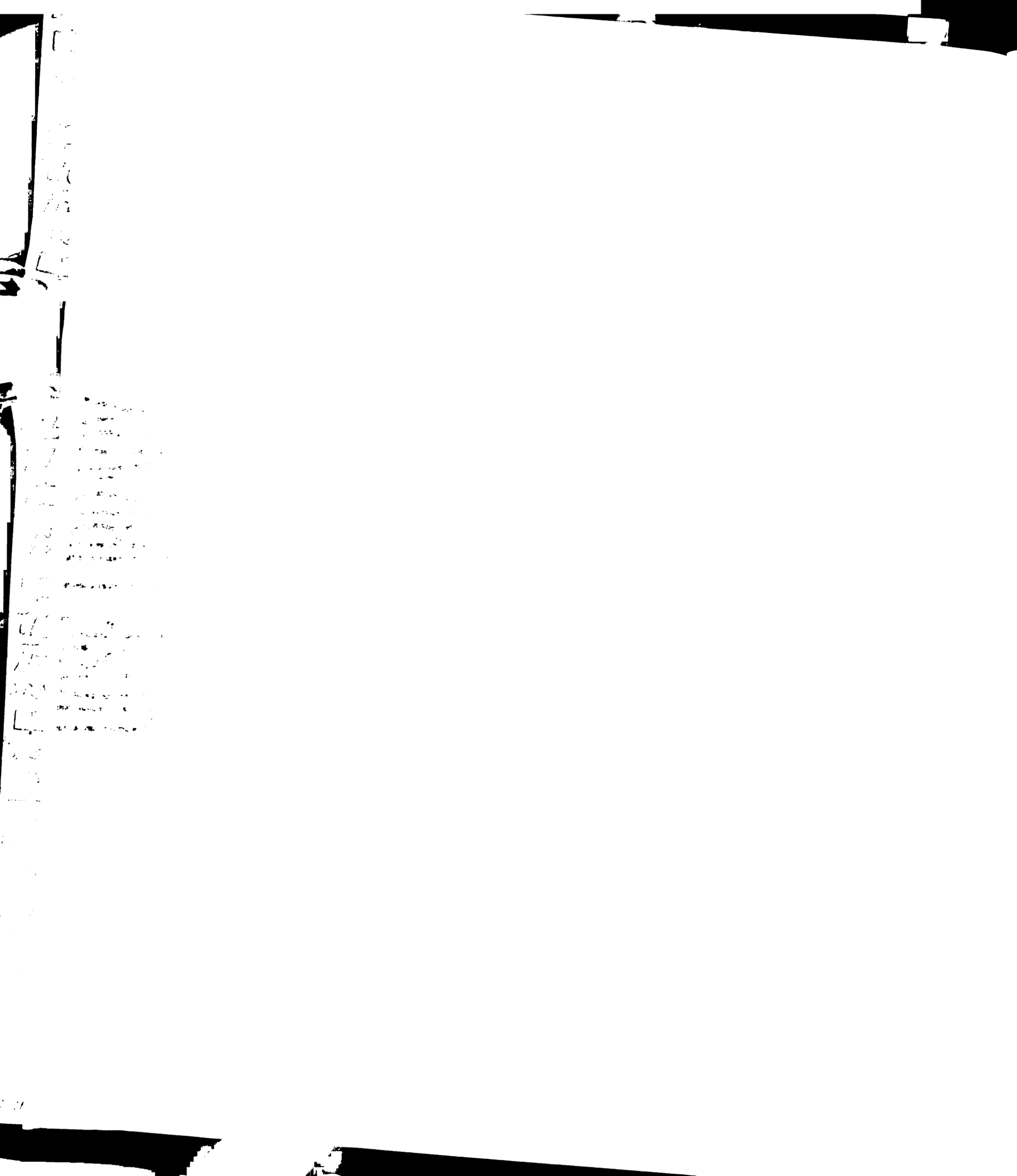

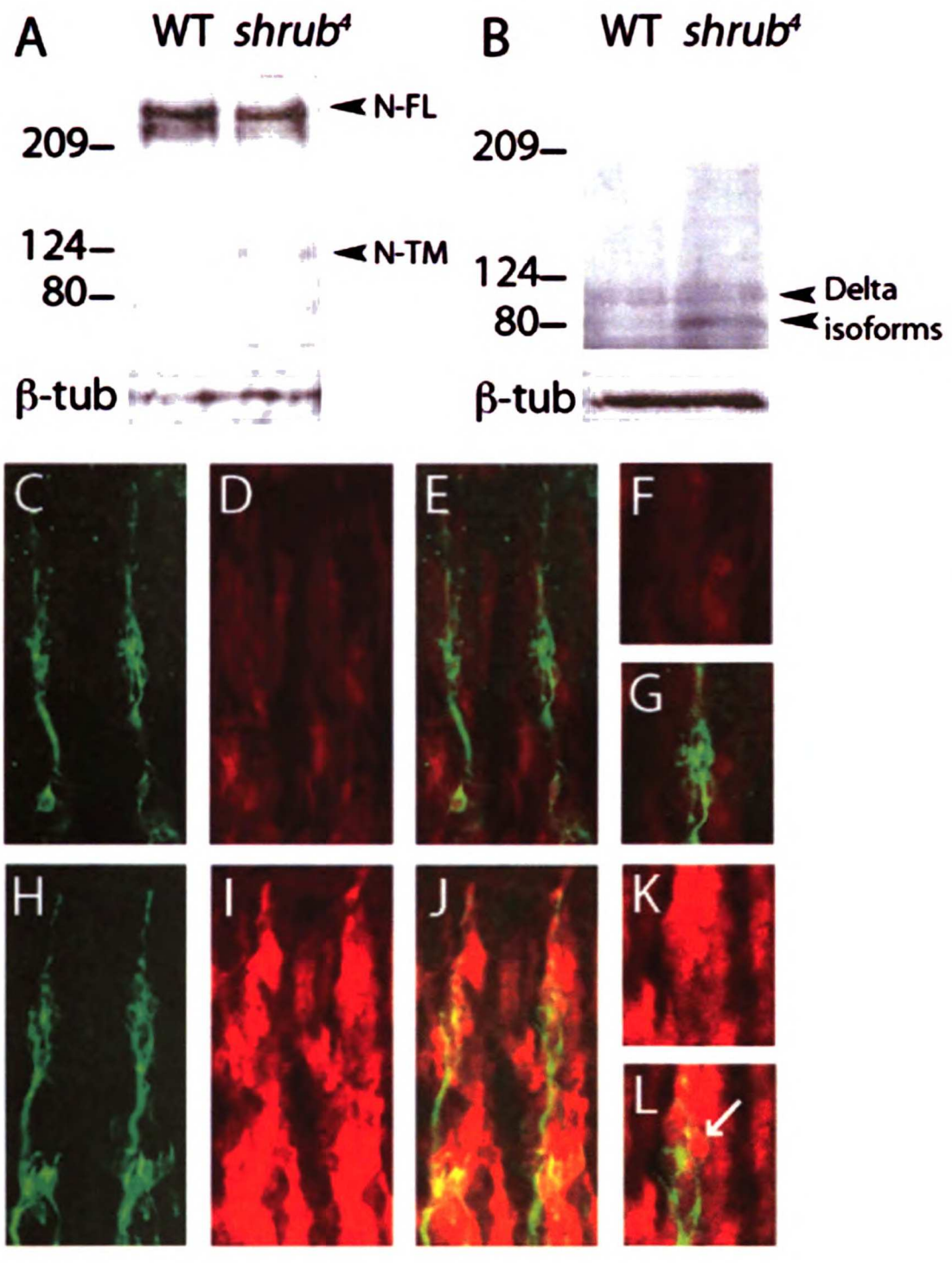
A
WT
shrub4
209–
124–
80–
N-FL
N-TM
β-tub
B
WT
shrub4
209–
124–
80–
Delta
isoforms
β-tub
C
D
E
F
G
H
I
J
K
L

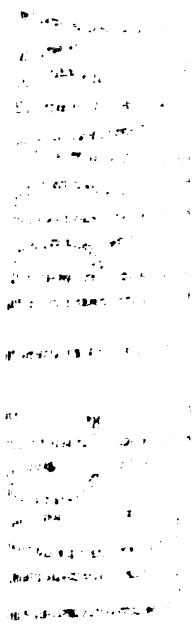

Figure 4-3. The cell-autonomous function of Notch in controlling dendritic morphogenesis

(A) A wild-type ddaC neuron clone labeled by MARCM. (B) A *Notch*$^{-}$ ddaC neuron clone exhibits decreased dendritic branching. (C) Quantification of dendritic branching. Bar 1: wild-type ddaC neuron clones generated by MARCM. Bar 2: *Notch*$^{-}$ ddaC neuron clones generated by MARCM. Bar 3: wild-type ddaC neurons as labeled by *Gal4*^{477}. Bar 4: ddaC neurons that express a constitutively active form of Notch under the control of *Gal4*^{477}. Bar 5: ddaC neurons that express a dominant-negative form of Notch. (D) A wild-type vpda neuron labeled with *Gal4*^{221}. (E) A vpda neuron expressing UAS-*Notch*$^{\Delta E}$. (F) Quantification of dendritic branching. Bar 1: wild-type vpda neurons as labeled by *Gal4*^{221}. Bar 2: vpda neurons that a constitutively active form of Notch under the control of *Gal4*^{221}. Values are mean ± SEM. ***: $p < 0.001$. Scale bar: 50 μm.

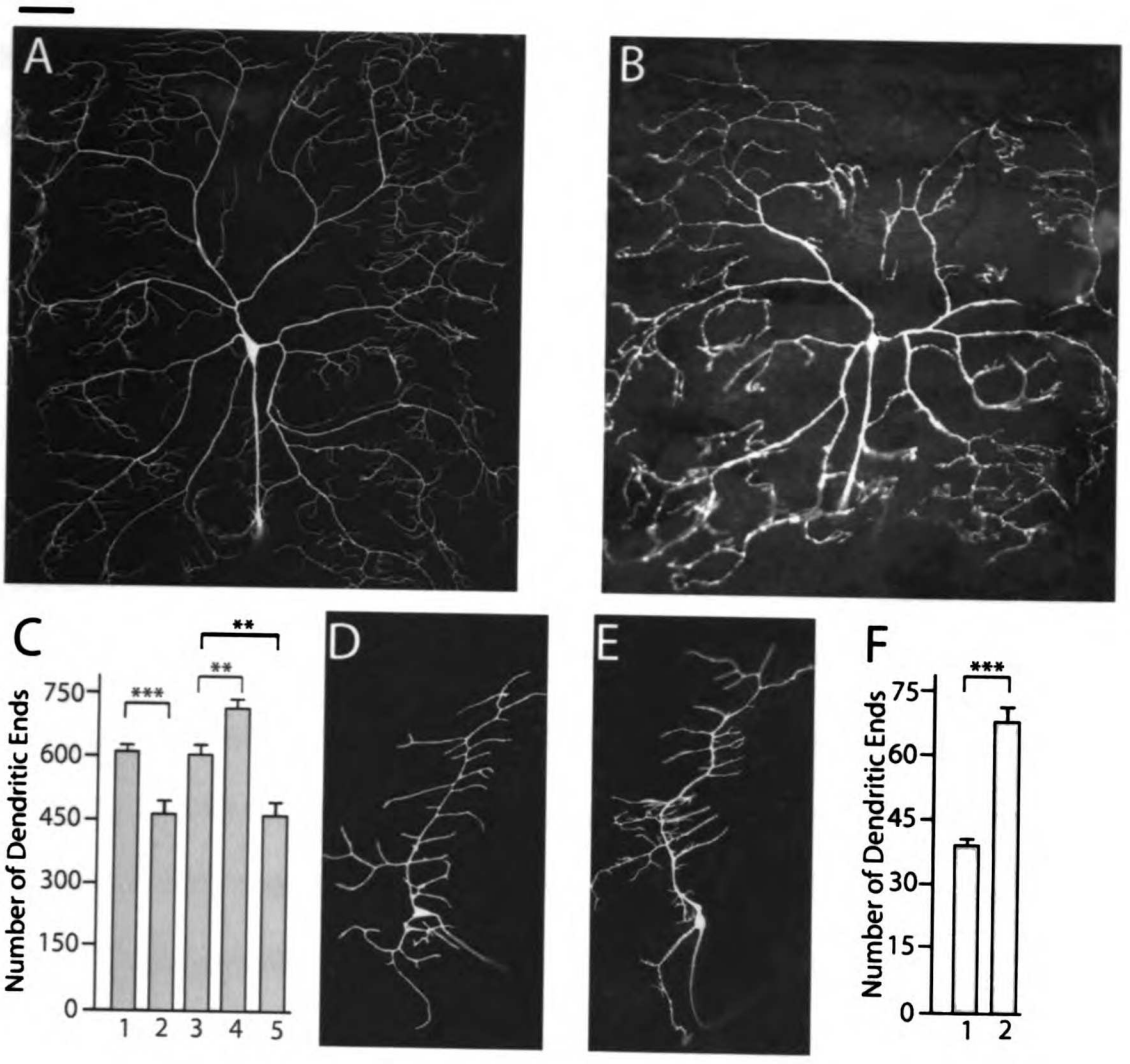
A
B
C
D
E
F
Number of Dendritic Ends
750
600
450
300
150
0
1 2 3 4 5
***
**
**
Number of Dendritic Ends
75
60
45
30
15
0
1 2
***

Figure 4-4. The cell-autonomous function of Delta in controlling dendritic morphogenesis

(A) Delta-GFP localization in a cluster of wild-type epithelial cells. (B) Delta-GFP localization in a cluster of epithelial cells expressing *shrub* RNAi. (C) Punctate Delta-GFP localization in a wild-type ddaE neuron. Arrowhead shows localization at dendritic terminal and arrow shows localization at dendritic branch point. (D) A wild-type ddaC neuron. (E) A *Delta*$^{-}$ ddaC neuron exhibits decreased dendritic branching. (F) Quantification of dendritic branching in wild-type and *Delta*$^{-}$ ddaC neurons generated with MARCM. (G) A wild-type ddaE neuron labeled with *Gal4*^{221}. (H) A ddaE neuron expressing UAS-*Delta-Truncated* (UAS-*Dl-D*) by *Gal4*^{221}. (I) A ddaE neuron expressing two copies of UAS-*Neuralized* (UAS-*Neur)* by *Gal4*^{221}. (J) Quantification of dendritic branching in ddaE neurons that are either wild-type (G), expressing UAS-*Delta-Truncated* (H), or expressing UAS-*Neuralized* (I). Values are mean ± SEM. ***: $p < 0.001$, *: $p < 0.05$. Scale bar: 50 μm.

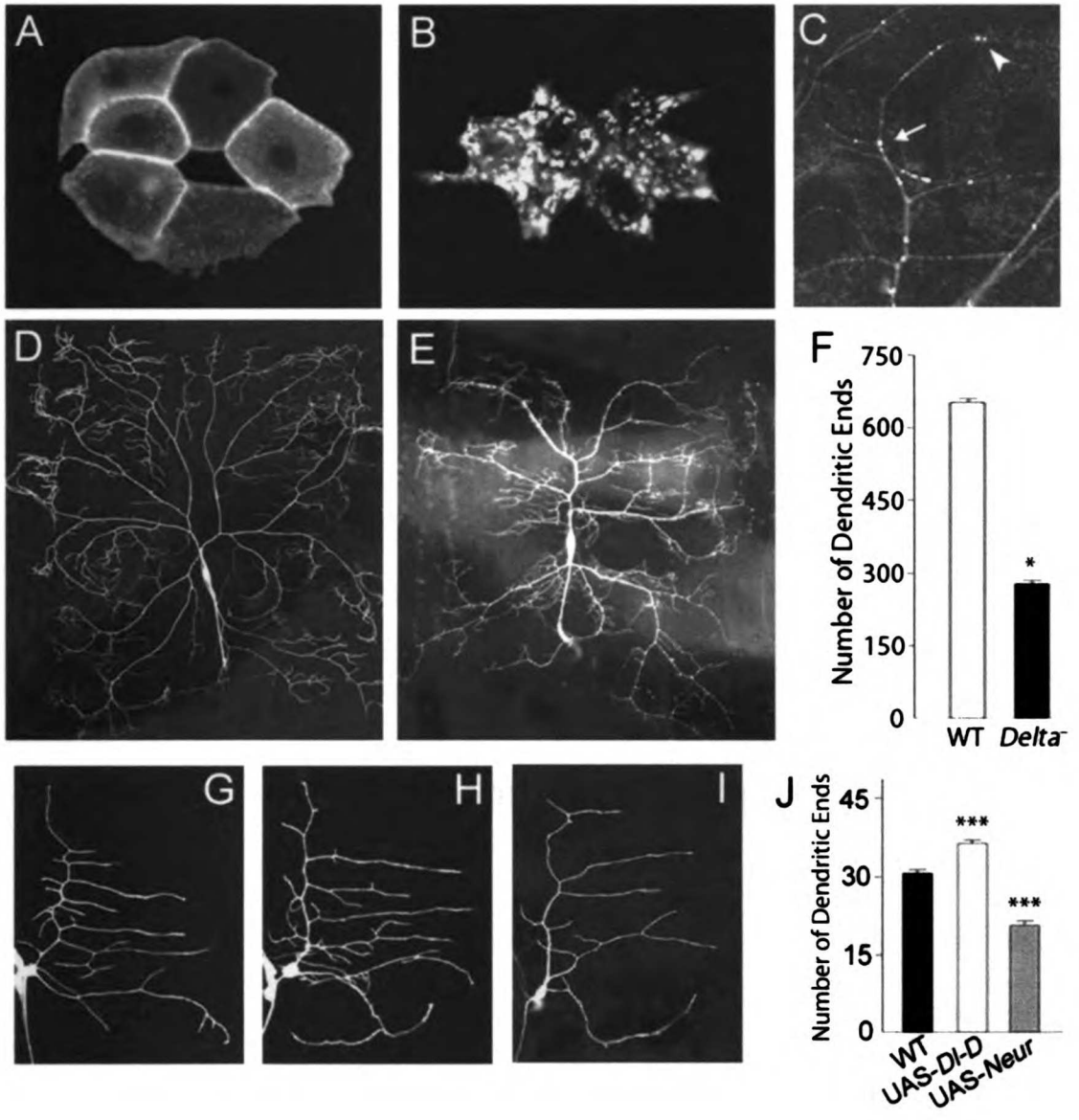
A
B
C
D
E
F
750
600
450
300
150
0
Number of Dendritic Ends
*
WT
Delta-
G
H
I
J
45
30
15
0
Number of Dendritic Ends
***
***
WT
UAS-Dl-D
UAS-Neur

Experimental Procedures

Fly Stocks and Genetic Crosses

Genetic crosses were carried out at 25° or 29°C with standard fly food medium. The following stocks were used: (1) *Gal4 109(2)80*, UAS-*GFP*, which labels all MD neurons and small cluster of epithelial cells in each segment, as well as a small number of CNS neurons; (2) y^1 *w*; flamingo*^{E59}*/Cyo*; (3) y^1 *w*; GAL4–109(2)80*, UAS-*GFP*, *flamingo*^{72}*/Cyo;* (4) *Gal4 109(2)80*, UAS-*GFP*, *shrub*^{4}*/CyO*, *Krüppel-Gal4*, UAS-*GFP*; (5) UAS-*shrub*; (6) UAS-*mSnf7-1*; (7) UAS-*mSnf7-3*; (8) *tubulin-Gal4*, which drives ubiquitous gene expression; (9) *FRT*^{G13}, *shrub*^{4}*/CyO*; (10) *Gal4*^{C155}, UAS-*mCD8::GFP*, *hs-FLP1*, which expresses GFP at a high level in all neurons but also detectable in epithelial cells in larvae; (11) *tubP-Gal80*, *FRT*^{G13}*/CyO*; (12) *FRT*^{G13} *P{ovoD1-18}2R/T(1;2)OR64/CyO;* (13) *hs-FLP1*, y^1 w^*; *Noc*^{Sco}*/CyO;* (14) *Gal4*^{221}, UAS-*mCD8::GFP*, which labels ddaE, ddaF, and vpda neurons in each segment, and *Gal4*^{477}, UAS-*mCD8::GFP*, which labels ddaC neurons. (15) UAS-*shrub-RNAi* (16) UAS-*shrub-GFP*; (17) UAS-*spinster-RFP* (gift from S. Sweeney and G. Davis); (18) UAS-*Rab4-RFP* (Bloomington); (19) UAS-*Rab7-GFP* and UAS-*Rab5-RFP* (kindly provided by M. González-Gaitán); (20) *E(spl)m8-lacZ* (kindly provided by F. Schweisguth); (21) *w N*$^{264-39}$ *FRT*^{19A}*/FM7*; (22) *eyeless-Gal4;* (23) UAS-*Notch-DN*; (24) UAS-*Notch*$^{\Delta E}$ (activated Notch); (25) *tub-Gal80, hs-FLP1, FRT*^{19A}*; Gal4109(2)80*, UAS-*mCD8::GFP/CyO;* (26) UAS-*Delta-GFP*; (27) *tubP-Gal80, FRT*^{82B}*/CyO*; (28) UAS-*Delta-Truncated* (UAS-*Dl-D)* (29) UAS-*Neuralized* (kindly provided by E. Lai); (30) *Gal4-1348*;. Maternal germline recombination was performed as described (Chou et al., 1993).

Single-Neuron MARCM

The cell-autonomous function of *flamingo, shrub, Notch and Delta* in single DA sensory neurons was analyzed as described (Li et al., 2004). For the *flamingo*^{E59}, *flamingo*^{72}, *and shrub*^{4} mutations, the protocol was similar, and it will be described here for *shrub*^{4}. The *shrub*^{4} mutation was first recombined onto the chromosome containing *FRT*^{G13}. *shrub*^{4}, *FRT*^{G13}*/CyO* male flies were crossed with *Gal4*^{C155}, UAS-*mCD8::GFP, hs-FLP1/FM7* virgin flies. Then, *Gal4*^{C155}, UAS-*mCD8::GFP, hs-FLP1*; *shrub*^{4}, *FRT*^{G13}/+ male flies were crossed with *Gal4*^{C155}, UAS-*mCD8::GFP, hs-FLP1; tubP-Gal80, FRT*^{G13}*/CyO* virgin flies. For *Notch* MARCM analysis, *w N*$^{264-39}$ *FRT*^{19A}*/FM7* and *tub-Gal80, hs-FLP1, FRT*^{19A} lines were used. *N*$^{264-39}$ is a loss-of-function *Notch* allele (Lehman et al., 1983). For *Delta* MARCM analysis, *P{neoFRT}82B P{lacW}Dl*$^{[S1485041]}$ and *tubP-Gal80, FRT*^{82B} lines were used. Images of dendritic morphology of single DA neurons were recorded with a Nikon confocal microscope (D-Eclipse C1). The significance of difference in dendritic termini number was determined with Student's t tests. The ability to infer cell-autonomous function from single DA sensory neuron clones in *Drosophila* larvae has been described (Sweeney et al., 2002).

Imaging and Quantitative Analysis of Dorsal Cluster DA Neuron Dendrites

Staged wild-type or *shrub*^{4} mutant embryos were collected on grape agar plates and processed as described (Gao et al., 1999). The dendritic morphology of GFP-labeled dorsal DA neurons was imaged by confocal microscopy (Nikon, D-Eclipse C1). The dendritic field area was calculated as described (Li et al., 2004). To calculate branching complexity, different orders of dendritic branches were counted by the centrifugal

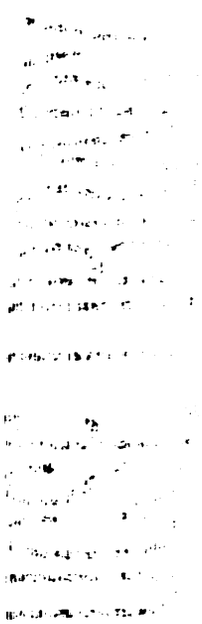

method (Uylings et al., 1975). All statistical analyses were done with Student's t tests. The number of dendritic ends of ddaE neurons was lower when *Gal4*^{221}, UAS-*mCD8::GFP* was used to visualize dendritic morphology as compared to ddaE MARCM clones (Li et al., 2004). The number also varies from early to late third instar larval stages.

Mapping and Sequence Analysis

The second chromosome deficiency kit (DK-2, Bloomington Stock Center) was used to identify deficiency lines that cover the lethal mutations in *shrub*^{4}. We then used P element insertion lines or small deletion lines (Bloomington Stock Center) to further narrow down the locus of the mutation in *shrub*^{4}. To identify the *shrub*^{4} mutations, we isolated genomic DNA from homozygous *shrub*^{4} mutant embryos. Primers were designed based on the wild-type gene sequence from FlyBase, and independent polymerase chain reactions were carried out to clone and sequence both strands of the mutant DNA. Coiled-coiled domains were predicted with the COILS program (Lupas et al., 1991).

Western Blot Analysis and Immunohistochemistry

The expression of Shrub, Notch, and Delta in *Drosophila* embryos was analyzed by western blot according to the standard protocol provided by Bio-Rad. For each antigen, western blot analysis was repeated at least twice. Protein extracts were prepared from wild-type or *shrub*^{4} mutants at 16–20 hr AEL. Anti-Shrub rabbit polyclonal antibody was generated with a purified fusion protein consisting of GST and the full-length Shrub.

The full-length *shrub* coding region was amplified by PCR and cloned into pGEX-4T-1 vector, and the resulting construct was used to transform *E. coli* for protein purification. For western blot, anti-Shrub antibody (1:500 dilution), mouse anti-Notch C17.9C6 (1:5000, Developmental Studies Hybridoma Bank (DSHB)), and mouse anti-Delta C594.9B (1:10,000, DSHB) were used as primary antibodies. Horseradish peroxidase-conjugated donkey anti-rabbit IgG and donkey anti-mouse antibody (Jackson ImmunoResearch Laboratories) were used as secondary antibodies (1:2000). For antibody immunostaining, embryos were fixed as described (Sweeney et al, 2002). Rabbit polyclonal antibody β-galactocidase (1:5000, Cappel) and mouse anti-Futsch 22C10 (1:20, DSHB) were used as primary antibodies, and Cy3-conjugated goat anti-rabbit and Cy2-conjugated goat anti-mouse IgG (Jackson ImmunoResearch Laboratories, 1:100) as secondary antibodies.

Generation of Transgenic Fly Lines

To generate UAS-*shrub*, the *shrub* ORF sequence was amplified by PCR using the primers 5'-GGCGAATTCATGAGTTTCTTCGGGAAGATGTTCGG-3' and 5'-GGC ATCTAGATTAGTTGGACCAGGATAAAAGCTGCTTC-3' and subcloned into the pUAST vector. Primers 5'-ATATATAGATCTATGTCGGTGTTCGGGAAGCT-3' and 5'-CGATCGTCTAGATTACATGGATCCGGCCCA-3' were used to amplify *mSnf7-1* from an EST clone and ligate into pUAST at the BglII/XbaI sites. Primers 5'-ATATGA ATTCATGAGCAAGTTGGGT-3' and 5'-ATATATTCTAGATTAAGTGGCCCAAGC-3' were used to amplify *mSnf7-3* from an EST clone and ligate into pUAST at the EcoRI/XbaI sites.

To generate UAS-*shrub-GFP*, 5'-ATATGAATTCATGAGTTTATTAGGGAAG-3' and 5'-GCGGGATCCCCTTAGTTGGACCAGGATAA-3' were used to amplify the *shrub* coding region that was subcloned together with GFP into the pUAST vector. To generate UAS-*shrub-RNAi*, a 782-bp DNA fragment corresponding to 198 bp at the end of the CG8055 coding region plus 584 bp of the 3' UTR was amplified by PCR and cloned into the pCR 2.1-TOPO vector (Invitrogen). The primers were: 5'-GAATTCG GGAACTCGACGAGCTG-3' and 5'-GGTGACACTATAGAACTCGAG-3'. This plasmid was then digested with EcoRI and BglII to give a 493-bp fragment. This fragment was cloned into pUAST at EcoRI/BglII sites. Then, the same fragment in a reverse orientation was cloned into the same vector between the BglII and XbaI sites with one blunt end.

Larval Viability Rescue Assay

To rescue larval viability of *shrub*^{4} mutants by UAS-*shrub*, *shrub*^{4}*/ CyO*, *Krüppel-Gal4*, UAS-*GFP*; *tubulin-GAL4*/+ flies were crossed with *shrub*^{4}*/ CyO*, *Krüppel-Gal4*, UAS-*GFP*; *UAS-shrub*/+ flies. The survival rate was calculated by dividing the number of observed larvae with the genotype *shrub*^{4}; UAS-*shrub*/*tubulin-Gal4* by the maximum possible larvae with this genotype. Since larval viability without rescue was 0% (calculated by crossing *shrub*^{4}*/CyO*, *Krüppel-Gal4*, UAS-*GFP; tub-GAL4*/+ flies with *shrub*^{4}*/ CyO, Krüppel-Gal4*, UAS-*GFP* flies), we assumed that both UAS-*shrub* and *tubulin-Gal4* must be present for viability. Rescue by mSnf7-1 or mSnf7-3 was quantified at the same time with UAS-*mSnf7-1* or UAS-*mSnf7-3* replacing UAS-*shrub* in the cross described above.

References

Aakalu, G., Smith, W.B., Nguyen, N., Jiang, C., and Schuman, E.M. (2001). Dynamic visualization of local protein synthesis in hippocampal neurons. Neuron *30*: 489-502.

Adams, C. M., Andersen, M. G., Motto, D. G., Price, M. P., Johnson, W. A., and Welsh, M. J. (1998). Ripped pocket and pickpocket, novel Drosophila DEG/EnaC subunits expressed in early development and in mechanosensory neurons. Journal of Cell Biology *140*, 143–152.

Altman, J., and Anderson, W.J. (1972). Experimental reorganization of the cerebellar cortex. I. Morphological effects of elimination of all microneurons with prolonged x-irradiation started at birth. Journal of Compative Neurology *146*: 355-406.

Andersen, R., Li, Y., Resseguie, M., and Brenman, J.E. (2005). Calcium/calmodulin-dependent protein kinase II alters structural plasticity and cytoskeletal dynamics in *Drosophila*. Journal of Neuroscience *25*, 8878–8888.

Artavanis-Tsakonas, S., Rand, M.D., and Lake, R.J. (1999). Notch signaling: cell fate control and signal integration in development. Science *284*, 770–776.

Babst, M. (2005). A protein's final ESCRT. Traffic *6*, 2–9.

Babst, M., Katzmann, D.J., Estepa-Sabal, E.J., Meerloo, T., and Emr, S.D. (2002a). ESCRT-III: an endosome-associated heterooligomeric protein complex required for MVB sorting. Developmental Cell *3*, 271–282.

Babst, M., Katzmann, D.J., Snyder, W.B., Wendland, B., and Emr, S.D. (2002b). Endosome-associated complex, ESCRT-II, recruits transport machinery for protein sorting at the multivesicular body. Developmental Cell *3*, 283–289.

Babst, M., Wendland, B., Estepa, E.J., and Emr, S.D. (1998). The Vps4p AAA ATPase regulates membrane association of a Vps protein complex required for normal endosome function. EMBO Journal *17*, 2982–2993.

Baker, R.E., Dijkhuizen, P.A., Van Pelt, J., and Verhaagen, J. (1998). Growth of pyramidal, but not non-pyramidal, dendrites in long-term organotypic explants of neonatal rat neocortex chronically exposed to neurotrophin-3. European Journal of Neuroscience *10*: 1037-44.

Baptista, C.A., Hatten, M.E., Blazeski, R., and Mason, C.A. (1994). Cell-cell interactions influence survival and differentiation of purified Purkinje cells *in vitro*. Neuron *12*: 243-60.

Berezovska, O., McLean, P., Knowles, R., Frosh, M., Lu, F.M., Lux, S.E., and Hyman, B.T. (1999). Notch1 inhibits neurite outgrowth in postmitotic primary neurons. Neuroscience *93*, 433–439.

Berezovska, O., Xia, M.Q., and Hyman, B.T. (1998). Notch is expressed in adult brain, is coexpressed with presenilin-1, and is altered in Alzheimer disease. Journal of Neuropathology and Experimental Neurology *57*, 738–745.

Bodmer, R., Carretto, R., and Jan, Y. N. (1989). Neurogenesis of the peripheral nervous system in *Drosophila* embryos: DNA replication patterns and cell lineages. Neuron *3*, 21–32.

Bodmer, R., and Jan, Y.N. (1987). Morphological differentiation of the embryonic peripheral neurons in *Drosophila*. Roux's Archive of Developmental Biology *196*, 69–77.

Bradke, F., and Dotti, C. G. (2000). Establishment of neuronal polarity: Lessons from cultured hippocampal neurons. Current Opinion in Neurobiology *10*, 574–581.

Brand, A. H., and Perrimon, N. (1993). Targeted gene expression as a means of altering cell fates and generating dominant phenotypes. Development *118*, 401–415.

Brenman, J.E., Gao, F.-B., Jan, L.Y., and Jan, Y.N. (2001). Sequoia, a tramtrack-related zinc finger protein, functions as a pan-neural regulator for dendrite and axon morphogenesis in *Drosophila*. Developmental Cell *1*, 667–677.

Brewster, R., and Bodmer, R. (1995). Origin and specification of type II sensory neurons in *Drosophila*. Development *121*, 2923– 2936.

Brose, K., and Tessier-Lavigne, M. (2000). Slit proteins: Key regulators of axon guidance, axonal branching, and cell migration. Current Opinion in Neurobiology *10*, 95–102.

Campos-Ortega, J. A., and Hartenstein, V. (1985). "The Embryonic Development of *Drosophila melanogaster*," Second edition. Springer-Verlag, New York.

Cantallops, I., Haas, K., and Cline, H. T. (2000). Postsynaptic CPG15 promotes synaptic maturation and presynaptic axon arbor elaboration *in vivo*. Nature Neuroscience *10*, 1004–1011.

Chae, J., Kim, M. J., Goo, J. H., Collier, S., Gubb, D., Charlton, J., Adler, P. N., and Park, W. J. (1999). The Drosophila tissue polarity gene starry night encodes a member of the protocadherin family. Development *126*, 5421–5429.

Chou, T.B., Noll, E. and Perrimon, N. (1993). Autosomal P[ovoD1] dominant female-sterile insertions in *Drosophila* and their use in generating germ-line chimeras. Development *119*, 1359–1369.

Clark, I.E., Jan, L.Y., and Jan, Y.N. (1997). Reciprocal localization of Nod and kinesin fusion proteins indicates microtubule polarity in the *Drosophila* oocyte, epithelium, neuron and muscle. Development *124*: 461-70.

Craig, A. M., and Banker, G. (1994). Neuronal polarity. Annual Review of Neuroscience *17*, 267–310.

Cline, H.T. (2001). Dendritic arbor development and synaptogenesis. Current Opinion in Neurobiology *11*: 118-26.

Crowner, D., Le Gall, M., Gates, M.A., and Giniger, E. (2003). Notch steers *Drosophila* ISNb motor axons by regulating the Abl signaling pathway. Current Biology *13*, 967–972.

Curtin, J.A., Quint, E., Tsipouri, V., Arkell, R.M., Cattanach, B., Copp, A.J., Henderson, D.J., Spurr, N., Stanier, P., Fisher, E.M., Nolan, P.M., Steel, K.P., Brown, S.D., Gray, I.C., and Murdoch, J.N. (2003). Mutation of Celsr1 disrupts planar polarity of inner ear hair cells and causes severe neural tube defects in the mouse. Current Biology *13*, 1129-33.

De Joussineau, C., Soule, J., Martin, M., Anguille, C., Montcourrier, P., and Alexandre, D. (2003). Delta-promoted filopodia mediate long-range lateral inhibition in *Drosophila*. Nature *426*, 555–559.

De Strooper, B., Annaert, W., Cupers, P., Saftig, P., Craessaerts, K., Mumm, J.S., Schroeter, E.H., Schrijvers, V., Wolfe, M.S,, Ray, W.J., Goate, A., and Kopan, R. (1999). A presenilin-1-dependent gamma-secretase-like protease mediates release of Notch intracellular domain. Nature *398*, 518–522.

Emoto, K., He, Y., Ye, B., Grueber, W.B., Adler, P.N., Jan, L.Y., and Jan, Y.N. (2004). Control of dendritic branching and tiling by the Tricornered-kinase/Furry signaling pathway in *Drosophila* sensory neurons. Cell *119*, 245–256.

Engert, F., and Bonhoeffer, T. (1999). Dendritic spine changes associated with hippocampal long-term synaptic plasticity. Nature *399*, 66–70.

Fehon, R.G., Kooh, P.J., Rebay, I., Regan, C.L., Xu, T., Muskavitch, M.A., Artavanis-Tsakonas, S. (1990). Molecular interactions between the protein products of the neurogenic loci *Notch* and *Delta*, two EGF-homologous genes in *Drosophila*. Cell *61*, 523–534.

Feng, G., Mellor, R. H., Bernstein, M., Keller-Peck, C., Nguyen, Q. T., Wallace, M., Nerbonne, J. M., Lichtman, J. W., and Sanes, (2000). Imaging multiple spectral variants of GFP. Neuron *28*, 41–51.

Franklin, J.L., Berechid, B.E., Cutting, F.B., Presente, A., Chambers, C.B., Foltz, D.R.,

Ferreira, A., and Nye, J.S. (1999). Autonomous and non-autonomous regulation of mammalian neurite development by Notch1 and Delta1. Current Biology *9*, 1448–1457.

Fuerstenberg, S., and Giniger, E. (1998). Multiple roles for notch in *Drosophila* myogenesis. Developmental Biology *201*, 66–77.

Furrer, M.P., Kim, S., Wolf, B., and Chiba, A. (2003). Robo and Frazzled/DCC mediate dendritic guidance at the CNS midline. Nature Neuroscience *6*: 223-30.

Gan, W.B., Kwon, E., Feng, G., Sanes, J.R., and Lichtman, J.W. (2003). Synaptic dynamism measured over minutes to months: age-dependent decline in an autonomic ganglion. Nature Neuroscience 6: 956-60.

Gao, F.-B., Brenman, J.E., Jan, L.Y., and Jan, Y.N. (1999). Genes regulating dendritic outgrowth, branching, and routing in *Drosophila*. Genes and Development *13*, 2549–2561.

Gao, F.-B., Kohwi, M., Brenman, J.E., Jan, L.Y., and Jan, Y.N. (2000). Control of dendritic field formation in *Drosophila*: The roles of Flamingo and competition between homologous neurons. Neuron *28*, 91–101.

Ghysen, A., Dambly-Chaudière, C., Aceves, E., Jan, L. Y., and Jan, Y. N. (1986). Sensory neurons and peripheral pathways in *Drosophila* embryos. Roux's Archive of Developmental Biology *195*, 281–289.

Giniger, E., Jan, L.Y., and Jan, Y.N. (1993). Specifying the path of the intersegmental nerve of the *Drosophila* embryo: a role for Delta and Notch. Development *117*, 431–440.

Goldberg, J.L., Klassen, M.P., Hua, Y., and Barres, B.A. (2002). Amacrine-signaled loss of intrinsic axon growth ability by retinal ganglion cells. Science *296*: 1860-4.

Grueber, W.B., Jan, L.Y., and Jan, YN. (2002). Tiling of the *Drosophila* epidermis by multidendritic sensory neurons. Development *129*, 2867–2878.

Grueber, W.B., Jan, L.Y., and Jan, Y.N. (2003). Different levels of the homeodomain protein cut regulate distinct dendrite branching patterns of *Drosophila* multidendritic neurons. Cell *112*, 805–818.

Gruenberg, J., and Stenmark, H. (2004). The biogenesis of multivesicular endosomes. Nature Reviews in Molecular and Cell Biology *5*, 317–323.

Howard, T.L., Stauffer, D.R., Degnin, C.R., and Hollenberg, S.M. (2001). CHMP1 functions as a member of a newly defined family of vesicle trafficking proteins. Journal of Cell Science *114*, 2395–2404.

Haas, H., Sin, W-C., Javaherian, A., Li, Z., and Cline, H. T. (2001). Single-cell electroporation for in vivo neuronal gene expression. Neuron *29*, 583–591.

Higgins, D., Burack, M., Lein, P., and Banker, G. (1997). Mechanisms of neuronal polarity. Current Opinion in Neurobiology *7*, 599–604.

Hitchcock, P.F. (1989). Exclusionary dendritic interactions in the retina of the goldfish. Development *106*: 589-98.

Huang, M.-L., Hsu, C. H., and Chien, C.-T. (2000). The proneural gene *amos* promotes multiple dendritic neuron formation in the *Drosophila* peripheral nervous system. Neuron *25*, 57–67.

Huppert, S.S., Jacobsen, T.L., and Muskavitch, M.A. (1997). Feedback regulation is central to Delta-Notch signalling required for *Drosophila* wing vein morphogenesis. Development *124*, 3283–3291.

Ikeuchi, T., and Sisodia, S.S. (2003). The Notch ligands, Delta1 and Jagged2, are substrates for presenilin-dependent "gamma-secretase" cleavage. Journal of Biological Chemistry *278*, 7751–7754.

Jan, Y. N., and Jan, L. Y. (1993). The peripheral nervous system. In "The Development of *Drosophila melanogaster*," pp. 1207– 1244. Cold Spring Harbor Press, Cold Spring Harbor, NY.

Jan, Y. N., and Jan, L. Y. (2000). Polarity in cell division: What frames thy fearful asymmetry? Cell *100*, 599–602.

Jan, Y. N., and Jan, L. Y. (2001). Dendrites. Genes and Development *15*, 2627–2641.

Jan, Y.N., and Jan L.Y. (2003). The control of dendrite development. Neuron *40*: 229-42.

Jefferis, G.S., Marin, E.C., Stocker, R.F., and Luo, L. (2001). Target neuron prespecification in the olfactory map of Drosophila. Nature *414*: 204-8.

Jefferis, G.S., Vyas, R.M., Berdnik, D., Ramaekers, A., Stocker, R.F., Tanaka, N.K., Ito, K., and Luo, L. (2004). Developmental origin of wiring specificity in the olfactory system of *Drosophila*. Development *131*: 117-30.

Jekely, G., and Rorth, P. (2003). Hrs mediates downregulation of multiple signaling receptors *in Drosophila*. EMBO Reports *4*, 1163–1168.

Jessell, T. M. (2000). Neuronal specification in the spinal cord: Inductive signals and transcriptional codes. Nature Reviews Genetics *1*, 20–29.

Jonsson, F., and Knust, E. (1996). Distinct functions of the *Drosophila* genes Serrate and Delta revealed by ectopic expression during wing development. Developmental Genetics and Evolution *206*, 91–101.

Jontes, J. D., and Smith, S. J. (2000). Filopodia, spines and the generation of synaptic diversity. Neuron *27*, 11–14.

Katoh, K., Shibata, H., Suzuki, H., Nara, A., Ishidoh, K., Kominami, E., Yoshimori, T., and Maki, M. (2003). The ALG-2-interacting protein Alix associates with CHMP4b, a human homologue of yeast Snf7 that is involved in multivesicular body sorting. Journal of Biological Chemistry *278*, 39104–39113.

Katoh, K., Shibata, H., Hatta, K., and Maki, M. (2004). CHMP4b is a major binding partner of the ALG-2-interacting protein Alix among the three CHMP4 isoforms. Archives of Biochemistry and Biophysics *421*, 159–165.

Katzmann, D.J., Babst, M., and Emr, S.D. (2001). Ubiquitin-dependent sorting into the multivesicular body pathway requires the function of a conserved endosomal protein sorting complex, ESCRT-I. Cell *106*, 145–155.

Kim S, Chiba A. (2004). Dendritic guidance. Trends in Neurosciences *27*: 194-202.

Klueg, K.M., Parody, T.R., Muskavitch, M.A. (1998). Complex proteolytic processing acts on Delta, a transmembrane ligand for Notch, during *Drosophila* development. Molecular Biology of the Cell *9*, 1709–1723.

Knoblich, J.A. (2001). *The Drosophila* nervous system as a model for asymmetric cell division. Symposia of the Society for Experimental Biology *53*: 75-89.

Koester, S.E., and O'Leary, D.D. (1992), Functional classes of cortical projection neurons develop dendritic distinctions by class-specific sculpting of an early common pattern. Journal of Neuroscience *12*: 1382-93.

Kolodziej, P.A., Jan, L.Y., and Jan, Y.N. (1995). Mutations that affect the length, fasciculation, or ventral orientation of specific sensory axons in the *Drosophila* embryo. Neuron *15*: 273-86.

Komiyama, T., Johnson, W.A., Luo, L., and Jefferis, G.S.X.E. (2003). From lineage to wiring specificity: POU domain transcription factors regulate precise connectivity of *Drosophila* olfactory projection neurons. Cell *112*, 157–167.

Kramer, A. P., Goldman, J. R., and Stent, G. S. (1985). Developmental arborization of sensory neurons in the leech *Haementeria ghilianii*. I. Origin of natural variations in the branching pattern. Journal of Neuroscience *5*, 759–767.

Kramer, A. P., and Stent, G. S. (1985). Developmental arborization of sensory neurons in the leech *Haementeria ghilianii*. II. Origin of natural variations in the branching pattern. Journal of Neuroscience *5*, 768–775.

Kuhl, D., and Skehel, P. (1998). Dendritic localization of mRNAs. Current Opinion inNeurobiology *8*: 600-6.

Kumar, J.P., and Moses, K. (2001). Eye specification in *Drosophila*: perspectives and implications. Seminars in Cellular and Developmental Biology *12*, 469–474.

Lai, E.C., Deblandre, G.A., Kintner, C., and Rubin, G.M. (2001). *Drosophila* neuralized is a ubiquitin ligase that promotes the internalization and degradation of delta. Developmental Cell *1*, 783–794.

Landgraf, M., Jeffrey, V., Fujioka, M., Jaynes, J.B., and Bate, M. (2003). Embryonic origins of a motor system: motor dendrites form a myotopic map in *Drosophila*. Public Library of Science Biology *1*: e41.

Le Borgne, R., Bardin, A., and Schweisguth, F. (2005). The roles of receptor and ligand endocytosis in regulating Notch signaling. Development *132*, 1751–1762.

Lecourtois, M., and Schweisguth, F. (1995). The neurogenic Suppressor of Hairless DNA-binding protein mediates the transcriptional activation of the Enhancer of split complex genes triggered by Notch signaling. Genes and Development *9*, 2598–2608.

Lee, A., Li, W., Xu, K., Bogert, B.A., Su, K., and Gao, F.-B. (2003). Control of dendritic development by the *Drosophila* fragile X-related gene involves the small GTPase Rac1. Development *130*, 5543–5552.

Lee, T., and Luo. L. (1999). Mosaic analysis with a repressible cell marker for studies of gene function in neuronal morphogenesis. Neuron *22*, 451–461.

Lee, T., Winter, C., Marticke, S.S., Lee, A., and Luo, L. (2000). Essential roles of *Drosophila* RhoA in the regulation of neuroblast proliferation and dendritic but not axonal morphogenesis. Neuron *25*: 307-16.

Lee, R.C., Clandinin, T.R., Lee, C.H., Chen, P.L., Meinertzhagen, I.A., and Zipursky, S.L. (2003). The protocadherin Flamingo is required for axon target selection in the *Drosophila* visual system. Nature Neuroscience *6*: 557-63.

Li, Z., Van Aelst, L., and Cline, H.T. (2000). Rho GTPases regulate distinct aspects of dendritic arbor growth in *Xenopus* central neurons *in vivo*. Nature Neuroscience *3*: 217-25.

Li, W., and Gao, F.-B. (2003). Actin filament-stabilizing protein tropomyosin regulates the size of dendritic fields. Journal of Neuroscience *23*, 6171–6175.

Li, W., Li, Y., and Gao, F.-B. (2005). Abelson, Enabled, and P120catenin exert distinct effects on dendritic morphogenesis in *Drosophila*. Developmental Dynamics *234*, 512–522.

Li, W., Wang, F., Menut, L., and Gao, F.-B. (2004). BTB/POZ-zinc finger protein Abrupt suppresses dendritic branching in a neuronal subtype-specific and dosage-dependent manner. Neuron *43*, 823–834.

Lin, D. M., and Goodman, C. S. (1994). Ectopic and increased expression of Fasciclin II alters motoneuron growth cone guidance. Neuron *13*, 507–523.

Liu, L., Yermolaieva, O., Johnson, W.A., Abboud, F.M., and Welsh, M.J. (2003). Identification and function of thermosensory neurons in *Drosophila* larvae. Nature Neuroscience *6*: 267-73.

Lom, B., and Cohen-Cory S. (1999). Brain-derived neurotrophic factor differentially regulates retinal ganglion cell dendritic and axonal arborization *in vivo*. Journal of Neuroscience *19*, 9928–9938.

Lu, B., Usui, T., Uemura, T., Jan, L. Y., and Jan, Y. N. (1999). Flamingo controls the planar polarity of sensory bristles and asymmetric division of sensory organ precursors in Drosophila. Current Biology *9*, 1247–1250.

Lu, B., Jan, L., and Jan, Y.N. (2000). Control of cell divisions in the nervous system: symmetry and asymmetry. Annual Review of Neuroscience *23*: 531-56.

Luo, L. (2000). Rho GTPases in neuronal morphogenesis. Nature Reviews Neuroscience *1*: 173-80.

Luo, L., Hensch, T.K., Ackerman, L., Barbel, S., Jan, L.Y., and Jan, Y.N. (1996). Differential effects of the Rac GTPase on Purkinje cell axons and dendritic trunks and spines. Nature *379*: 837-40.

Lupas, A., Van Dyke, M., and Stock, J. (1991). Predicting coiled coils from protein sequences. Science *252*, 1162–1164.

Maletic-Savatic, M., Malinow, R., and Svoboda, K. (1999). Rapid dendritic morphogenesis in CA1 hippocampal dendrites induced by synaptic activity. Science *283*, 1923–1927.

Mari-Beffa, M., de Celis, J.F., and Garcia-Bellido, A. (1991). Genetic and developmental analyses of chaetae pattern formation in *Drosophila* tergites. Roux's Archives of Developmental Biology *200*, 132–142.

Masland, R. H. (2001). Neuronal diversity in the retina. Current Opinion in Neurobiology *11*, 431–436.

Masland, R.H. (2004). Neuronal cell types. Current Biology *14*, R497–500.

Matus, A. (2000). Actin-based plasticity in dendritic spines. Science *290*, 754–758.

McAllister, A. K., Lo, D. C., and Katz, L. C. (1995). Neurotrophins regulate dendritic growth in developing visual cortex. Neuron *15*, 791–803.

McAllister, A.K., Katz, L.C., and Lo, D.C. (1997). Opposing roles for endogenous BDNF and NT-3 in regulating cortical dendritic growth. Neuron *18*: 767-78.

McAllister, A. K. (2000). Cellular and molecular mechanisms of dendrite growth. Cerebral Cortex *10*, 963–973.

Medina, P.M., Swick, L.L., Andersen, R., Blalock, Z., and Brenman, J.E. (2006). A novel forward genetic screen to identify mutations affecting larval neuronal dendrite development in *Drosophila melanogaster*. Genetics *172* (4).

Moberg, K.H., Schelble, S., Burdick, S.K., and Hariharan, I.K. (2005). Mutations in erupted, the *Drosophila* ortholog of mammalian *tumor susceptibility gene 101*, elicit non-cell-autonomous overgrowth. Developmental Cell *9*, 699–710.

Moore, A.W,, Jan, L.Y., and Jan,Y.N. (2002). *hamlet*, a binary genetic switch between single- and multiple- dendrite neuron morphology. Science *297*: 1355-8.

Myers, P.Z., Eisen, J.S., and Westerfield, M. (1986). Development and axonal outgrowth of identified motoneurons in the zebrafish. Journal of Neuroscience *6*: 2278-89.

Nedivi, E., Wu, G. Y., and Cline, H. T. (1998). Promotion of dendritic growth by CPG15, an activity-induced signaling molecule. Science *281*, 1863–1866.

Neumann, C.J., and Cohen, S.M. (1996). A hierarchy of cross-regulation involving Notch, wingless, vestigial and cut organizes the dorsal/ventral axis of the *Drosophila* wing. Development *122*: 3477-85.

Niblock, M.M., Brunso-Bechtold, J.K., and Riddle, D.R. (2001). Laminar variation in neuronal viability and trophic dependence in neocortical slices. Journal of Neuroscience Research *65*: 455-62.

Nixon, R.A. (2005). Endosome function and dysfunction in Alzheimer's disease and other neurodegenerative diseases. Neurobiology of Aging *26*, 373–382.

Orgogozo, V., Schweisguth, F., and Bellaiche, Y. (2001). Lineage, cell polarity and inscuteable function in the peripheral nervous system of the *Drosophila* embryo. Development *128*, 631–643.

Quinlan, E.M., Olstein, D.H., and Bear, M.F. (1999). Bidirectional, experience-dependent regulation of N-methyl-D-aspartate receptor subunit composition in the rat visual cortex during postnatal development. Proceedings of the National Academy of Sciences U S A. *96*: 12876-80.

Parks, A.L., Klueg, K.M., Stout, J.R., and Muskavitch, M.A. (2000). Ligand endocytosis drives receptor dissociation and activation in the Notch pathway. Development *127*, 1373–1385.

Parrish, J.Z., Kim, M.D., Jan, L.Y., and Jan, Y.N. (2006). Genome-wide analyses identify transcription factors required for proper morphogenesis of Drosophila sensory neuron dendrites. Genes and Development *20*: 820-35.

Peck, J.W, Bowden, E.T., and Burbelo, P.D. (2004). Structure and function of human Vps20 and Snf7 proteins. Biochemistry Journal *377*, 693–700.

Perry, V. H., and Linden, R. (1982). Evidence for dendritic competition in the developing retina. Nature *297*, 683–685.

Peters, A., and Kaiserman-Abramof, I. R. (1970). The small pyramidal neuron of the rat cerebral cortex. The perikaryon, dendrites and spines. American Journal of Anatomy *127*, 321–355.

Piddini, E., and Vincent, J.P. (2003). Modulation of developmental signals by endocytosis: different means and many ends. Current Opinion in Cell Biology *15*, 474–481.

Polleux, F., Giger, R.J., Ginty, D.D., Kolodkin, A.L., and Ghosh, A. (1998). Patterning of cortical efferent projections by semaphorin-neuropilin interactions. Science *282*: 1904-6.

Polleux, F., Morrow, T., and Ghosh, A. (2000). Semaphorin 3A is a chemoattractant for cortical apical dendrites. Nature *404*, 567–573.

Posern, G., Rapp, U.R., and Feller, S.M. (2000). The Crk signaling pathway contributes to the bombesin-induced activation of the small GTPase Rap1 in Swiss 3T3 cells. Oncogene *19*: 6361-8.

Prokop, A., Uhler, J., Roote, J., and Bate, M. (1998). The *kakapo* mutation affects terminal arborization and central dendritic sprouting of *Drosophila* motorneurons. Journal of Cell Biology *143*: 1283-94.

Rakic, P., and Sidman, R.L. (1973). Organization of cerebellar cortex secondary to deficit of granule cells in weaver mutant mice. Journal of Comparative Neurology *152*: 133-61.

Ramón y Cajal, S. (1995). Histology of the nervous system of man and vertebrates (New York, Oxford University Press).

Raymond, C.K., Howald-Stevenson. I., Vater, C.A., and Stevens, T.H. (1992). Morphological classification of the yeast vacuolar protein sorting mutants: evidence for a prevacuolar compartment in class E vps mutants. Molecular Biology of the Cell *3*, 1389–1402.

Redmond, L., and Ghosh, A. (2001) . The role of Notch and Rho GTPase signaling in the control of dendritic development. Current Opinion in Neurobiology *11*, 111–117.

Redmond, L., Oh, S.R., Hicks, D., Weinmaster, G., and Ghosh, A. (2000). Nuclear Notch1 signaling and the regulation of dendritic development. Nature Neuroscience *3*, 30–40.

Reichardt, L. F., and Farinas, I. (1997). Neurotrophic factors and their receptors: Roles in neuronal development and function. In "Molecular and Cellular Approaches to Neural Development," pp. 220–263. Oxford Univ. Press, New York.

Reichman-Fried, M., Dickson, B., Hafen, E., and Shilo, B.Z. (1994). Elucidation of the role of *breathless*, a *Drosophila* FGF receptor homolog, in tracheal cell migration. Genes and Development *8*, 428–439.

Reid, E., Connell, J., Edwards, T.L., Duley, S., Brown, S.E., and Sanderson, C.M. (2005). The hereditary spastic paraplegia protein spastin interacts with the ESCRT-III complex-associated endosomal protein CHMP1B. Human Molecular Genetics *14*, 19–38.

Reuter, J.E., Nardine, T.M., Penton, A., Billuart, P., Scott, E.K., Usui, T., Uemura, T., and Luo, L. (2003). A mosaic genetic screen for genes necessary for *Drosophila* mushroom body neuronal morphogenesis. Development *130*, 1203–1213.

Roayaie, K., Crump, J. G., Sagasti, A., and Bargmann, C. I. (1998). The G alpha protein ODR-3 mediates olfactory and nociceptive function and controls cilium morphogenesis in *C. elegans* olfactory neurons. Neuron *20*, 55–67.

Sagasti, A., Guido, M.R., Raible, D.W., and Schier, A.F. (2005). Repulsive interactions shape the morphologies and functional arrangement of zebrafish peripheral sensory arbors. Current Biology *15*: 804–14.

Sakata, T., Sakaguchi, H., Tsuda, L., Higashitani, A., Aigaki, T., Matsuno, K., and Hayashi, S. (2004). *Drosophila* Nedd4 regulates endocytosis of notch and suppresses its ligand-independent activation. Current Biology *14*, 2228–2236.

Salzberg, A., Prokopenko, S.N., He, Y., Tsai, P., Pal, M., Maroy, P., Glover, D.M., Deak, P., and Bellen, H.J. (1997). P-element insertion alleles of essential genes on the third chromosome of *Drosophila melanogaster*: Mutations affecting embryonic PNS development. Genetics *147*,1723–1741.

Schrader, S., and Merritt, D. J. (2000). Central projections of *Drosophila* sensory neurons in the transition from embryo to larva. Journal of Comparative Neurology *425*, 34–44.

Scott, E. K., and Luo, L. (2001). How do dendrites take their shape? Nature Neuroscience *4*, 359–365.

Senti, K.A., Usui, T., Boucke, K., Greber, U., Uemura, T., and Dickson, B.J. (2003). Flamingo regulates R8 axon-axon and axon-target interactions in the *Drosophila* visual system. Current Biology *13*: 828-32.

Sestan, N., Artavanis-Tsakonas, S., and Rakic, P. (1999). Contact-dependent inhibition of cortical neurite growth mediated by Notch signaling. Science *286*, 741–746.

Shankland, M., and Goodman, C. S. (1982). Development of the dendritic branching pattern of the medial giant interneuron in the grasshopper embryo. Developmental Biology *92*, 489–506.

Shaye, D.D., and Greenwald, I. (2002). Endocytosis-mediated downregulation of LIN-12/Notch upon Ras activation in *Caenorhabditis elegans*. Nature *420*, 686–690.

Shen, Q., Zhong, W., Jan. Y.N., and Temple, S. (2002). Asymmetric Numb distribution is critical for asymmetric cell division of mouse cerebral cortical stem cells and neuroblasts. Development *129*: 4843-53.

Shi, S., Hayashi, Y., Esteban, J.A., and Malinow, R. (2001). Subunit-specific rules governing AMPA receptor trafficking to synapses in hippocampal pyramidal neurons. Cell *105*: 331-43.

Skibinski, G., Parkinson, N.J., Brown, J.M., Chakrabarti, L., Lloyd, S.L., Hummerich, H., Nielsen, J.E., Hodges, J.R., Spillantini, M.G., Thusgaard, T., Brandner, S., Brun, A., Rossor, M.N., Gade, A., Johannsen, P., Sorensen, S.A., Gydesen, S., Fisher, E.M., and Collinge, J. (2005). Mutations in the endosomal ESCRTIII-complex subunit CHMP2B in frontotemporal dementia. Nature Genetics *37*, 806–808.

Six, E., Ndiaye, D., Laabi, Y., Brou, C., Gupta-Rossi, N., Israel, A., and Logeat, F. (2003). The Notch ligand Delta1 is sequentially cleaved by an ADAM protease and gamma-secretase. Proceedings of the National Academy of Sciences U. S. A. *100*, 7638–7643.

Song, H., Ming, G., He, Z., Lehmann, M., McKerracher, L., TessierLavigne, M., and Poo, M. (1998). Conversion of neuronal growth cone responses from repulsion to attraction by cyclic nucleotides. Science *281*, 1515–1518.

Sorkin, A., and Von Zastrow, M. (2002). Signal transduction and endocytosis: close encounters of many kinds. Nature Reviews Molecular Cell Biology *3*, 600–614.

Stevens, C.F. (1998). Neuronal diversity: too many cell types for comfort? Current Biology *8*: R708-10.

Sugimura, K., Satoh, D., Estes, P., Crews, S., and Uemura, T. (2004). Development of morphological diversity of dendrites in *Drosophila* by the BTB-zinc finger protein abrupt. Neuron *43*, 809–822.

Sweeney, S.T., and Davis, G.W. (2002). Unrestricted synaptic growth in spinster-a late endosomal protein implicated in TGF-beta-mediated synaptic growth regulation. Neuron *36*, 403–416.

Sweeney, N.T., Li, W., and Gao, F.-B. (2002). Genetic manipulation of single neurons *in vivo* reveals specific roles of Flamingo in neuronal morphogenesis. Developmental Biology *247*, 76–88.

Thompson, B.J., Mathieu, J., Sung, H.H., Loeser, E., Rorth, P., and Cohen, S.M. (2005). Tumor suppressor properties of the ESCRT-II complex component Vps25 in *Drosophila*. Developmental Cell *9*, 711–720.

Tracey, W.D. Jr., Wilson, R.I., Laurent, G., and Benzer, S. (2003). *painless*, a *Drosophila* gene essential for nociception. Cell *113*: 261-73.

Tu, J., Vallier, L.G., Carlson, M. (1993). Molecular and genetic analysis of the SNF7 gene in *Saccharomyces cerevisiae*. Genetics *135*, 17–23.

Usui, T., Shima, Y., Shimada, Y., Hirano, S., Burgess, R. W., Schwarz, T. L., Takeichi, M., and Uemura, T. (1999). Flamingo, a seven-pass transmembrane cadherin, regulates epithelial planar cell polarity under the control of Frizzled. Cell *98*, 585–595.

Uylings, H.B., Smit, G.J., and Veltman, W.A. (1975). Ordering methods in quantitative analysis of branching structures of dendritic trees. Advances in Neurology *12*, 347–354.

Vaccari, T., and Bilder, D. (2005). The *Drosophila* tumor suppressor Vps25 prevents nonautonomous overproliferation by regulating Notch trafficking. Developmental Cell *9*, 687–698.

Vercelli, A., Assal. F., and Innocenti, G.M. (1992). Emergence of callosally projecting neurons with stellate morphology in the visual cortex of the kitten. Experimental Brain Research *90*: 346-58.

Vervoort, M., Merritt, D. J., Ghysen, A., and Dambly-Chaudière, C. (1997). Genetic basis of the formation and identity of type I and type II neurons in *Drosophila* embryos. Development *124*, 2819– 2828.

von Schwedler, U.K., Stuchell, M., Muller, B., Ward, D.M., Chung, H.Y., Morita, E., Wang, H.E., Davis, T., He, G.P., Cimbora, D.M., Scott, A., Krausslich, H.G., Kaplan, J., Morham, S.G., and Sundquist, W.I. (2003). The protein network of HIV budding. Cell *114*: 701-13.

Wang, H., and Macagno, E. R. (1998). A detached branch stops being recognized as self by other branches of a neuron. Journal of Neurobiology *35*, 53–64.

Wassle, H., Peichl, L., and Boycott, B.B. (1981). Dendritic territories of cat retinal ganglion cells. Nature *292*: 344-5.

Westerfield, M., McMurray, J.V., and Eisen, J.S. (1986). Identified motoneurons and their innervation of axial muscles in the zebrafish. Journal of Neuroscience *6*: 2267-77.

Whitford, K.L., Dijkhuizen, P., Polleux, F., and Ghosh, A. (2002). Molecular control of cortical dendrite development. Annual Review of Neuroscience *25*: 127-49.

Whitford, K. L., Marillat, V., Stein, E., Goodman, C. S., Tessier-Lavigne, M., Chedotal, A., and Ghosh A. (2002). Regulation of cortical dendrite development by slit-robo interactions. Neuron *33*,47–66.

Wilkin, M.B., Carbery, A.M., Fostier, M., Aslam, H., Mazaleyrat, S.L., Higgs, J., Myat, A., Evans, D.A., Cornell, M., and Baron, M. (2004). Regulation of notch endosomal sorting and signaling by *Drosophila* Nedd4 family proteins. Current Biology *14*, 2237–2244.

Wills, Z., Bateman, J., Korey, C.A., Comer, A., and Van Vactor, D. (1999). The tyrosine kinase Abl and its substrate enabled collaborate with the receptor phosphatase Dlar to control motor axon guidance. Neuron *22*: 301-12.

Wong, W.T., Faulkner-Jones, B.E., Sanes, J.R., and Wong, R.O. (2000). Rapid dendritic remodeling in the developing retina: dependence on neurotransmission and reciprocal regulation by Rac and Rho. Journal of Neuroscience *20*: 5024-36.

Wong, W. T., and Wong, R. O. (2000). Rapid dendritic movement during synapse formation and rearrangement. Current Opinion in Neurobiology *10*, 118–124.

Wu, G.Y., and Cline, H.T. (1998). Stabilization of dendritic arbor structure in vivo by CaMKII. Science *279*: 222-6.

Wu, G.Y., Deisseroth, K., and Tsien, R.W. (2001). Spaced stimuli stabilize MAPK pathway activation and its effects on dendritic morphology. Nature Neuroscience *4*: 151-8.

Xu, B., Zang, K., Ruff, N. L., Zhang, Y. A., McConnell, S. K., Stryker, M. P., and Reichardt, L. F. (2000). Cortical degeneration in the absence of neurotrophin signaling: Dendritic retraction and neuronal loss after removal of the receptor TrkB. Neuron *26*, 233–245.

Yoon, K., and Gaiano, N. (2005). Notch signaling in the mammalian central nervous system: insights from mouse mutants. Nature Neuroscience *8*, 709–715.

Zanata, S.M., Hovatta, I., Rohm, B., and Puschel, A.W. (2002). Antagonistic effects of Rnd1 and RhoD GTPases regulate receptor activity in Semaphorin 3A-induced cytoskeletal collapse. Journal of Neuroscience. *22*: 471-7.

Zhu, J.J., Esteban, J.A., Hayashi, Y., and Malinow, R. (2000). Postnatal synaptic potentiation: delivery of GluR4-containing AMPA receptors by spontaneous activity. Nature Neuroscience *3*: 1098-106.

Zhu, H., and Luo, L. (2004). Diverse functions of N-cadherin in dendritic and axonal terminal arborization of olfactory projection neurons. Neuron *42*: 63-75.

Zhu, S., Perez, R., Pan, M., and Lee, T. (2005). Requirement of Cul3 for axonal arborization and dendritic elaboration in *Drosophila* mushroom body neurons. Journal of Neuroscience *25*, 4189–4197.

Zong, H., Espinosa, J.S., Su, H.H., Muzumdar, M.D., and Luo, L. (2005). Mosaic analysis with double markers in mice. Cell *121*: 479-92.

Zou, D.J., and Cline, H.T. (1999). Postsynaptic calcium/calmodulin-dependent protein kinase II is required to limit elaboration of presynaptic and postsynaptic neuronal arbors. Journal of Neuroscience *19*: 8909-18.